

THE RADIATION FROM A LINEAR ANTENNA

IN THE PRESENCE OF A WEDGE

A MASTER'S THESIS

IN

Electrical and Electronics Engineering

Middle East Technical University

By

Mohammad B. ABACHI

September 1989

W. E.
Tükseköğretim Kurulu
Dokümantasyon Merkezi

Approval of the Graduate School of Natural and Applied Sciences.


Prof.Dr.Alpay Ankara

Director

I certify that this thesis satisfies all the requirements as a thesis for the degree of Master of Science in Electrical and Electronics Engineering.


Assoc.Prof.Dr.Erol Kocaoğlan

Chairman of the Department

We certify that we have read this thesis and that in our opinion it is fully adequate,in scope and quality,as a thesis for the degree of Master of Science in Electrical and Electronics Engineering.


Assoc.Prof.Dr.Merih Buyukdura

Supervisor

Examining Committee in Charge :

Prof.Dr. Altunkan Hizal (Chairman)

Assoc.Prof.Dr.Fatih Canatan

Assoc.Prof.Dr.Nilgun Gunalp

Assoc.Prof.Dr.Merih Buyukdura

Assoc.Prof.Dr.Sencer Koc

ABSTRACT

THE RADIATION FROM A LINEAR ANTENNA IN THE PRESENCE OF A WEDGE

ABACHI,Mohammad B.

M.SC. in Electrical and Electronics Engineering

Supervisor: Assoc.Prof.Dr.Merih Buyukdura

September 1989,92 pages

The purpose of this study is to predict accurately the behaviour of a monopole antenna mounted near the edge of a perfectly conducting half-plane. The approach used is to combine the method of moments (MM) with ray-optical techniques as proposed by D. Pozar.

The ray-optical method employed is the extended UTD,which was found to yield results for the antenna impedance virtually indistinguishable from those obtained using the exact Green's function for a half-plane. The radiation pattern of the antenna is also investigated.

Keywords: Method of Moments (MM)-Uniform geometric theory of diffraction (UTD)

Extended uniform geometric theory of diffraction (Extended UTD)

609.02.03

ÖZET

AÇILI BİR KÖSEDE DOĞRUSAL ANTENİN İŞİNİMİ

Mohammad B. ABACHI

Yüksek Lisans Tezi, Elektrik ve Elektronik Muh. Bölümü

Tez Yöneticisi Y. Doç. Dr. Merih Büyükdura

Eylül 1989, 93 sayfa

Bu çalışmanın amacı tam iletken yarı düzlem kenarına monte edilmiş bir monopol anten davranışının olabildiğince hassas olarak saptanmasıdır. Kullanılan yaklaşım Momentler yöntemi ile D. Pozar tarafından önerilen ray-optik teknığının bir birleşimidir.

Kullanılan Ray-optik teknigi genişletilmiş UTD olup, anten empedansı için bir yarı düzlemede Green fonksiyonları ile elde edilen sonuçlardan ayırtedilmiyecek kadar yakın sonuçlar verdiği görülmüştür.

Anten empedansının işinim dizgesi de araştırılmıştır.

Anahtar Kelimeler: Momentler yöntemi (MM)-Geometrik düzgün kırılma teorisi (UTD)
genişletilmiş Geometrik düzgün kırılma teorisi (UTD)

ACKNOWLEDGMENTS

I would like to express my sincere gratitude to Assoc.Prof.Dr. O. Merih Büyükdura for his supervision and guidance of this project.

I would like to thank my best friend,my sister,for her support and encouragement.

My special thanks go to my family and my friends.

TABLE OF CONTENTS

ABSTRACT	i
ÖZET	iii
ACKNOWLEDGMENTS	v
TABLE OF CONTENTS	vi
LIST OF FIGURES	viii
1. INTRODUCTION	1
2. THE MOMENT METHOD FOR THIN-WIRE ANTENNAS	4
2.1 Introduction	4
2.2 Pocklington's Integral Equation	4
2.3 Galerkin's Method using piecewise sinusoidal basis functions. (Dipole)	7
2.4 Calculating The Input Impedance of a Monopole Antenna on an Infinite Electric Conductor	13
3. EDGE DIFFRACTION	20
3.1 Introduction	20
3.2 Geometrical Theory of Diffraction.....	20
3.3 Uniform Geometrical Theory of Diffraction (UTD)	24
3.4 Extended UTD	27

4. Hybrid MM-GTD APPROACH	31
4.1 Introduction	31
4.2 Combining the MM with ray techniques	31
4.3 MM-UTD	34
4.4 Hybrid MM-Extended UTD Method	38
5. COMPARISON OF RESULTS	47
6. CONCLUSIONS	53
7. REFERENCES	54
8. APPENDICES	
A. Computer Program for calculating Input Impedance of a Dipole Antenna	56
B. Computer Program for calculating Input Impedance of a Monopole Antenna on an infinite ground plane	63
C. Computer Program for calculating Input Impedance of a Monopole Antenna on an infinite half-plane	72

LIST OF FIGURES

Figure		Page
2.2.1	Perfectly conducting wire in free space.	5
2.3.1	Piecewise sinusoidal basis function.	9
2.4.1	Monopole antenna mounted on an infinite conducting ground plane.	14
2.4.2	Monopole antenna over perfect ground plane with its image (dashed).	16
3.2.1	Wedge geometry for edge diffraction.	21
4.3.1	Monopole antenna mounted on a perfect ground half-plane.	35
4.4.1	Monopole antenna mounted on a perfect ground half-plane showing fields.	40
5.1.1	Input resistance of a $\lambda/4$ monopole versus distance d from edge of half-plane using MM-UTD and MM-extended UTD.	49
5.1.2	Input reactance of a $\lambda/4$ monopole versus distance d from edge of half-plane using MM-UTD and MM-extended UTD.	50

Figure	Page
5.1.3 Input resistance of a $\lambda/4$ monopole versus distance d from edge of half-plane using exact Green's function and UTD Green's function.	51
5.1.2 Input reactance of a $\lambda/4$ monopole versus distance d from edge of half-plane using exact Green's function and UTD Green's function.	52

CHAPTER 1 : INTRODUCTION

The object of this thesis is to find the input impedance of a monopole antenna mounted near the edge of a perfectly conducting half-plane. To achieve this,a hybrid moment method-extended UTD approach is devised.

As is well known, the moment method involves the setting up of an integral equation which enforces the tangential component of the total (radiated field) electric field to vanish. The unknown current density on the antenna is approximated by a series of known (basis) functions with unknown coefficients. The radiated field is then calculated in terms of unknown coefficients using a suitable method. This in turn is examined on the surface of the antenna and its tangential component is set equal to the negative feed field,thus enforcing the null tangential field condition. What is obtained at this point is an approximate functional equality involving a finite number of unknown coefficients. To convert this equality into a set of algebraic equations, both sides of the equality are multiplied in turn by a set of so-called testing (or weighting) functions and integrated over the length of the antenna. The set of algebraic equations thus obtained are solved easily on a digital computer using one of the available matrix-inversion

techniques, allowing one to obtain an approximate expression for the current density on the antenna.

In this thesis the extended UTD (extended Uniform Geometrical Theory of Diffraction)[1] is used to calculate the field radiated by the antenna in the presence of the half-plane. The extended UTD is a more accurate version of the UTD in that higher order, non ray-optical terms are retained in the expression for the diffracted field. This higher order terms become important close to the edge of the half-plane where accuracy is important if the monopole is situated close to the edge.

On the moment method side of the hybrid technique, the Galerkin's method is employed using subsectional piecewise sinusoidal functions. The Galerkin's method was chosen for its well tested numerical stability. The advantage to the choice of piecewise sinusoidal basis functions is two-fold: 1) The free-space field of a piecewise sinusoidal current distribution is known in closed form. This leaves only the testing integrals to be evaluated numerically, saving computational time. 2) As mentioned above, the total radiated field is calculated using the extended UTD which, to calculate the diffracted field requires the field incident on the edge to be ray-optical. The closed form free space field of a piecewise sinusoidal current is in the form of three spherical waves each of which of course is ray-optical.

In chapter 2, the application of the moment method to thin-wire antennas is illustrated. For this purpose the input impedance of first a dipole antenna in free-space,then a monopole antenna mounted on an infinite ground plane are calculated. Chapter 3 describes the ray-optical techniques used in the following chapter.The GTD (Geometrical Theory of Diffraction), the UTD and the extended UTD techniques are presented in turn. Finally the object problem of a monopole near the edge of a half-plane be solved in chapter 4, using first a moment method-UTD approach,then a moment method-extended UTD approach.

It should be pointed out at this point that the general hybrid method employed here was suggested and used earlier by D.Pozar[2]. The problem of the radiation by a monopole mounted near the edge of a half-plane was solved in his work using two different approaches. The first is a moment method solution which employs the exact (eigenfunction expansion) Green's function for the half-plane. The second is a hybrid moment method-UTD approach in which the UTD is used in place of the exact Green's function.The two results are compared and as expected,found to be in good agreement when the monopole is not very close to the edge.Pozar's results based on the hybrid approach are duplicated here.Furthermore the hybrid method was used employing the extended UTD in place of the UTD with the aim of improving accuracy.The results are found to be in much better agreement with the exact Green's function solution. Thus our results may be seen as a verification of the superior accuracy of the extended UTD as compared to the conventional UTD.

CHAPTER 2 : The Moment Method for Thin-Wire Antennas

2.1. Introduction

In this chapter, the method of moments is discussed in the context of thin wire antennas. First Pocklington's integral equation is derived and converted into a set of algebraic equations using a general moment method approach. Then the specific Galerkin method is employed using piecewise sinusoidal basis (and testing) functions.

A dipole in free-space and a monopole mounted on an infinite ground plane are examined.

2.2. Pocklington's Integral Equation

One of the common integral equations that arises in the treatment of wire antennas or scatterers is that derived by Pocklington [3,4]. The problem of interest is shown in Fig.2.1, in which a cylindrical perfectly conducting wire of radius a is surrounded by free-space (permittivity ϵ_0 , permeability μ_0). It is assumed that a , the wire radius is very small compared to both L , the length of the wire and λ the wavelength at the frequency of operation. When this antenna is excited by a time harmonic source

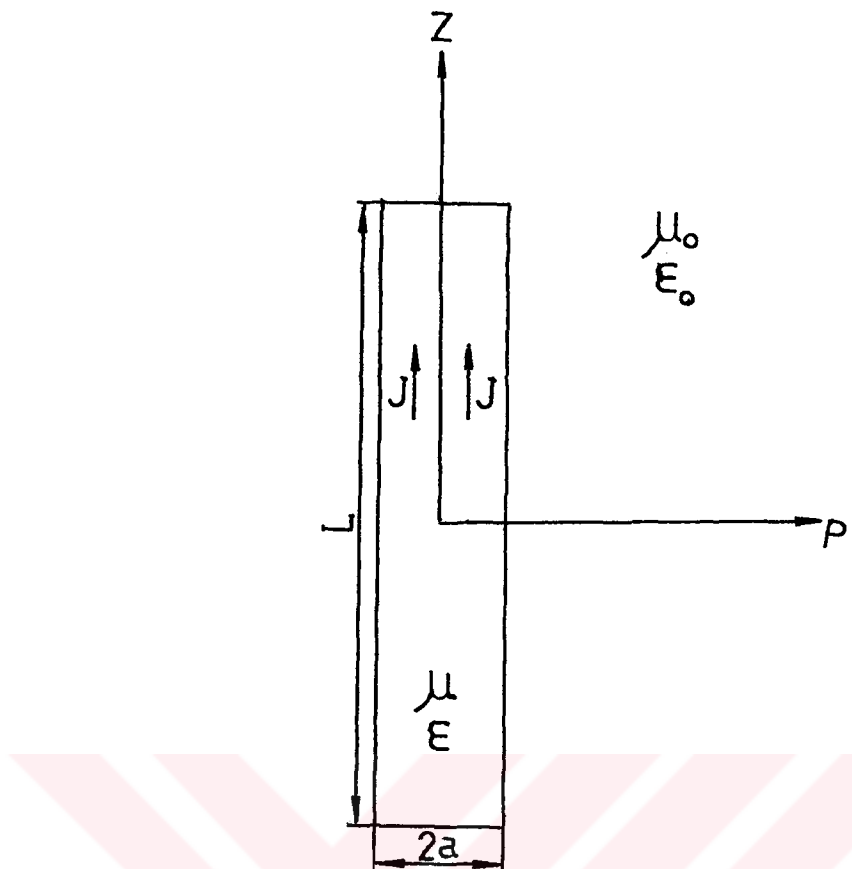


Figure 2.2.1. Perfectly conducting wire in free space.

of electromagnetic fields, a surface current distribution denoted by \bar{J} will be induced on the wire which in turn will radiate itself. It is assumed that $a \ll \lambda$ and $a \ll L$ here; we may safely assume that \bar{J} is purely z -directed, i.e. $\bar{J} = \hat{z} J_z$. The vector potential \bar{A} due to this current distribution is well known to be given by

$$\bar{A} = \hat{z} \iint_s J_z \frac{e^{-jkR}}{4\pi R} ds' \quad (2.2.1).$$

Here $k = \omega \sqrt{\mu_0 \epsilon_0}$ is the free-space wave number, R is the distance between the source point (x', y', z') and the

observation point (x, y, z) , i.e.,

$$R = \sqrt{(x-x')^2 + (y-y')^2 + (z-z')^2} \quad (2.2.2).$$

and S is the surface of the wire. Note that in (2.2.1), as well as throughout the thesis an $e^{j\omega t}$ time dependence is assumed and suppressed. Note also that the Lorentz Gauge has been used in (2.2.1). Accordingly, the z -component of the electric field due to \bar{J} is given by

$$E_z^S = \frac{1}{j\omega\epsilon_0} \int \int_S \left[\frac{\partial^2}{\partial z^2} + k^2 \right] \frac{e^{-jkR}}{4\pi R} J_z ds' \quad (2.2.3).$$

Since a is small we may assume the current density to be uniform with respect to the polar coordinate ϕ' such that

$$E_z^S = \frac{1}{j\omega\epsilon_0} \int_{-L/2}^{+L/2} \left[\frac{\partial^2}{\partial z^2} + k^2 \right] \frac{e^{-jkR}}{4\pi R} I(z') dz' \quad (2.2.4).$$

where

$$I(z') = 2\pi a J_z(z') \quad (2.2.5).$$

Since the axis of the wire is in a perfectly conducting region, the total field there (i.e. $\rho=0, -L/2 \leq z \leq L/2$) should vanish, i.e.,

$$E_z^S (\rho=0, -L/2 \leq z \leq L/2) = -E_z^I (\rho=0, -L/2 \leq z \leq L/2) \quad (2.2.6)$$

which, using (2.2.4) can be expressed as

$$\frac{1}{j\omega\epsilon_0} \int_{-L/2}^{+L/2} I(z') \left[\frac{\partial^2 \psi(z, z')}{\partial z^2} + k^2 \psi(z, z') \right] dz' = -E_z^i(z) \quad (2.2.7)$$

which is true for $-L/2 \leq z \leq L/2$. Here,

$$\psi(z, z') = \frac{e^{-jkR}}{4\pi R} \quad (2.2.8)$$

and only the z, z' dependence is retained since now, from the circular cross-section of the wire

$$R = \sqrt{(z-z')^2 + a^2} \quad (2.2.9)$$

It should be pointed out at this point that (2.2.7) can be used to solve both a scattering problem, in which case E_z^i would be the free-space field of a distant source, and an antenna radiation problem in which case E_z^i should be taken as the free-space field of the feed structure.

2.3 Galerkin's Method using Piecewise Sinusoidal Basis Functions. (Dipole).

In this thesis we shall use piecewise sinusoidal basis functions to approximate the current distribution on the wire. Thus

$$I(z') = \sum_{n=-(N-1)/2}^{(N-1)/2} I_n F_n(z') \quad (2.3.1)$$

where

$$F_n(z') = \begin{cases} \frac{\sin[k(z' - z_{n-1})]}{\sin(k\Delta z)} & , \quad z_{n-1} < z' \leq z_n \\ \frac{\sin[k(z_{n+1} - z')]}{\sin(k\Delta z)} & , \quad z_n \leq z' < z_{n+1} \end{cases} \quad (2.3.2)$$

true for $n=-(N-1)/2, \dots, (N-1)/2$, and N , the total number of subsections is chosen to be an odd number, and

$$\Delta z = \frac{L}{N+1} \quad (2.3.3).$$

We also have

$$z_n = n\Delta z \quad (2.3.4).$$

The approximate representation of $I(z')$ as in (2.3.1) is illustrated in Fig.2.3.1.

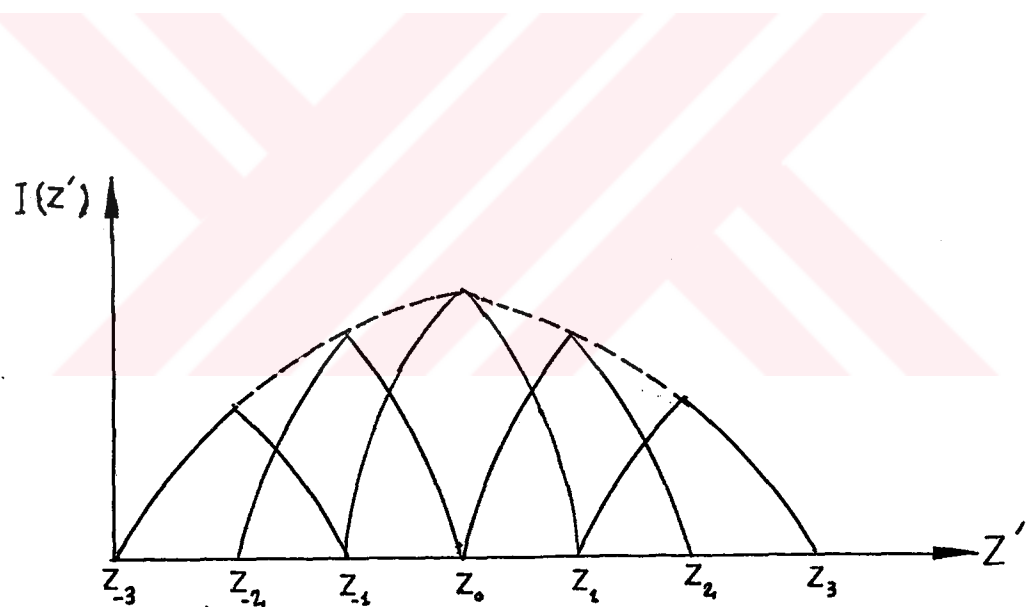
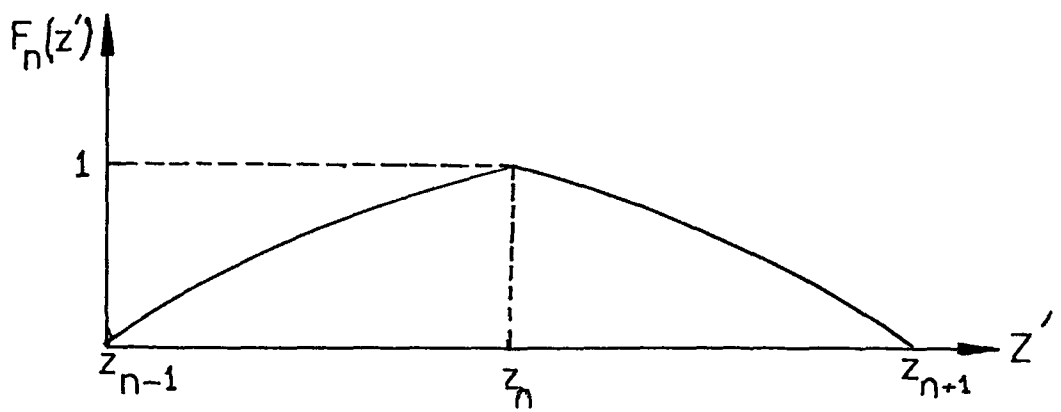


Figure 2.3.1 a) The piecewise sinusoidal basis function.
b) The representation of $I(z')$ in terms of the piecewise sinusoidal basis. ($N=5$).

Incorporating (2.3.1) in (2.2.7),

$$\sum_{n=-(N-1)/2}^{(N-1)/2} I_n \frac{1}{j\omega\epsilon_0} \int_{-L/2}^{+L/2} F_n(z') \left[\frac{a^2\psi(z,z')}{az^2} + k^2\psi(z,z') \right] dz' = -E(z) \quad (2.3.5)$$

is obtained. But since $F_n(z')$ vanishes for $z' > z_{n+1}$ and $z' < z_{n-1}$, we may write

$$\sum_{n=-(N-1)/2}^{(N-1)/2} I_n \frac{1}{j\omega\epsilon_0} \int_{z_{n-1}}^{z_{n+1}} F_n(z') \left[\frac{a^2\psi(z,z')}{az^2} + k^2\psi(z,z') \right] dz' = -E(z) \quad (2.3.6)$$

The integral appearing on the left hand side of this equation is given in closed form by [5]

$$\begin{aligned} \frac{1}{j\omega\epsilon_0} \int_{z_{n-1}}^{z_{n+1}} F_n(z') \left[\frac{a^2\psi(z,z')}{az^2} + k^2\psi(z,z') \right] dz' = \\ -j30 \left[\frac{e^{-jkR_{n-1}}}{R_{n-1} \sin(k\Delta z)} - \frac{e^{-jkR_n} \sin(2k\Delta z)}{R_n \sin^2(k\Delta z)} + \frac{e^{-jkR_{n+1}}}{R_{n+1} \sin(k\Delta z)} \right] \end{aligned} \quad (2.3.7)$$

where

$$\begin{aligned} R_n &= \sqrt{a^2 + (z - z_n)^2} \\ R_{n-1} &= \sqrt{a^2 + (z - z_{n-1})^2} \\ R_{n+1} &= \sqrt{a^2 + (z - z_{n+1})^2} \end{aligned} \quad (2.3.8)$$

Observe that the field of a piecewise sinusoidal current distribution is a sum of three spherical waves, one emanating from the mid-point of the section, the other two from the end points. It is this ray-optical nature of the field which will enable us to employ the UTD and the extended UTD for the hybrid formulation in the following chapters.

Substituting (2.3.7) in (2.3.6) we obtain

$$\sum_{n=-(N-1)/2}^{(N-1)/2} I_n (-j30) \left[\frac{e^{-jkR_{n-1}}}{R_{n-1} \sin(k\Delta z)} - \frac{e^{-jkR_n} \sin(2k\Delta z)}{R_n \sin^2(k\Delta z)} \right. \\ \left. + \frac{e^{-jkR_{n+1}}}{R_{n+1} \sin(k\Delta z)} \right] = -E_z(z) \quad (2.3.9)$$

The next step, in accordance with the Galerkin's method is to multiply both sides of (2.3.9) by $F_m(z)$ and integrate over the wire length. Thus

$$\sum_{n=-(N-1)/2}^{(N-1)/2} I_n \int_{z_{m-1}}^{z_{m+1}} F_m(z) \frac{-j30}{\sin(k\Delta z)} \left[\frac{e^{-jkR_{n-1}}}{R_{n-1}} \right. \\ \left. - 2\cos(k\Delta z) \frac{e^{-jkR_n}}{R_n} + \frac{e^{-jkR_{n+1}}}{R_{n+1}} \right] dz = \\ - \int_{z_{m-1}}^{z_{m+1}} F_m(z) E_z(z) dz \quad (2.3.10)$$

$m=-(N-1)/2, \dots, (N-1)/2$

is obtained.(2.3.10) is now a set of algebraic equations which can be expressed as

$$\sum_{n=-(N-1)/2}^{(N-1)/2} Z_{mn} I_n = V_m \quad (2.3.11)$$

where

$$Z_{mn} = - \int_{z_{m-1}}^{z_{m+1}} \frac{\sin k(\Delta z - |z - z_m|)}{\sin(k\Delta z)} \cdot \left[\frac{e^{-jkR_{n-1}}}{R_{n-1}} - 2\cos(k\Delta z) \frac{e^{-jkR_n}}{R_n} + \frac{e^{-jkR_{n+1}}}{R_{n+1}} \right] dz \quad (2.3.12)$$

and

$$V_m = - \int_{z_{m-1}}^{z_{m+1}} F_m(z) E_z^i(z) dz \quad (2.3.13)$$

In this thesis we have used a delta-gap voltage generator for the feed. Therefore we can write V_m as

$$V_m = - \int_{z_{m-1}}^{z_{m+1}} F_m(z) \delta(z) V_0 dz \quad (2.3.14)$$

And from the definition of the Dirac delta function we have

$$V_m = \begin{cases} V_0, & z=0 \\ 0, & z \neq 0 \end{cases} \quad (2.3.15)$$

What remains now is to solve the matrix equation (2.3.11) to find the unknown coefficients I_n . Then, since the terminal current $I(z=0)$ is given by I_0 (see Fig.2.3.1) the input impedance is given simply by

$$Z_{in} = \frac{V_0}{I_0} \quad (2.3.16)$$

2.4 CALCULATING THE INPUT IMPEDANCE OF A MONPOLE ANTENNA ON AN INFINITE ELECTRIC CONDUCTOR

The problem with which will be dealing in this section is that of a monopole antenna mounted on an infinite conducting ground plane, as shown in Fig.(2.4.1). Obviously, the solution of a center-fed dipole given in the previous section along with image theory considerations can be used directly to find say the input impedance. Nevertheless we have chosen to set up a new integral equation in which the total scattered field (the field due to the current distribution on the antenna) is obtained using geometrical optics(GO). In other words the field of a piecewise sinusoidal current distribution is expressed as (2.3.7) plus three more similar terms representing the field reflected by the ground plane. This approach will serve as an intermediate step towards our final solution in which the diffracted fields emanating from a nearby edge will also be included in the analysis.

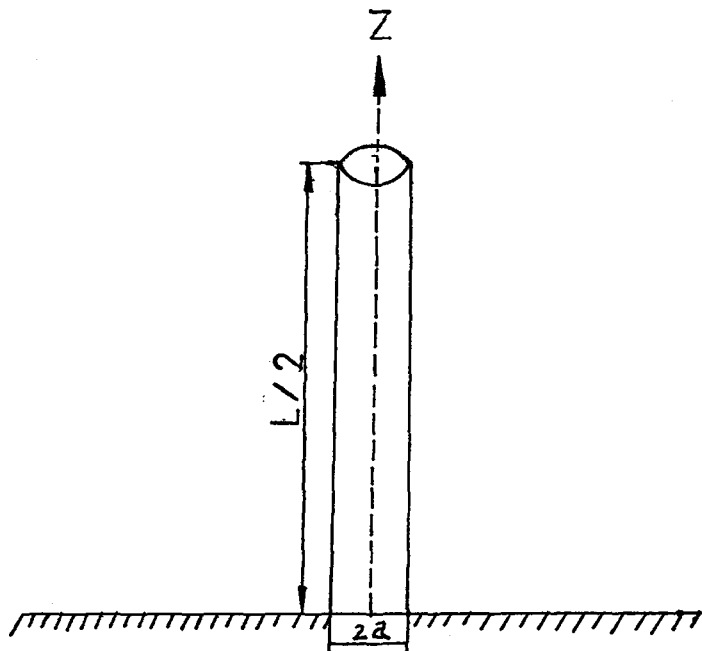


Figure 2.4.1 Monopole antenna mounted on an infinite conducting ground plane.

From image theory, the essential feature to remember is that the fields above a perfect ground plane from a primary source acting in the presence of the perfect ground plane (perfect conducting plane) are found by summing the contributions of the primary source and the image, each acting in free space. The z-component of the total field due to current distribution on the monopole is given by

$$E_z^s = E_z^{GO} = E_z^{\text{in}} + E_z^{\text{re}} \quad (2.4.1)$$

Here E_z^{in} represents the "incident" or the free-space field of the current distribution whereas E_z^{re} represents the "reflected" component, emanating from the image of the current distribution. The incident field of a piecewise sinusoidal current distribution is as given in (2.3.7).

We can calculate E_z^{re} (image effect)from the following expression:

$$E_z^{re} = \frac{-j30}{\sin(k\Delta z)} \left[\frac{e^{-jkR'_n}}{R'_n} - 2\cos(k\Delta z) \frac{e^{-jkR'_n}}{R'_n} + \frac{e^{-jkR'_{n+1}}}{R'_{n+1}} \right] \quad (2.4.2)$$

where

$$\begin{aligned} R'_n &= \sqrt{a^2 + (z + z_n)^2} \\ R'_{n-1} &= \sqrt{a^2 + (z + z_{n-1})^2} \\ R'_{n+1} &= \sqrt{a^2 + (z + z_{n+1})^2} \end{aligned} \quad (2.4.3)$$

Note that R'_n , R'_{n+1} and R'_{n-1} are the distances from the observation point to the mid point and the end points, respectively, of the image of the particular piecewise sinusoidal of interest.

Now we can find an expression for the generalized impedance matrix.

$$Z_{mn} = \int_{z_{m-1}}^{z_m} \frac{\sin k(z-z_{m-l})}{\sin(k\Delta z)} \hat{z} \cdot (\bar{E}_n^{\text{in}} + \bar{E}_n^{\text{re}}) dz +$$

$$\int_{z_m}^{z_{m+1}} \frac{\sin k(z_{m+1}-z)}{\sin(k\Delta z)} \hat{z} \cdot (\bar{E}_n^{\text{in}} + \bar{E}_n^{\text{re}}) dz$$

$m, n = 0, 1, 2, \dots, (N-1)/2$

(2.4.4)

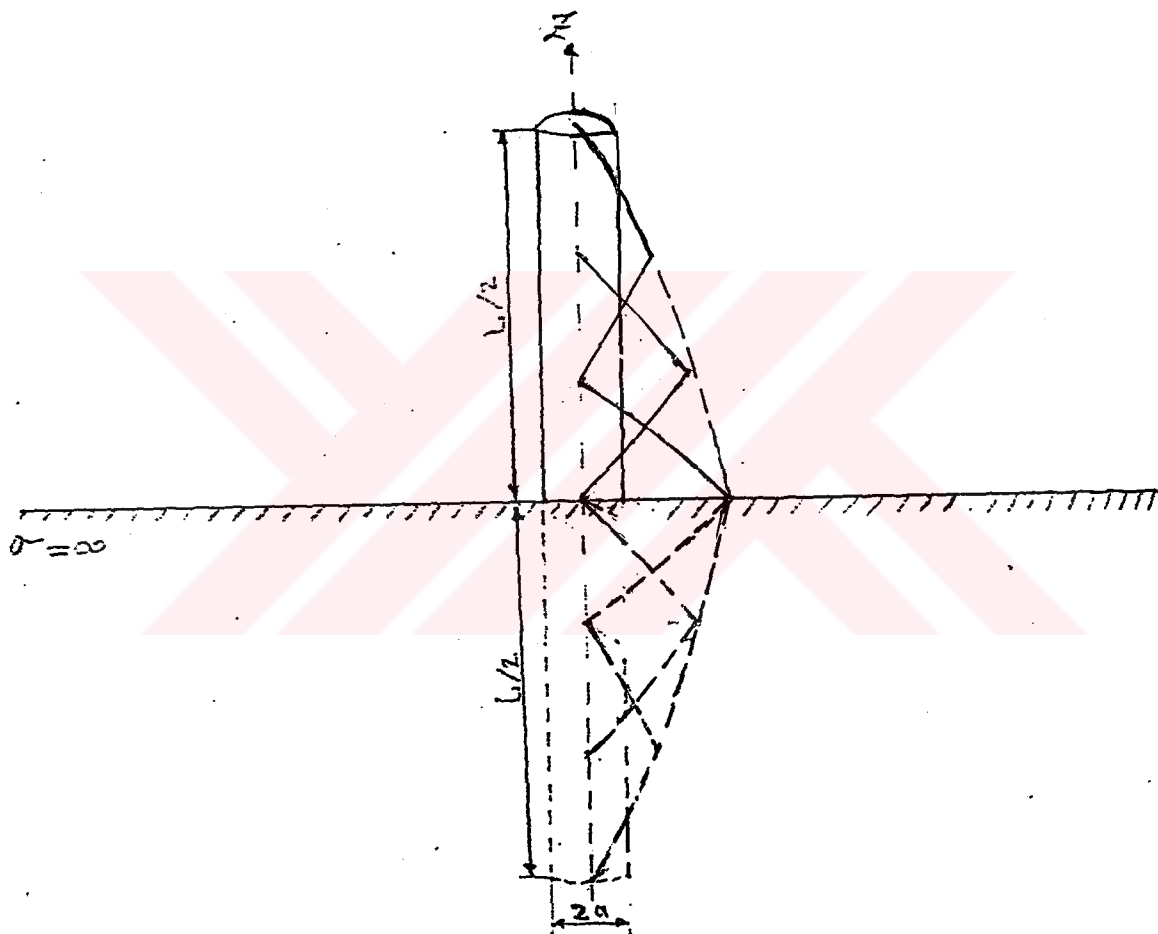


Figure 2.4.2. Monopole antenna over perfect ground plane with its image (dashed).

If we substitute for E_n^{in} and E_n^{re} we have

$$Z_{mn} = - \int_{z_{m-1}}^{z_m + i \sin k(\Delta z - |z - z_m|)} \frac{\sin(k(\Delta z - |z - z_m|))}{\sin(k\Delta z)} dz$$

$$= \frac{j30}{\sin(k\Delta z)} \cdot \left[\frac{e^{-jkR'_{n-1}}}{R_{n-1}} \right.$$

$$- 2\cos(k\Delta z) \frac{e^{-jkR'_n}}{R_n} + \frac{e^{-jkR'_{n+1}}}{R_{n+1}}$$

$$\left. \frac{e^{-jkR'_{n-1}}}{R_{n-1}} - 2\cos(k\Delta z) \frac{e^{-jkR'_n}}{R_n} + \frac{e^{-jkR'_{n+1}}}{R_{n+1}} \right] dz$$

(2.4.5)

This expression is valid for each value of m and n, except for m=0 and/or n=0

If m=0 and n>0 we use the following expression

$$Z_{0n} = - \int_0^{\Delta z} \frac{\sin k(z_1 - z)}{\sin(k\Delta z)} dz$$

$$= \frac{j30}{\sin(k\Delta z)} \cdot \left[\frac{e^{-jkR'_{n-1}}}{R_{n-1}} \right.$$

$$- 2\cos(k\Delta z) \frac{e^{-jkR'_n}}{R_n} + \frac{e^{-jkR'_{n+1}}}{R_{n+1}}$$

$$\left. \frac{e^{-jkR'_{n-1}}}{R_{n-1}} - 2\cos(k\Delta z) \frac{e^{-jkR'_n}}{R_n} + \frac{e^{-jkR'_{n+1}}}{R_{n+1}} \right] dz$$

(2.4.6)

If $m > 0$ and $n = 0$ we use the following expression

$$Z_{m0} = - \int_{z_{m-1}}^{z_{m+1}} \frac{\sin k(\Delta z - |z - z_m|)}{\sin(k\Delta z)} \cdot \left[\frac{e^{-jkR_1}}{R_1} - 2\cos(k\Delta z) \left(\frac{e^{-jkR_0}}{R_0} + \frac{e^{-jkR_1'}}{R_1'} \right) dz \right] \quad (2.4.7)$$

And lastly for $m=n=0$ we use

$$Z_{00} = - \int_0^{\Delta z} \frac{\sin k(z_1 - z)}{\sin(k\Delta z)} \cdot \left[\frac{e^{-jkR_1}}{R_1} - 2\cos(k\Delta z) \left(\frac{e^{-jkR_0}}{R_0} + \frac{e^{-jkR_1'}}{R_1'} \right) dz \right] \quad (2.4.8)$$

In this case the set of equations to be solved are

$$\sum_{n=0}^{(N-1)/2} Z_{mn} I_n = V_m \quad (2.4.9)$$

$$m=0,1,\dots,(N-1)/2$$

where Z_{mn} are given by (2.4.5),(2.4.6),(2.4.7),and

$$V_m = \begin{cases} V_0, & m=0 \\ 0, & m \neq 0 \end{cases} \quad (2.4.10)$$

The input impedance is again given by

$$Z_{in} = \frac{V_0}{I_0}$$

The currents and charges on a monopole are the same as on the upper half of its dipole counterpart, but the terminal voltage is only half that of the dipole.

The voltage is half because the gap width of input terminals is half that of the dipole, and the same electric field over half the distance gives half the voltage.

The input impedance for a monopole is therefore half that of its dipole counterpart, or

$$Z_{in,mono} = \frac{V_{in,mono}}{I_{in,mono}} = \frac{1}{2} \frac{V_{in,dipole}}{I_{in,dipole}} = \frac{1}{2} Z_{in,dipole} \quad (2.4.11)$$

This indeed is the result we have obtained with our more involved, roundabout approach.

CHAPTER 3 : EDGE DIFFRACTION

3.1. Introduction

In this chapter the two ray techniques to be used in the following chapter,namely the Uniform Geometrical Theory of Diffraction (UTD) and the extended UTD techniques are described. The description will be limited to the phenomenon of edge diffraction since this is the only mechanism important for our purposes.

3.2. Geometrical Theory of Diffraction

Consider the total high frequency field at any point exterior to the infinite perfectly conducting wedge shown in Fig.3.2.1. One well known high frequency method is Geometrical Optics(GO) [6]which would predict the field as

$$\bar{E} \sim \bar{E}^{GO} = \bar{E}^{in} u^{in} + \bar{E}^{re} u^{re} \quad (3.2.1)$$

where the symbol \sim means "asymptotically equal to";i.e., the approximation becomes more accurate as the frequency is increased. \bar{E}^{in} denotes the incident field or in other words the field of the primary source in the absence of the wedge; and u^{in} is an appropriate unit step function which, referring to Fig.3.2.1, equals unity in regions I and II and vanishes in region III,

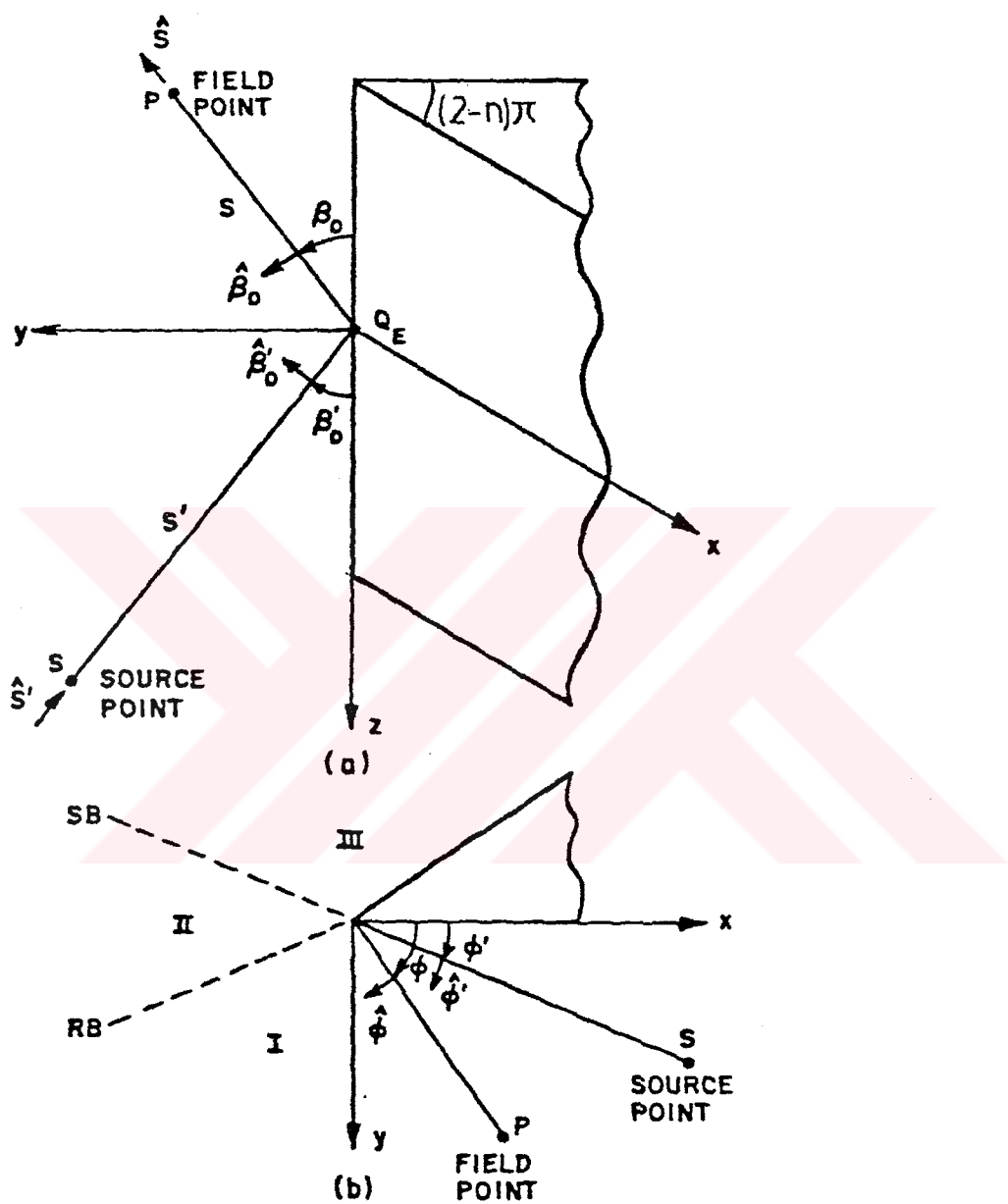


Figure 3.2.1 Wedge geometry for edge diffraction.

Likewise, \bar{E}^{re} denotes the reflected field, i.e., the image field were the $y=0$ face of the wedge infinite in extent. Again u^{re} is a unit step function which vanishes outside region I.

Obviously the field predicted by the GO is discontinuous across the boundaries of regions I, II and III, called the reflection shadow boundary (R.B) and the incident shadow boundary (S.B). This is evidence of errors in the GO which become more pronounced as the frequency is pulled lower. Note also that the GO predicts a null field in region III, known as the shadow region.

A generalization of the GO which systematically introduces diffracted rays was suggested in the 50's by J. B. Keller and his co-workers and is known as Geometrical Theory of Diffraction (GTD) [7,8,9]. The postulates of Keller's theory are:

1. The diffracted field propagates along ray paths that include points on the boundary surface. These ray paths obey the principle of Fermat, known also as the principle of shortest optical path.
2. Diffraction, like reflection and transmission, is a local phenomenon at high frequencies. That is, it depends only on the nature of the boundary surface and the incident field in the immediate neighborhood of the point of diffraction.

3. A diffraction wave propagates along its ray path so that
- power is conserved in a tube of rays, and
 - phase delay equals the wave number times the distance along the ray path.

In the GTD, the total high frequency field of the problem shown in Fig.3.2.1 is given by

$$\bar{E} \sim \bar{E}^{GO} + \bar{E}^d \quad (3.2.2)$$

where \bar{E}^d refers to the so called "edge diffracted field"; it is given by

$$\bar{E}^d = \bar{E}^i(Q_E) \cdot \bar{D} \cdot \sqrt{\frac{s'}{s(s+s')}} e^{-jks} \quad (3.2.3)$$

for spherical wave incidence, i.e., an incident field with a spherical wavefront.

Here Q_E is the so-called point of diffraction. It is a point on the edge determined by the condition $\beta_0 = \beta_0'$, a direct consequence of the generalized Fermat's principle. This principle states that the total path from the source to the point of observation, subject to the condition that one point on the edge be included in the path, is an extremum, in this case a minimum. The angles β_0 and β_0' are shown in Fig.3.2.1, as well as the angles ϕ , ϕ' , the distances s and s' and the unit vectors $\hat{\phi}$, $\hat{\phi}'$, $\hat{\beta}_0$, $\hat{\beta}_0'$, \hat{s} and \hat{s}' .

\tilde{D} is the so-called dyadic edge diffraction coefficient given by

$$\tilde{D} = -D_s \hat{\beta}_0' \hat{\beta}_0 - D_h \hat{\phi}_0' \hat{\phi}_0 \quad (3.2.4)$$

where D_s and D_h are the so-called soft and hard diffraction coefficients. They are functions of the aspect angles β_0 , ϕ and ϕ' but not a function of s or s' such that the diffracted field is a ray optical field.

The explicit formulas for D_s and D_h will not be given here since we will not use the GTD. Suffice it to say that among others, one drawback of the GTD is that it is not valid in regions adjacent to the SB and RB, known as transition regions. Specifically, as one approaches these boundaries, the diffraction coefficients and hence the diffracted field predicted by the GTD blows up. Obviously a more satisfactory theory would predict diffracted fields which are not only finite at these boundaries but which have discontinuities there which compensate those of the GO field.

3.3. Uniform Geometrical Theory of Diffraction (UTD)

The UTD is an extention of the GTD which overcomes the difficulties mentioned at the end of the previous section. The expressions given there are also valid in the UTD except that the diffraction coefficients differ from the GTD only in the transition

regions. The extent of these regions will become clear presently. The edge diffraction coefficients of the UTD are given by [10]

$$D_s(L, \phi, \phi') = \frac{-e^{-j(\pi/4)}}{2n\sqrt{2\pi k} \sin \beta_0} \cdot$$

$$[\cot(\frac{\pi+(\phi-\phi')}{2n}) F[kLa^+(\phi-\phi')] + \cot(\frac{\pi-(\phi-\phi')}{2n}) F[kLa^-(\phi-\phi')]$$

$$\mp \{ \cot(\frac{\pi+(\phi+\phi')}{2n}) F[kLa^+(\phi+\phi')] + \cot(\frac{\pi-(\phi+\phi')}{2n}) F[kLa^-(\phi+\phi')] \}]$$
(3.3.1)

where, if the argument of F is represented by X,

$$F(X) = 2j\sqrt{X} e^{jX} \int_{\sqrt{X}}^{\infty} e^{-j\tau^2} d\tau$$
(3.3.2)

$$L = \frac{s \cdot s'}{s+s'} \sin^2 \beta_0$$
(3.3.3)

for spherical wave incidence, and the factor a which is measure of the separation of the observation point from a SB or an RB is given by

$$a^\pm(\phi \pm \phi') = 2 \cos^2 \left[\frac{2\pi n N^\pm - (\phi \pm \phi')}{2} \right]$$
(3.3.4)

in which N^\pm are the integers which most nearly satisfy the four equations

$$2\pi n N^\pm - (\phi \pm \phi') = \pi$$
(3.3.5)

and

$$2\pi n N - (\phi \pm \phi') = -\pi \quad (3.3.6)$$

The factor n is related to the wedge angle as shown in Fig.3.2.1. In our problem involving a half-plane, we will take $n=2$. The function F defined in (3.3.2) is called the transition function. When its argument is small it is given approximately by

$$F(X) \approx \left[\sqrt{\pi X} - 2X \exp(j\frac{\pi}{4}) - \frac{2}{3}X^2 \exp(-j\frac{\pi}{4}) \right] \cdot \exp\left[j(\frac{\pi}{4}+X)\right] \quad (3.3.7)$$

and when X is large

$$F(X) \approx 1 + j\frac{1}{2X} - \frac{3}{4}X^{-2} \quad (3.3.8)$$

Note from (3.3.4) that the case of a zero argument for the transition function corresponds to the observation point being on either a shadow or a reflection boundary. In this case one of the cotangent factors in (3.3.1) blows up and the associated transition function vanishes. The resulting finite limits are different as one approaches the boundary from the two sides(lit and shadow), giving rise to a discontinuity in the diffraction coefficient and hence the diffracted field which exactly compensates the discontinuity in the GO field.

Note also that as its argument increases the transition function approaches unity. If in (3.3.1) all the transition functions are replaced by unity, the four terms can be rearranged to yield the same diffraction coefficients as those of the GTD. Hence, outside the transition regions UTD and GTD are identical, the definition of the transition regions being those regions adjacent to the S.B. and R.B. in which all four transition functions appearing in (3.3.1) can not be approximated by unity. Since the arguments of the transition functions involve s , the diffracted field is ray-optical only outside the transition regions. Inside the transition regions the dependence of the diffracted field is not simply as shown explicitly in (3.2.3), but more involved.

3.4 Extended UTD

As was mentioned in section 3.1, the most important high-frequency scattering mechanism(excluding those phenomena accounted for by geometrical optics, i.e., reflection and shadowing)is edge diffraction. Although the UTD solution for edge diffraction properly compensates all jump discontinuities in the geometrical optics, some components of the geometrical optics field have discontinuous derivatives across the shadow and reflection boundaries, which are not compensated by the UTD. These discontinuities are evidence of error. These errors become more pronounced as the frequency is decreased or the distances from the edge to the observation or

source points become moderate. The diffraction coefficients of UTD given in the previous section are such that only terms of order up to $k^{-1/2}$ have been retained.

An attempt to overcome these difficulties and improve the accuracy has resulted in the so-called extended UTD [1], in which terms of order $k^{-3/2}$ have been added to the solution. Improved accuracy has indeed been observed in numerical tests, especially in the case of a half-plane. Specifically in the case of plane-wave incidence on a half-plane, the expressions of the extended UTD are exact. We note also that the total field predictions of the extended UTD are not only continuous but continuous in derivative as well.

In the extended UTD, the components of the edge diffracted field are given by

$$\begin{aligned} \begin{bmatrix} E_{\beta_0}^d \\ E_{\phi}^d \\ E_s^d \end{bmatrix} &= \left\{ \begin{bmatrix} -D_s + D_1 & D_2 \\ D_3 & -D_h + D_4 \\ D_5 & D_6 \end{bmatrix} \begin{bmatrix} E_{\beta_0}^i(Q_E) \\ E_{\phi}^i(Q_E) \end{bmatrix} \right. \\ &\quad \left. + \begin{bmatrix} -d_s d_2 \\ d_3 - d_h \\ 0 \ 0 \end{bmatrix} \begin{bmatrix} aE_{\beta_0}^i(Q_E) \\ \frac{an'}{aE_{\phi}^i(Q_E)} \\ \frac{an'}{aE_{\phi}^i(Q_E)} \end{bmatrix} \right\} e^{-jks} \cdot \sqrt{\frac{s'}{s(s+s')}} \quad (3.4.1) \end{aligned}$$

where

$$D_1 = \frac{\cot^2 \beta_0}{jk} \left[\left(\frac{s+s'}{s'} \right) \frac{a}{as} - \frac{1}{2s} \right] . D_s . \frac{s+s'}{s'} \quad (3.4.2)$$

$$D_2 = -\frac{\cos \beta_0}{jks \sin^2 \beta_0} . \frac{s+s'}{s'} . \frac{aD_h}{a\phi} \quad (3.4.3)$$

$$D_3 = \frac{\cos \beta_0}{jks \sin^2 \beta_0} . \frac{s+s'}{s'} . \frac{aD_s}{a\phi} \quad (3.4.4)$$

$$D_4 = \frac{1}{jk \sin^2 \beta_0} \frac{s+s'}{s'} \left[\left(\frac{s+s'}{s'} \right) \frac{a}{as} - \frac{1}{2s} \right] . D_h \quad (3.4.5)$$

$$D_5 = \frac{\cot \beta_0}{jk} \left[\left(\frac{s+s'}{s'} \right) \frac{a}{as} - \frac{1}{2s} \right] . D_s \quad (3.4.6)$$

$$D_6 = -\frac{1}{jks \sin \beta_0} \frac{aD_h}{a\phi} \quad (3.4.7)$$

$$d_h = \frac{1}{jk \sin \beta_0} \frac{aD_h}{a\phi'} \quad (3.4.8)$$

$$d_s = \frac{1}{jk \sin \beta_0} \frac{aD_s}{a\phi'} \quad (3.4.9)$$

where d_h and d_s are hard and soft slope diffraction coefficients respectively.

$$d_2 = \frac{s \cot \beta_0}{jk} \left[\left(\frac{s+s'}{s'} \right) \frac{a}{as} - \frac{1}{2s} \right] . D_s \quad (3.4.10)$$

$$d_3 = -\frac{s \cot \beta_0}{jk} \left[\left(\frac{s+s'}{s'} \right) \frac{a}{as} - \frac{1}{2s} \right] . D_h \quad (3.4.11)$$

We will use these formulas for a hybrid approach in the following chapter.

All the terms appearing here and not in UTD, i.e., D_1 , D_2 , ... , D_6 , d_s , d_h , d_2 and d_3 are of order $k^{-3/2}$. Note that as opposed to the UTD, the extended UTD predicts a radial diffracted field component as well as transverse components. Note also that terms proportional to not only the field incident at the point of diffraction but also those proportional to the spatial derivative of the incident field appear in (3.4.1). Here,

$$\frac{a}{\sin'} = \hat{n}' \cdot \nabla \quad (3.3.12)$$

in which \hat{n}' is a unit vector normal to the plane of diffraction (the plane determined by the edge and the diffracted ray), pointing into the lit region.

CHAPTER 4 : HYBRID MM-GTD APPROACH

4.1 Introduction

In this chapter, the problem of the radiation by a monopole antenna mounted near the edge of a perfectly-conducting half-plane is considered. The geometry of the problem is illustrated in Fig.4.3.1.

In section 4.2., it is demonstrated how the edge diffraction mechanism can be incorporated into the moment of methods. The hybrid technique thus illustrated is employed in section 4.3 using the UTD and in section 4.4 using the extended UTD.

4.2 Combining the MM with ray techniques

Recall from chapter 2 that the m^{th} element of the generalized impedance matrix for a dipole radiating in free space was given by

$$Z_{mn} = \int_{-L/2}^{L/2} F_m(z) E_{zn}^s dz \quad (4.2.1)$$

in which $F_m(z)$ is the piecewise sinusoidal testing function defined in equation (2.3.2) and E_{zn}^s is the z-component of the field at the axis of the antenna due to the n^{th} basis function radiating in free-space. Recall also that E_{zn}^s was given in closed form in equation (2.2.4). Again referring to chapter 2, the mn^{th} element of the generalized impedance matrix for a monopole mounted on an infinite ground plane is similarly given by

$$Z_{mn} = \int_0^{L/2} F_m(z) E_{zn}^s dz \quad (4.2.2)$$

where this time E_{zn}^s is the z-component of the total field at the axis of the antenna radiating in the presence of the ground plane, i.e.

$$E_{zn}^s = E_{zn}^{\text{in}} + E_{zn}^{\text{re}} = E_{zn}^{\text{GO}} \quad (4.2.3)$$

Since we know from chapter 3 that the field of a source of ray-optical fields radiating in the presence of a wedge (in our case a half plane, $n=2$) is given by

$$E_z^s = E_z^{\text{GO}} + E_z^d \quad (4.2.4)$$

the generalized impedance matrix elements should again be given by (4.2.2), but with the total field due to the n^{th} basis function replaced by

$$E_{zn}^s(z) = E_{zn}^{GO}(z) + E_{zn}^d(z) \quad (4.2.5)$$

where $E_{zn}^d(z)$ is the diffracted component. Since the integral in (4.2.2) is obviously a linear operation we may write

$$Z'_{mn} = Z_{mn} + Z_{mn}^g \quad (4.2.6)$$

where Z'_{mn} is the impedance matrix of the problem of interest here (i.e., a monopole mounted near the edge of a half-plane), Z_{mn} is that of the problem studied in section 2.4 (i.e. a monopole mounted on an infinite ground plane) given in (2.4.5), (2.4.6), (2.4.7) and (2.4.8) and Z_{mn}^g is given by

$$Z_{mn}^g = \int_0^{L/2} F_m(z) E_{zn}^d dz \quad (4.2.7)$$

once these elements are calculated and the matrix in (4.2.6) is filled, the procedure for obtaining the unknown current coefficients and in turn finding the antenna input impedance is straightforward as described in chapter 2. In the following sections we shall employ first the UTD and then the extended UTD to find $E_{zn}^d(z)$.

4.3 MM-UTD

The field incident on the edge due to the n^{th} piecewise sinusoidal basis function is given by

$$E_z^{\text{in}}(Q) = \frac{-j30}{\sin(k\Delta z)} \left[\frac{e^{-jks'_{n-1}}}{s'_{n-1}} - 2 \cos(k\Delta z) \frac{e^{-jks'_n}}{s'_n} + \frac{e^{-jks'_{n+1}}}{s'_{n+1}} \right] \quad (4.3.1)$$

where s'_n , s'_{n-1} and s'_{n+1} are the distances from the edge to the mid-point, the lower and upper end points, respectively, of the n^{th} sub-section, i.e.,

$$s'_{n-1} = \sqrt{d^2 + z_{n-1}^2} \quad (4.3.2)$$

$$s'_n = \sqrt{d^2 + z_n^2} \quad (4.3.3)$$

and

$$s'_{n+1} = \sqrt{d^2 + z_{n+1}^2} \quad (4.3.4)$$

Recall that to find the diffracted field the UTD requires that the field incident on the edge be ray-optical. The field given in (4.3.1) is not ray-optical, but each of the three terms is (specifically they are spherical waves). Therefore while calculating the diffracted field we should consider each as a separate incident field and superpose the three resulting diffracted fields. But first some preliminaries; referring to Fig.4.3.1,

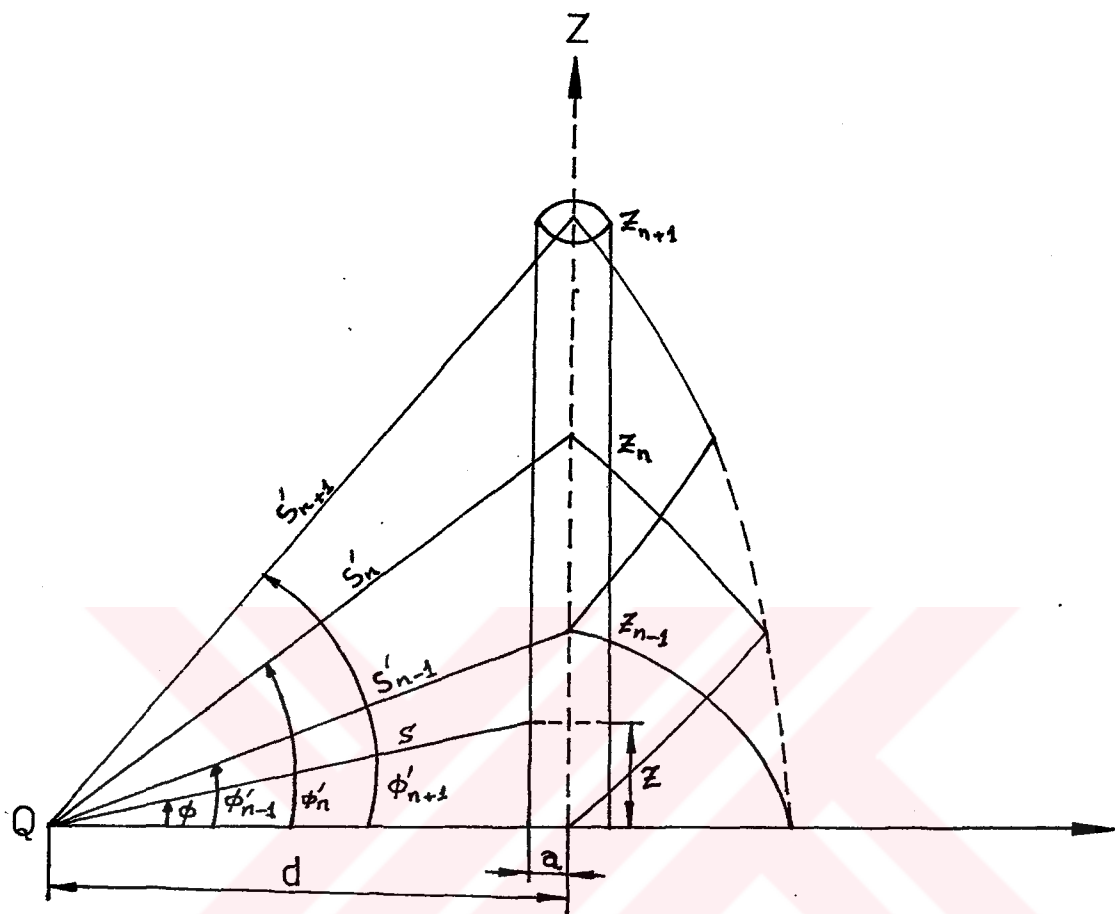


Figure 4.3.1 Monopole antenna mounted on a perfect ground half-plane.

$$s = \sqrt{d^2 + z^2} \quad (4.3.5)$$

$$\phi = \cos^{-1} \frac{d}{s} \quad (4.3.6)$$

$$\phi'_n = \cos^{-1} \frac{d}{s'_n} \quad (4.3.7)$$

Since the UTD diffracted field is given in a ray-fixed coordinate format, we also note that for each of the three spherical waves we have

$$E_{\phi}^d(z) = -E_{\phi'}^{in}(Q) \cdot D_h(\phi, \phi', s, s') \cdot \sqrt{\frac{s'}{s(s+s')}} \cdot e^{-jks} \quad (4.3.8)$$

$$E_{\phi'}^{in}(Q) = \frac{E_z^{in}(Q)}{\cos \phi'} \quad (4.3.9)$$

$$E_z^d(z) = E_{\phi}^d(Q) \cdot \cos \phi \quad (4.3.10)$$

resulting in

$$E_z^d(z) = -E_z^{in}(Q) \cdot \frac{\cos \phi}{\cos \phi'} D_h(\phi, \phi', s, s') \cdot \sqrt{\frac{s'}{s(s+s')}} \cdot e^{-jks} \quad (4.3.11)$$

Note that in the argument of the diffraction coefficient β_0 does not appear explicitly since the point of diffraction is always that point on the edge closest to the monopole, hence $\beta_0 = \pi/2$.

Incorporating all these, we have for the diffracted field at the axis of the monopole due to the n^{th} piecewise sinusoidal current distribution.

$$E_{zn}^d(z) = - \frac{j30}{\sin(k\Delta z)} \cdot$$

$$\begin{aligned}
 & \left[\frac{e^{-jks'_{n-1}}}{s'_{n-1} \cos \phi'_{n-1}} \cdot D_h(\phi, \phi'_{n-1}, s, s'_{n-1}) \cdot \sqrt{\frac{s'_{n-1}}{s(s+s'_{n-1})}} \right. \\
 & - 2 \cos(k\Delta z) \frac{e^{-jks'_n}}{s'_n \cos \phi'_n} \cdot D_h(\phi, \phi'_n, s, s'_n) \cdot \sqrt{\frac{s'_n}{s(s+s'_n)}} \\
 & \left. + \frac{e^{-jks'_{n+1}}}{s'_{n+1} \cos \phi'_{n+1}} \cdot D_h(\phi, \phi'_{n+1}, s, s'_{n+1}) \cdot \sqrt{\frac{s'_{n+1}}{s(s+s'_{n+1})}} \right] \cdot \\
 & \cos \phi \cdot e^{-jks} \\
 & \quad (4.3.12)
 \end{aligned}$$

Note that ϕ and s are functions of z while their primed counterparts are not. Once (4.3.12) is evaluated as a function of z , we can find the "diffracted component" of the impedance matrix as

$$Z_{mn}^g = \int_0^L F_m(z) E_{zn}^d dz \quad (4.3.13)$$

4.4 Hybrid MM-Extended UTD Method

In this section we explain hybrid moment method-extended UTD approach. We start by using the formulas which are introduced in chapter 3, section 4.

In our problem for a monopole mounted at or near a half-plane edge we have $\beta_0 = \pi/2$, therefore

$$D_1=D_2=D_3=D_5=0 \quad (4.4.1)$$

and

$$d_3=d_2=0 \quad (4.4.2)$$

$$\begin{aligned} \begin{bmatrix} E_{\beta_0}^d \\ E_{\phi}^d \\ E_S^d \end{bmatrix} &= \left\{ \begin{bmatrix} -D_s & 0 & E_{\beta_0}^i(Q_E) \\ 0 & -D_h + D_4 & E_{\phi}^i(Q_E) \\ 0 & D_6 & E_{\phi}^i(Q_E) \end{bmatrix} \right. \\ &+ \left. \begin{bmatrix} -d_s & 0 & aE_{\beta_0}^i(Q_E) \\ 0 & -d_h & \frac{an'}{aE_{\phi}^i(Q_E)} \\ 0 & 0 & \frac{an'}{aE_{\phi}^i(Q_E)} \end{bmatrix} \right\} e^{-jks} \cdot \sqrt{\frac{s'}{s(s+s')}} \quad (4.4.3) \end{aligned}$$

second part of the right side of the above expression vanishes; then we have

$$\begin{aligned} \begin{bmatrix} E_{\beta_0}^d \\ E_{\phi}^d \\ E_S^d \end{bmatrix} &= \left\{ \begin{bmatrix} -D_s & 0 & E_{\beta_0}^i(Q_E) \\ 0 & -D_h + D_4 & E_{\phi}^i(Q_E) \\ 0 & D_6 & E_{\phi}^i(Q_E) \end{bmatrix} \right. \\ &\left. e^{-jks} \cdot \sqrt{\frac{s'}{s(s+s')}} \right\} \quad (4.4.4) \end{aligned}$$

Now we may write

$$E_{\phi}^d = (-D_h + D_4) E_{\phi}^i(Q_E) e^{-jks} \cdot \sqrt{\frac{s'}{s(s+s')}} \quad (4.4.5)$$

$$E_s^d = D_6 E_{\phi}^i(Q_E) e^{-jks} \cdot \sqrt{\frac{s'}{s(s+s')}} \quad (4.4.6)$$

The z-components of these fields are from Figure 4.4.1

$$E_z^d = E_{\phi}^d \cos \phi + E_s^d \sin \phi \quad (4.4.7)$$

$$E_z^d = (-D_h + D_4) E_{\phi}^i(Q_E) e^{-jks} \cdot \sqrt{\frac{s'}{s(s+s')}} \cos \phi$$

$$+ D_6 E_{\phi}^i(Q_E) e^{-jks} \cdot \sqrt{\frac{s'}{s(s+s')}} \sin \phi \quad (4.4.8)$$

where

$$E_{\phi}^i(Q) = \frac{E_z^i(Q)}{\cos \phi} \quad (4.4.9)$$

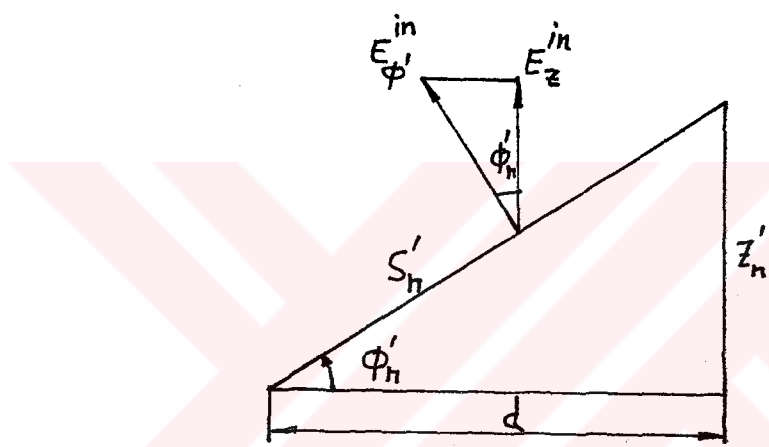
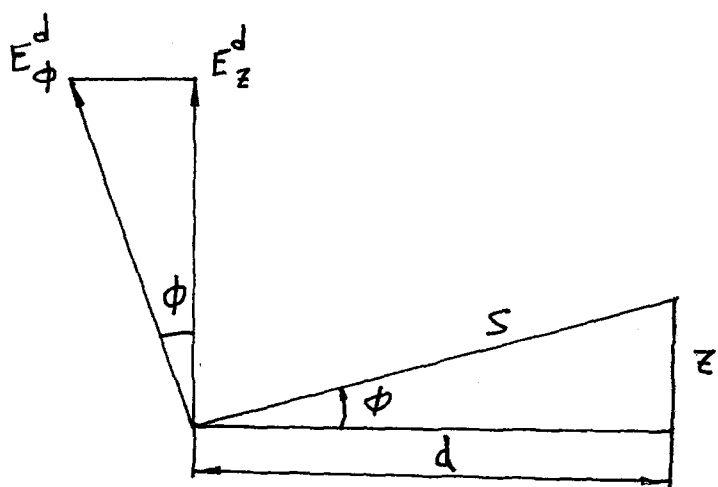


Figure 4.4.1 Monopole antenna mounted on a perfect ground half-plane showing fields.

And as in the previous section, each term of the incident field given in (4.3.1) is treated separately yielding

$$E_{zn}^d(z) = \frac{j30}{\sin(k\Delta z)} .$$

$$\begin{aligned}
 & \left[\frac{e^{-jks'n-1}}{s'n-1 \cos \phi'n-1} \cdot [-D_h(\phi, \phi'n-1, s, s'n-1) + D_4(\phi, \phi'n-1, s, s'n-1)] \right] \cdot \sqrt{\frac{s'n-1}{s(s+s'n-1)}} \\
 & - 2\cos(k\Delta z) \frac{e^{-jks'n}}{s'n \cos \phi'n} \cdot [-D_h(\phi, \phi'n, s, s'n) + D_4(\phi, \phi'n, s, s'n)] \cdot \sqrt{\frac{s'n}{s(s+s'n)}} \\
 & + \frac{e^{-jks'n+1}}{s'n+1 \cos \phi'n+1} \cdot [-D_h(\phi, \phi'n+1, s, s'n+1) + D_4(\phi, \phi'n+1, s, s'n+1)] \cdot \sqrt{\frac{s'n+1}{s(s+s'n+1)}} \cdot \\
 & \quad \cos \phi \cdot e^{-jks} \\
 & \left[\frac{e^{-jks'n-1}}{s'n-1 \cos \phi'n-1} \cdot [D_5(\phi, \phi'n-1, s, s'n-1)] \right] \cdot \sqrt{\frac{s'n-1}{s(s+s'n-1)}} \\
 & - 2\cos(k\Delta z) \frac{e^{-jks'n}}{s'n \cos \phi'n} \cdot [D_5(\phi, \phi'n, s, s'n)] \cdot \sqrt{\frac{s'n}{s(s+s'n)}} \\
 & + \frac{e^{-jks'n+1}}{s'n+1 \cos \phi'n+1} \cdot [D_5(\phi, \phi'n+1, s, s'n+1)] \cdot \sqrt{\frac{s'n+1}{s(s+s'n+1)}} \cdot \\
 & \quad \sin \phi \cdot e^{-jks}
 \end{aligned}$$

(4.4.10)

Again, the elements Z_{mn}^g are calculated using

(4.4.6). Now we need to find D_4 and D_6 .

We have [10,11]

$$D_n(\phi, \phi', s, s') = \frac{-e^{-j(\pi/4)}}{2n\sqrt{2\pi k} \sin \beta_0}$$

$$\begin{aligned} & [\cot(\frac{\pi+(\phi-\phi')}{2n}) F[kLa^+(\phi-\phi')] + \cot(\frac{\pi-(\phi-\phi')}{2n}) F[kLa^-(\phi-\phi')]] \\ & + \{ \cot(\frac{\pi+(\phi+\phi')}{2n}) F[kLa^+(\phi+\phi')] + \cot(\frac{\pi-(\phi+\phi')}{2n}) F[kLa^-(\phi+\phi')]\} \end{aligned} \quad (4.4.11)$$

where, if the argument of F is represented by X,

$$F(X) = 2j \sqrt{X} e^{jX} \int_{\sqrt{X}}^{\infty} e^{-j\tau^2} d\tau \quad (4.4.12)$$

$$X = kLa^\pm(\phi \pm \phi') = k \frac{ss'}{s+s'} a^\pm(\phi \pm \phi') \quad (4.4.13)$$

$$a^\pm(\phi \pm \phi') = 2 \cos^2[\frac{2\pi n N^\pm - (\phi \pm \phi')}{2}] \quad (4.4.14)$$

in which N^\pm are the integers which most nearly satisfy the four equations

$$2\pi n N^+ - (\phi \pm \phi') = \pi \quad (4.4.15)$$

and

$$2\pi n N^- - (\phi \pm \phi') = -\pi \quad (4.4.16)$$

A subroutine computes the wedge transition function which is given in (4.4.12).

When X is small

$$F(X) \cong [\sqrt{\pi X} - 2X \exp(j\frac{\pi}{4}) - \frac{2}{3}X^2 \exp(-j\frac{\pi}{4})] \cdot \exp[j(\frac{\pi}{4} + X)] \quad (4.4.17)$$

and when X is large

$$F(X) \cong 1 + j\frac{1}{2X} - \frac{3}{4}X^{-2} \quad (4.4.18)$$

When $0.3 < X < 5.5$ a linear interpolation scheme is used such that

$$F(X) = F(X_i) + (F(X_{i+1}) - F(X_i)) \frac{(X - X_i)}{(X_{i+1} - X_i)} \quad (4.4.19)$$

where the $F(X_i), \frac{F(X_{i+1}) - F(X_i)}{(X_{i+1} - X_i)}$ and X_i are tabulated.

when $X < 0$

$$F(X) = F^*(|X|)$$

where the * indicates the complex conjugate.

For D_4 we should differentiate $D_h(\phi, \phi', s, s')$ w.r.t s , this means we should differentiate $F(X)$ w.r.t s . We may use either an analytical method or an approximation method. First we start by the analytical method.

$$\frac{\partial F(X)}{\partial s} = \frac{\partial F(X)}{\partial X} \frac{\partial X}{\partial s} \quad (4.4.20)$$

$$X = kLa^\pm(\phi \pm \phi') = k \frac{ss'}{s+s'} a^\pm(\phi \pm \phi') \quad (4.4.21)$$

after some manipulation we have

$$\frac{\partial X}{\partial s} = X \frac{s'}{s(s+s')} \quad (4.4.22)$$

and

$$\frac{\partial F(X)}{\partial X} = \frac{1}{2X} F(X) + jF(X) - j \quad (4.4.23)$$

$$\frac{\partial F(X)}{\partial s} = [\frac{1}{2X} F(X) + jF(X) - j] \cdot X \frac{s'}{s(s+s')} \quad (4.4.24)$$

Now the approximation method:

When X is large we have

$$F(X) \approx (1 + j\frac{1}{2X} - \frac{3}{4}X^{-2}) \quad (4.4.25)$$

the result of derivative is then

$$\frac{dF(X)}{ds} = \frac{s'}{2s(s+s')} \left(\frac{-j}{X} + \frac{3}{X^2} \right) \quad (4.4.26)$$

when X is small we have

$$F(X) = \left[\sqrt{\pi X} - 2X \exp(j\frac{\pi}{4}) - \frac{2}{3}X^2 \exp(-j\frac{\pi}{4}) \right] \cdot \exp[j(\frac{\pi}{4}+X)] \quad (4.4.27)$$

and

$$\frac{dF(X)}{ds} = \left\{ \left[\frac{\sqrt{\pi X}}{2} - 2X \exp(j\frac{\pi}{4}) - \frac{4}{3}X^2 \exp(-j\frac{\pi}{4}) \right] \cdot \exp[j(\frac{\pi}{4}+X)] + jXF(X) \right\} \frac{s'}{s(s+s')} \quad (4.4.28)$$

When $0.3 < X < 5.5$ a linear interpolation scheme is used such that

$$F(X) = F(X_i) + (F(X_{i+1}) - F(X_i)) \frac{(X-X_i)}{(X_{i+1}-X_i)} \quad (4.4.29)$$

$$\frac{dF(X)}{ds} = \frac{F(X_{i+1}) - F(X_i)}{(X_{i+1}-X_i)} \times \frac{s'}{s(s+s')} \quad (4.4.30)$$

while differentiating $F(X)$ w.r.t s , we can differentiate D_h and calculate D_4 . This is done in a subroutine which is enclosed in appendix c.

For calculating D_6 we need to differentiate $F(X)$ w.r.t. ϕ .

we know from (4.4.11) that D_h is

$$D_h(\phi, \phi', s, s') = \frac{-e^{-j(\pi/4)}}{2n\sqrt{2\pi k} \sin \beta_0}$$

$$\left[\cot\left(\frac{\pi + (\phi - \phi')}{2n}\right) F[kLa^+(\phi - \phi')] + \cot\left(\frac{\pi - (\phi - \phi')}{2n}\right) F[kLa^-(\phi - \phi')]\right]$$

$$+ \left\{ \cot\left(\frac{\pi + (\phi + \phi')}{2n}\right) F[kLa^+(\phi + \phi')] + \cot\left(\frac{\pi - (\phi + \phi')}{2n}\right) F[kLa^-(\phi + \phi')]\right\}$$

$$\frac{\partial F(X)}{\partial \phi} = \frac{\partial F(X)}{\partial X} \frac{\partial X}{\partial \phi} \quad (4.4.31)$$

we know

$$X = kLa^\pm(\phi \pm \phi') \quad (4.4.32)$$

$$a^\pm(\phi \pm \phi') = 2 \cos^2\left[\frac{2n\pi N^\pm - (\phi \pm \phi')}{2}\right] \quad (4.3.33)$$

therefore we have

$$\frac{\partial X}{\partial \phi} = kL \frac{\partial}{\partial \phi} a^\pm(\phi \pm \phi')$$

or

$$\frac{\partial X}{\partial \phi} = X \tan\left[\frac{2n\pi N^\pm - (\phi \pm \phi')}{2}\right] \quad (4.4.34)$$

therefore

$$\frac{\partial F(X)}{\partial \phi} = \frac{\partial F(X)}{\partial X} X \tan\left[\frac{2n\pi N^\pm - (\phi \pm \phi')}{2}\right] \quad (4.4.35)$$

according to above formulas we know the first part of second side of this formula.

$$\text{By using } \frac{\partial}{\partial X} \cot x = -(1 + \cot^2 x) = -\frac{1}{\cos^2 x}$$

we may write derivative of D_h as follows

$$\begin{aligned}
\frac{\partial D_n}{\partial \phi} &= \frac{-e^{-j(\pi/4)}}{2n \sqrt{2\pi k} \sin \beta_0}, \\
&+ \left[\frac{-1}{2n \cos^2 \left(\frac{\pi + (\phi - \phi')}{2n} \right)} \cdot F[kLa^+(\phi - \phi')] \right] \\
&\quad + \cot \left(\frac{\pi + (\phi - \phi')}{2n} \right) \cdot \frac{\partial}{\partial X} F[kLa^+(\phi - \phi')] \\
&+ \left[\frac{1}{2n \cos^2 \left(\frac{\pi - (\phi - \phi')}{2n} \right)} \cdot F[kLa^-(\phi - \phi')] \right] \\
&\quad + \cot \left(\frac{\pi - (\phi - \phi')}{2n} \right) \cdot \frac{\partial}{\partial X} F[kLa^-(\phi - \phi')] \\
&+ \left[\frac{-1}{2n \cos^2 \left(\frac{\pi + (\phi + \phi')}{2n} \right)} \cdot F[kLa^+(\phi + \phi')] \right] \\
&\quad + \cot \left(\frac{\pi + (\phi + \phi')}{2n} \right) \cdot \frac{\partial}{\partial X} F[kLa^+(\phi + \phi')] \\
&+ \left[\frac{1}{2n \cos^2 \left(\frac{\pi - (\phi + \phi')}{2n} \right)} \cdot F[kLa^-(\phi + \phi')] \right] \\
&\quad + \cot \left(\frac{\pi - (\phi + \phi')}{2n} \right) \cdot \frac{\partial}{\partial X} F[kLa^-(\phi + \phi')]
\end{aligned}$$

(4.4.36)

With this expression and using (4.4.8) we can calculate D_6 using an appropriate subroutine.

CHAPTER 5 : COMPARISON OF RESULTS

The first numerical result we obtained was to check the basic moment method program. For this purpose we calculated the input impedance of a dipole of length $\lambda/2$ radiating in free space. The radius of the wire is 0.001λ . The dipole was separated into 5 sections (the number which appears as N in the text). The weighting integrals which appear in chapter 2 (Eq. (2.2.10)) were evaluated using Simson's rule using 17 points. The value we obtained for the input impedance is $82.98+j41.93 \Omega$ compared to the value found in the literature [13] of $82.95 +j41.91 \Omega$. This corresponds to an error in magnitude of 0.03%.

The next step was to calculate the input impedance of a monopole of length $\lambda/4$ mounted on a ground plane as described in section 2.4. The result is $41.49+j20.96 \Omega$, as expected one-half the result obtained for the corresponding dipole in free-space.

Finally the input impedance of a monopole mounted in the vicinity of the edge of a half-plane is considered. The wire radius 0.001λ , the length of the monopole is $\lambda/4$. The input impedance is calculated for d , the edge-monopole distance

ranging from 0 to λ . The results obtained from the hybrid MM-UTD method and the MM-extended UTD method as well as that obtained using the MM along with the exact Green's function for a half-plane are shown in figures 5.1.1, 5.1.2, 5.1.3 and 5.1.4. In each case two subsections were used and the necessary numerical integrals were evaluated using 10 Simpson intervals. Note the excellent agreement between the MM-extended UTD method and the MM using the exact Green's function. Observe also that the MM-UTD results are excellent at moderately larger distances but not at small distances, as expected.

*Input Resistance of $\lambda/4$ Monopole versus
distance d from edge of half-plane*

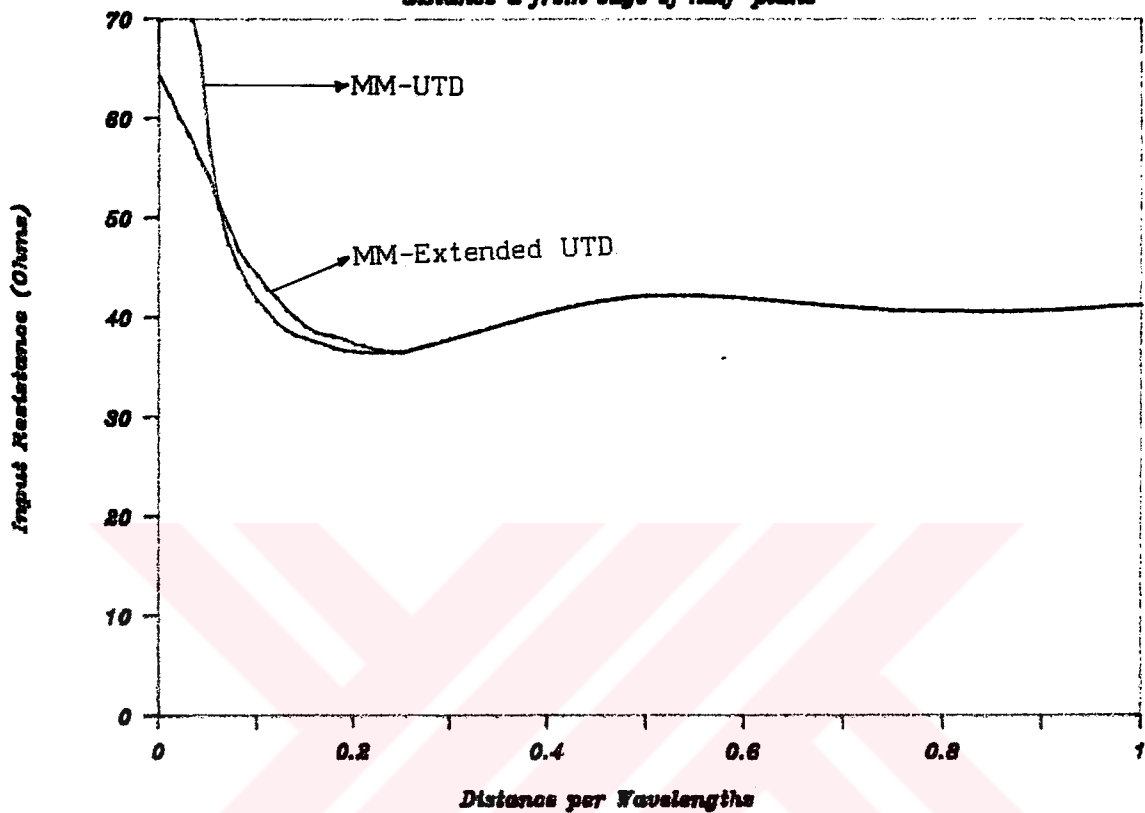


Fig. 5.1.1. Input resistance of $\lambda/4$ monopole versus distance d from edge of half-plane computed using MM-UTD and MM-Extended UTD.

*Input Reactance of $\lambda/4$ Monopole versus
distance d from edge of half-plane*

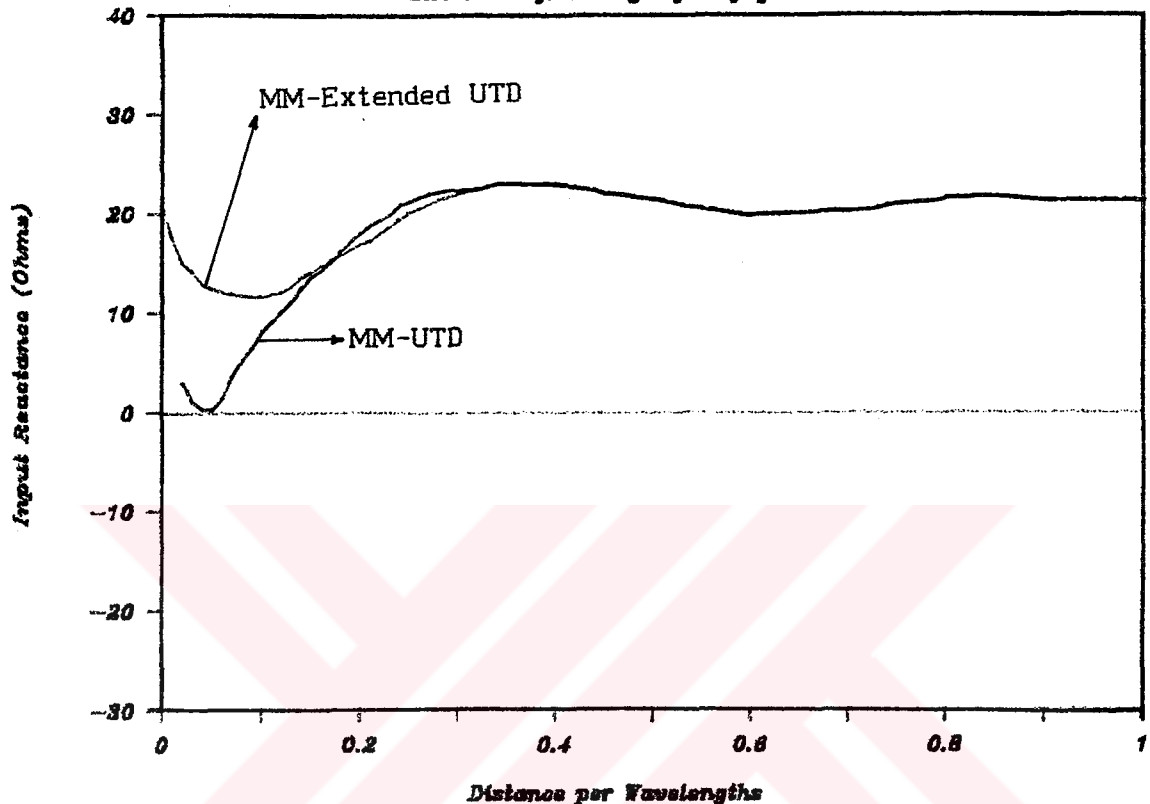


Fig. 5.1.2. Input reactance of $\lambda/4$ monopole versus
distance d from edge of half-plane computed
using MM-UTD and MM-Extended UTD.

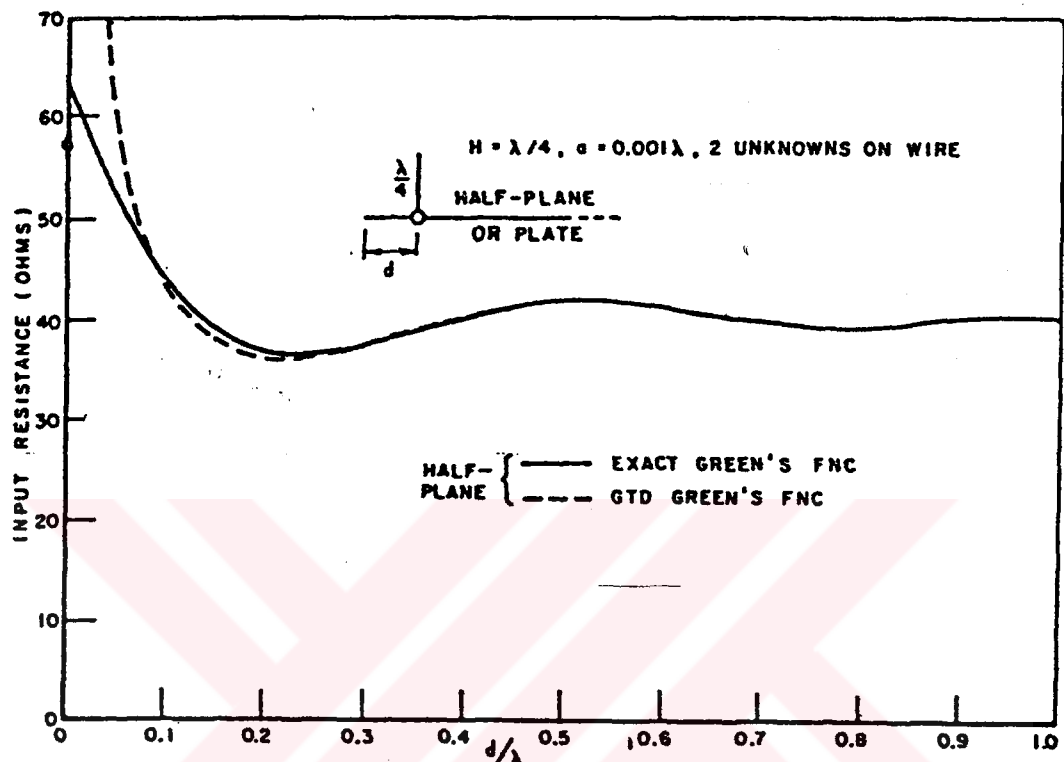


Fig. 5.1.3. Input resistance of $\lambda/4$ monopole versus distance d from edge of half-plane computed using exact Green's function and UTD Green's function.

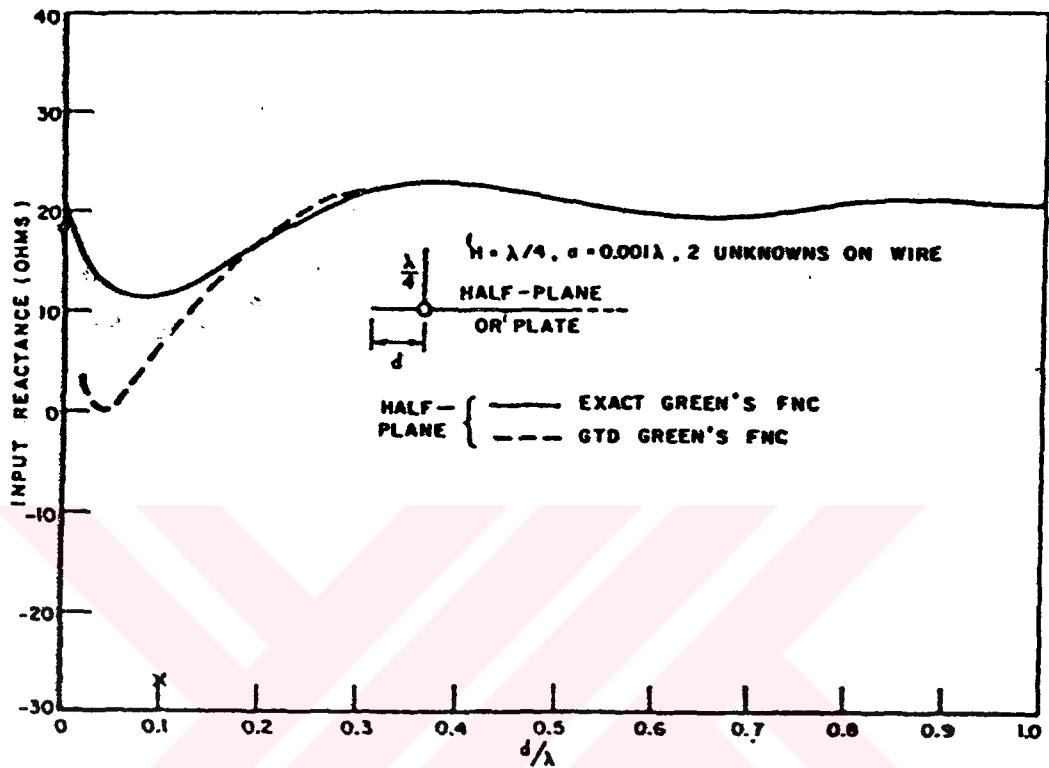


Fig. 5.1.4. Input reactance of $\lambda/4$ monopole versus distance d from edge of half-plane computed using exact Green's function and UTD Green's function.

CHAPTER 6: CONCLUSION

In this thesis we have shown how the method of moments (a low-frequency method) can be combined with ray techniques such as the UTD or the extended UTD (high-frequency methods). The hybrid technique is demonstrated to encompass a higher class of problems than possible with either MM or ray-techniques alone.

The problem of calculating the input impedance of a monopole antenna mounted near the edge of a perfectly conducting half-plane was considered in the context of hybrid techniques. Both the MM-UTD and the MM-extended UTD techniques were used as described in chapter 4.

As shown in chapter 5, the MM-UTD hybrid technique (recall that the UTD is accurate to order $k^{-1/2}$) was found to yield excellent results down to a value of 0.3λ for the monopole-edge separation. In contrast, the MM-extended UTD technique (the extended UTD is accurate to order $k^{-3/2}$) surprisingly yields accurate results down to zero separation. As a result this thesis may be considered as not only an exercise in combining two distinct methods, but also a testimony to the accuracy of the extended UTD.

REFERENCES

1. O.M. Buyukdura, "Radiation from sources and scatterers near the edge of a perfectly conducting wedge", PhD. dissertation, 1984.
2. David M. POZAR and Edward H. Newman, " Analysis of a Monopole Mounted near or at the Edge of a Half-Plane," IEEE Transactions on Antennas and Propagation, vol. AP-29, No.3, MAY 1981.
3. Gary A. Thiele and T. H. Newhous, "A Hybrid Technique for Combining Moment Methods with the Geometrical Theory of Diffraction," IEEE Transactions on Antennas and Propagation, vol. AP-23, No.1 January 1975.
4. Warren L. Stutzman and Gary A. Thiele, 1981, "Antenna Theory and Design." John Wily & Sons, Inc.
5. R. W. P. King, The Theory of Linear Antenna, Harvard University Press, Cambridge, 1956.
6. M. Born and E. Wolf, "Principles of Optics," 1970.
7. J. B. Keller, "Geometrical theory of diffraction," J. Opt. Soc. of Am., Vol. 52, pp. 116-130, 1962.

8. L. M. Graves, Editor, "A geometrical theory of diffraction," in Calculus of Variations and its Applications, McGraw Hill, 1958; pp. 27-52.
9. G. L. James, Geometrical Theory of Diffraction, Peter Peregrinus Ltd., England, 1976.
10. R. G. Kouyoumjian and P. H. Pathak, " A uniform geometrical theory of diffraction for an edge in a perfectly conducting surface," Proc. IEEE, Vol. 62, pp. 1448-1461, 1974.
11. R. G. Kouyoumjian, "Asymtotic High-Frequency Methods," Proc. IEEE, vol. 53, pp. 864-876, Aug. 1965.
12. R. G. Kouyoumjian, "The geometrical theory of diffraction and its application," in Numerical and Asymptotic Techniques in Electromagnetics, Springer-Verlag, New York, 1975.
13. R. S. Elliot, Antenna Theory and Design, Prentice-Hall, Inc., Englewood Cliffs, N.J., 1981.



APPENDICES

```

C*
C* ***** M O M E N T   M E T H O D   P R O G R A M   F O R   A   C E N T E R - F E D   D I P O L E   W I T H   D E L T A - G A P ****
C*   * V O L T A G E   G E N E R A T O R . *
C*   * T H I S   C O M P U T E R   P R O G R A M   U S E S   P I E C E W I S E   S I N U S O I D A L   B A S I S   *
C*   * F U N C T I O N S   A N D   G A L E R K I N ' S   M E T H O D   T O   A N A L Y S E   A   C E N T E R - F E D   *
C*   * L I N E A R   D I P O L E . A   G E N E R A L   S U B R O U T I N E   F O R   I N V E R S I O N   O F   A   *
C*   * C O M P L E X   M A T R I X   I S   I N C L U D E D . *
C*   * T H E   V A R I A B L E S   I N   T H E   M A I N   P R O G R A M   A R E : *
C*   *          A = R A D I U S   O F   W I R E   I N   W A V E L E N G T H S   *
C*   *          N = N U M B E R   O F   S E G M E N T S   ( O D D )   *
C*   *          L = L E N G T H   O F   T H E   D I P O L E   I N   W A V E L E N G T H S   *
C*   *          N I N T = N U M B E R   O F   S I M P S O N S ' S   R U L E   D I V I S I O N   *
C*   *
C*   *
C*   *
C*   ***** D I M E N S I O N   Z M A G ( 1 5 ) , Z P H A S E ( 1 5 ) *
REAL L,LL,LLP,IMAX,ZINMAG,ZINPHA
REAL IMAG(15),IPHASE(15)
COMPLEX I(15),V(15),J,ZZ(5,5),ZIN,IIN
COMPLEX INGRLK,KERNEL
COMPLEX IZ(15),ZLOAD
COMMON/ARRAY/IZ,V
COMMON /CNSTNS/J,B2,A2,B
OPEN(UNIT=5,FILE='D1.DAT',STATUS='OLD')
OPEN(UNIT=6,FILE='DUT7.DAT',STATUS='NEW')
DATA DEGRAD,RADDEG/.0174532,57.29577/
READ(5,1000) A,N,L,NINT
1000 FORMAT(F6.4,I2,F4.2,I2,2X)
WRITE(6,10) N,L,A,NINT
10 FORMAT(1H1,26X,'INPUT PARAMETERS'//1H ,25X,'N=' ,I3,' SEGMENTS' ,
      //1H ,25X,'L=' ,F5.2,' WAVELENGTHS'//1H ,25X,'A=' ,F9.6,' WAVELENGTH
      *S'//25X,'NINT=' ,I3//1H ,15X,'IMPEDANCE MATRIX Z(IJ,JJ)'//1H ,3X,
      *'N' ,2X,'REAL' ,5X,'IMAGINARY' /)
NP02P1=N/2+1
DZ=L/(N+1)
PI=3.14159265
J=(0.,1.)
B=2.*PI
B2=B*B
A2=A*A
M=N
ZMM=-0.5*L
Z=ZMM+DZ
C* FILL THE IMPEDANCE AND VOLTAGE MATRICES
DO 600 II=1,M
ZM=ZMM+DZ
ZMP=ZMM+2.*DZ
ZNM=-.5*L
DO 100 JJ=1,N
ZN=ZNM+DZ
ZNP=ZNM+2.*DZ
C* CALL INGRLK(NINT,ZMM,ZM,ZMP,ZNM,ZN,ZNP)
IF(II.EQ.1)GO TO 350

```

```

      IF(II.EQ.NN.AND.JJ.EQ.MM) GO TO 351
      IF(II.EQ.MM+1.AND.JJ.EQ.NN+1) GO TO 351
350  ZZ(II,JJ)=INGRLK(NINT,ZMM,ZM,ZMP,ZNM,ZN,ZNP,A)
      GO TO 352
351  ZZ(II,JJ)=ZZ(MM,NN)
352  MM=II
      NN=JJ
100  ZMM=ZN
      ZM=ZM
600  CONTINUE
C*   WRITE OUT INPUT PARAMETERS AND IMPEDANCE MATRIX
      DO 250 II=1,N
      WRITE(6,20) II,(ZZ(II,JJ),JJ=1,N)
20    FORMAT(2X,I3,1X,3(F6.2,'+j',F6.1,1X)/4(F6.2,'+j',F6.1,1X)/1)
      250 CONTINUE
C*   CALL COMPLEX MATRIX SOLVING SUBROUTINE
      CALL LINEQ(ZZ,N)
      WRITE(6,35)
35    FORMAT(//15X,'INVERSION OF COMPLEX MATRIX',//15X,'NN=1',10X,'NN=2
     *10X,'NN=3')
      DO 1250 II=1,N
      WRITE(6,120) II,(ZZ(II,JJ),JJ=1,N)
120   FORMAT(2X,I3,1X,3(F6.4,'+j',F6.4,1X)/4(5X,4(F6.4,'+j',F6.4,1X)/1)
     *5X,3(F6.4,'+j',F6.4,1X)/5X,2(F6.4,'+j',F6.4,1X))
      1250 CONTINUE
C*   COMPUTE INPUT IMPEDANCE
      DO 203 II=1,N
      V(II)=(0.,0.)
      IF (II.EQ.NP02P1) V(II)=(1.,0.)
      203 CONTINUE
C*   WRITE OUT VOLTAGE VECTOR
      WRITE(6,130)
130   FORMAT(1H //1H //,15X,'VOLTAGE VECTOR V(N)'//1H ,4X,'N',5X,'REAL
     *,2X,'IMAGINARY')
      DO 310 KK=1,N
      310 WRITE(6,140) KK,V(KK)
140   FORMAT(1H ,2X,I3,4X,F6.3,' + j ',7X,F6.3)
C*   COMPUTE CURRENT VECTOR I(II)
      DO 666 II=1,N
      DO 667 JJ=1,N
      I(II)=I(II)+ZZ(II,JJ)*V(JJ)
      667 CONTINUE
      IMAG(II)=1000.*CABS(I(II))
      SS2=REAL(I(II))
      SS1=AIMAG(I(II))
      SS3=SS1/SS2
      IPHASE(II)=RADDEG*ATAN(SS3)
666  CONTINUE
      MP=NP02P1
      IIN=I(MP)
      V(MP)=(1.,0.)
      ZIN=V(MP)/IIN
C*   ZIN(MP)=ZIN(MP)+ZLOAD
C*   WRITE OUT CURRENT VECTOR
      WRITE(6,30)

```

```

30 FORMAT(1H //1H //,20X,'CURRENT VECTOR I(N)''/1H ,8X,'N',2X,'REAL
     ',4X,'IMAGINARY',4X,'MAGNITUDE (mA)',2X,'IPHASE')
     DO 300 KK=1,N
     WRITE(6,40) KK,I(KK),IMAG(KK),IPHASE(KK)
40 FORMAT(1H ,6X,I3,2X,F6.4,' + j ',F6.4,5X,F9.5,7X,F9.5)
300 CONTINUE
ZINMAG=CABS(ZIN)
S2=REAL(ZIN)
S1=AIMAG(ZIN)
S=S1/S2
ZINPHA=RADDEG*ATAN(S)
WRITE(6,444) ZIN,ZINMAG,ZINPHA
444 FORMAT(//5X,* INPUT IMPEDANCE =',F11.2,' + j ',F11.2,1X,'*'//8X,'['
     *1X,'ZINMAG =',F11.2,2X,', ZINPHASE =',F11.2,1X,']')
STOP
END
C* THIS SUBROUTINE USES SIMPSON'S RULE TO NUMERICALLY INTEGRATE
C* FOR IMPEDANCE ELEMENTS USING EQUATION(2.3.12)
COMPLEX FUNCTION INGRLK(NINT,ZMM,ZM,ZMP,ZNM,ZN,ZNP,A)
COMPLEX K1,K2,S1,S2,HALF1,HALF2,INGRL1,INGRL2,J
COMMON/CNSTNS/J,B2,A2,B
H1=(ZM-ZMM)/NINT
H2=(ZMP-ZM)/NINT
H102=0.5*H1
H202=0.5*H2
S1=(0.,0.)
S2=S1
CALL KERNEL(K1,K2,ZMM,ZM,ZMP,ZNM,ZN,ZNP,ZMM+H102,ZM+H202,A)
HALF1=K1
HALF2=K2
NINTM1=NINT-1
DO 100 I=1,NINTM1
Z1=ZMM+I*H1
Z2=ZM+I*H2
CALL KERNEL(K1,K2,ZMM,ZM,ZMP,ZNM,ZN,ZNP,Z1,Z2,A)
S1=S1+K1
S2=S2+K2
CALL KERNEL(K1,K2,ZMM,ZM,ZMP,ZNM,ZN,ZNP,Z1+H102,Z2+H202,A)
HALF1=HALF1+K1
100 HALF2=HALF2+K2
INGRL1=4.*HALF1+2.*S1
INGRL2=4.*HALF2+2.*S2
CALL KERNEL(K1,K2,ZMM,ZM,ZMP,ZNM,ZN,ZNP,ZMM,ZM,A)
INGRL1=INGRL1+K1
INGRL2=INGRL2+K2
CALL KERNEL(K1,K2,ZMM,ZM,ZMP,ZNM,ZN,ZNP,ZM,ZMP,A)
INGRL1=H1*(INGRL1+K1)/6.
INGRL2=H2*(INGRL2+K2)/6.
INGRLK=INGRL1+INGRL2
RETURN
END
C* THIS SUBROUTIN COMPUTES VALUES OF INTEGRAND IN EQUTION (2.3.12)
SUBROUTINE KERNEL(K1,K2,ZMM,ZM,ZMP,ZNM,ZN,ZNP,Z1,Z2,A)
COMPLEX K1,K2,J
COMMON/CNSTNS/J,B2,A2,B

```

```

Z12=Z1#Z1
Z22=Z2#Z2
DZM=ZMP-ZM
DZN=ZNP-ZN
RNH1=SQRT(A2+(Z1-ZNM)*(Z1-ZNM))
RN1=SQRT(A2+(Z1-ZN)*(Z1-ZN))
RNP1=SQRT(A2+(Z1-ZNP)*(Z1-ZNP))
RNM2=SQRT(A2+(Z2-ZNM)*(Z2-ZNM))
RN2=SQRT(A2+(Z2-ZN)*(Z2-ZN))
RNP2=SQRT(A2+(Z2-ZNP)*(Z2-ZNP))
K1=30.*J1(CEXP(-J*B*RNH1)/RNH1-2.*COS(B*DZN)*CEXP(-J*B*RN1)/RN1+
*CEXP(-J*B*RNP1)/RNP1)/SIN(B*DZN)
K2=30.*J1(CEXP(-J*B*RNH2)/RNH2-2.*COS(B*DZN)*CEXP(-J*B*RN2)/RN2+
*CEXP(-J*B*RNP2)/RNP2)/SIN(B*DZN)
K1=K1*SIN(B*(Z1-ZNM))/SIN(B*DZN)
K2=K2*SIN(B*(ZMP-Z2))/SIN(B*DZN)
RETURN
END
C* INVERSION OF A COMPLEX MATRIX ZZ, OF ORDER N, INVERSE IS RETURNED
C* IN PLACE OF ZZ
SUBROUTINE LINEQ(ZZ,N)
COMPLEX ZZ(1),STOR,ST0,ST,S
DIMENSION LR(77)
COMPLEX X
CABQ(X)=REAL(X)*REAL(X)+AIMAG(X)*AIMAG(X)
DO 20 I=1,N
LR(I)=I
20 CONTINUE
M1=0
DO 18 M=1,N
K=M
DO 2 I=M,N
K1=M1+I
K2=M1+K
IF(CABQ(ZZ(K1))-CABQ(ZZ(K2))) 2,2,6
6 K=I
2 CONTINUE
LS=LR(M)
LR(M)=LR(K)
LR(K)=LS
K2=M1+K
STOR=ZZ(K2)
J1=0
DO 7 J=1,N
K1=J1+K
K2=J1+M
ST0=ZZ(K1)
ZZ(K1)=ZZ(K2)
ZZ(K2)=ST0/STOR
J1=J1+N
7 CONTINUE
K1=M1+M
ZZ(K1)=1./STOR
DO 11 I=1,N
IF (I-M)12,11,12

```

```
12 K1=M1+I
ST=ZZ(K1)
ZZ(K1)=(0.,0.)
J1=0
DO 10 J=1,N
K1=J1+I
K2=J1+M
ZZ(K1)=ZZ(K1)-ZZ(K2)*ST
J1=J1+N
10 CONTINUE
11 CONTINUE
M1=M1+N
18 CONTINUE
J1=0
DO 9 J=1,N
IF (J-LR(J)) 14,8,14
14 LRJ=LR(J)
J2=(LRJ-1)*N
21 DO 13 I=1,N
K2=J2+I
K1=J1+I
S=ZZ(K2)
ZZ(K2)=ZZ(K1)
ZZ(K1)=S
13 CONTINUE
LR(J)=LR(LRJ)
LR(LRJ)=LRJ
IF (J-LR(J)) 14,8,14
8 J1=J1+N
9 CONTINUE
RETURN
END
```

1

INPUT PARAMETERS

N= 5 SEGMENTS

L= .50 WAVELENGTHS

A= .001000 WAVELENGTHS

NINT= 17

IMPEDANCE MATRIX Z(II,JJ)

N REAL IMAGINARY

1	5.69+j-692.3	5.54+j 372.5	5.10+j 47.8
	4.42+j 8.6	3.58+j 2.9	
2	5.54+j 372.5	5.69+j-692.3	5.54+j 372.5
	5.10+j 47.8	4.42+j 8.6	
3	5.10+j 47.8	5.54+j 372.5	5.69+j-692.3
	5.54+j 372.5	5.10+j 47.8	
4	4.42+j 8.6	5.10+j 47.8	5.54+j 372.5
	5.69+j-692.3	5.54+j 372.5	
5	3.58+j 2.9	4.42+j 8.6	5.10+j 47.8
	5.54+j 372.5	5.69+j-692.3	

INVERSION OF COMPLEX MATRIX

	NN=1	NN=2	NN=3
1	.0028+j-.0003	.0045+j-.0024	.0052+j-.0034
	.0045+j-.0034	.0028+j-.0022	
2	.0045+j-.0024	.0074+j-.0033	.0084+j-.0051
	.0074+j-.0051	.0045+j-.0034	
3	.0051+j-.0034	.0084+j-.0051	.0096+j-.0049
	.0084+j-.0051	.0052+j-.0034	
4	.0045+j-.0034	.0074+j-.0051	.0084+j-.0051
	.0074+j-.0033	.0045+j-.0024	
5	.0028+j-.0022	.0045+j-.0034	.0052+j-.0034
	.0045+j-.0024	.0028+j-.0003	

VOLTAGE VECTOR V(M)

N REAL IMAGINARY

1	.000	+ j	.000
2	.000	+ j	.000
3	1.000	+ j	.000
4	.000	+ j	.000
5	.000	+ j	.000

CURRENT VECTOR I(N)

N	REAL	IMAGINARY	MAGNITUDE (mA)	IPHASE
1	.0052 + j -.0034		6.20371	-33.66762
2	.0084 + j -.0051		9.86479	-31.40116
3	.0096 + j -.0049		10.75601	-26.80561
4	.0084 + j -.0051		9.86479	-31.40116
5	.0052 + j -.0034		6.20371	-33.66763

* INPUT IMPEDANCE = 82.98 +j 41.93 *

[ZINMAG = 92.97 , ZINPHASE = 26.81]

```

C
C ***** M O M E N T   M E T H O D   P R O G R A M   F O R   A   B O T T O M - F E D   M O N O P O L E   W I T H   D E L T A -
C   *   G A P   V O L T A G E   G E N E R A T O R   O N   A N   I N F I N I T E   G R O U N D   P L A N E .
C   *   T H I S   C O M P U T E R   P R O G R A M   U S E S   P I E C E W I S E   S I N U S O I D A L   B A S I S   F U N C T -
C   *   I O N S   A N D   G A L E R K I N ' S   M E T H O D   T O   A N A L Y S E   A   B O T T O M - F E D   L I N E A R
C   *   M O N O P O L E .
C
C   *   T H E   V A R I A B L E S   I N   T H E   M A I N   P R O G R A M   A R E :
C   *           A = R A D I U S   O F   A N T E N N A   I N   W A V E L E N G T H S
C   *           N = N U M B E R   O F   S E G M E N T S
C   *           L = L E N G T H   O F   T H E   M O N O P O L E   I N   W A V E L E N G T H S
C   *           N I N T = N U M B E R   O F   S I M P S O N ' S   R U L E   D I V I S I O N
C
C *****

C
      DIMENSION ZMAG(23),ZPHASE(23)
      REAL L,LL,LLP,IMAX,ZINMAG,ZINPHA
      REAL IMAG(23),IPHASE(23)
      COMPLEX I(23),V(23),J,ZZ(3,3),ZIN,IIN
      COMPLEX INGRLI,KERNEI,INGRLM,KERNEM
      COMPLEX IZ(23),ZLOAD
      COMMON/ARRAY/ZZ,V
      COMMON /CNSTNS/J,B2,A2,B
      OPEN(UNIT=5,FILE='DA2.DAT',STATUS='OLD')
      OPEN(UNIT=6,FILE='OUTPUT.DAT',STATUS='NEW')
      DATA DEGRAD,RADDEG/.0174532,57.29577/
      READ(5,1000) A,N,L,NINT
1000 FORMAT(F7.5,I2,F4.2,I2)
C*   WRITE OUT INPUT PARAMETERS AND IMPEDANCE MATRIX
      WRITE(6,10) N,L,A,NINT
10  FORMAT(1H1,26X,'INPUT PARAMETERS'//1H ,25X,'N=',I3,' SEGMENTS',
     //1H ,25X,'L=',F5.2,' WAVELENGTHS'//1H ,25X,'A=',F9.6,' WAVELENGTH
     $'//23X,'NINT=',I3//1H ,26X,'IMPEDANCE MATRIX Z(IJ,JJ)'//1H ,
     *'N',2X,'REAL',1X,'IMAGINARY'/)
      NP02P1=1
      DZ=L/N
      PI=3.14159265
      J=(0.,1.)
      B=2.*PI
      B2=B*B
      A2=A*A
      M=N
      ZMM=0.
      DO 600 II=2,M
      ZM=ZMM+DZ
      ZMP=ZMM+2.*DZ
      ZNM=0.
      DO 100 JJ=2,N
      ZN=ZN+DZ
      ZNP=ZN+2.*DZ
C*   CALL INGRLK(NINT,ZMM,ZM,ZMP,ZNM,ZN,ZNP)
      ZZ(IJ,JJ)=INGRLI(NINT,ZMM,ZM,ZMP,ZNM,ZN,ZNP,A)
100 ZNM=ZN

```

```

ZMM=ZN
600 CONTINUE
ZMM=0.
ZNM=0.
ZM=0.
ZN=0.
ZMP=DZ
ZNP=DZ
ZZ( 1, 1)=INGRLM(NINT,ZMM,ZN,ZMP,ZNM,ZN,ZNP,A)
ZMM=0.
DO 350 MM=2,M
ZN=0.
ZNM=0.
ZNP=DZ
ZN=ZNM+DZ
ZMP=ZNM+2.*DZ
ZZ( 1,MM)=INGRLM(NINT,ZMM,ZN,ZMP,ZNM,ZN,ZNP,A)
350 ZNM=ZN
DO 351 NN=2,N
ZMM=0.
ZM=0.
ZNP=DZ
ZN=ZNM+DZ
ZNP=ZNM+2.*DZ
ZZ(NN, 1)=INGRLI(NINT,ZMM,ZN,ZMP,ZNM,ZN,ZNP,A)
351 ZNM=ZN
DO 250 II=1,M
WRITE(6,20) II,(ZZ(II,JJ),JJ=1,N)
20 FORMAT(I2,5(F6.2,'+j',F6.1,1X)/4(2X,4(F7.2,'+j',F6.1    )/))
250 CONTINUE
C CALL COMPLEX MATRIX SOLVING SUBROUTINE
CALL LINEB(ZZ,N)
WRITE (6,35)
35 FORMAT(//15X,'INVERSION OF COMPLEX MATRIX',//15X,'NN=1',10X,'NN=2
*10X,'NN=3')
DO 1250 II=1,M
WRITE(6,120) II,(ZZ(II,JJ),JJ=1,N)
120 FORMAT(1X,I2,2X,3(F6.4,'+j',F6.4,1X)/4(5X,4(F6.4,'+j',F6.4,1X)/
*5X,3(F6.4,'+j',F6.4,1X)/5X,2(F6.4,'+j',F6.4,1X))
1250 CONTINUE
C COMPUTE INPUT IMPEDANCE
DO 203 II=1,M
V(II)=(0.,0.)
IF (II.EQ.NP02P1) V(II)=(1.,0.)
203 CONTINUE
C WRITE OUT VOLTAGE VECTOR
WRITE(6,130)
130 FORMAT(1H //1H //,25X,'VOLTAGE VECTOR V(M)'//1H ,2X,'N',12X,'REAL
*',14X,'IMAGINARY')
DO 310 KK=1,N
310 WRITE(6,140) KK,V(KK)
140 FORMAT(1H ,I3,11X,F6.3,' + j ',7X,F6.3)
DO 666 II=1,M
DO 667 JJ=1,N
I(II)=I(II)+ZZ(II,JJ)*V(JJ)

```

```

IMAG(II)=1000.*CABS(I(II))
SS2=REAL(I(II))
SS1=AIMAG(I(II))
SS=SS1/SS2
IPHASE(II)=RADDEG*ATAN(SS)
667 CONTINUE
666 CONTINUE
MP=NPO2P1
IIN=I(MP)
V(MP)=(1.,0.)
ZIN=V(MP)/IIN
C   WRITE OUT CURRENT VECTOR
WRITE(6,30)
30 FORMAT(1H //1H //,20X,'CURRENT VECTOR I(N)''//1H ,8X,'N',2X,'REAL
*' ,4X,'IMAGINARY',4X,'IMAGNITUDE (mA)',2X,'IPHASE' '/')
DD 300 KK=1,N
WRITE(6,40) KK,I(KK),IMAG(KK),IPHASE(KK)
40 FORMAT(1H ,6X,13,2X,F6.4,' + j ',F6.4,5X,F9.3,7X,F9.3)
300 CONTINUE
C   WRITE(6,51)
C 51 FORMAT(1H //1H //,'

C   /*-----*/
C   /*          CALCULATING ANTENNA INPUT IMPEDANCE           */
C   /* THE INPUT IMPEDANCE OF AN ANTENNA IS THE IMPEDANCE PRESENTED BY    */
C   /* THE ANTENNA AT ITS TERMINALS. THE INPUT IMPEDANCE WILL BE AFFECTED   */
C   /* BY OTHER ANTENNAS OR OBJECTS THAT ARE NEARBY.                      */
C   /* THE INPUT IMPEDANCE IS COMPOSED OF REAL AND IMAGINARY PARTS. THE     */
C   /* INPUT RESISTANCE, RIN, REPRESENTS DISSIPATION(HEATING AND RADIATION)  */
C   /* IN THE ANTENNA. THE INPUT REACTANCE, XIN, REPRESENTS POWER STORED IN THE NEARBY FIELD OF THE ANTENNA. */
C   /*-----*/
ZINMAG=CABS(ZIN)
S2=REAL(ZIN)
S1=AIMAG(ZIN)
S=S1/S2
ZINPHA=RADDEG*ATAN(S)
WRITE(6,444) ZIN,ZINMAG,ZINPHA
444 FORMAT(//5X,'* INPUT IMPEDANCE =',F11.2,' +j ',F11.2,1X,'*//8X,'I'
*' ,1X,'ZINMAG =',F11.2,2X,', ZINPHASE =',F11.2,1X,'J')
STOP
END
C* THIS SUBROUTINE USES SIMPSON'S RULE TO NUMERICALLY INTEGRATE
C* FOR IMPEDANCE ELEMENTS USING EQUATION (2.4.5)
COMPLEX FUNCTION INGR1(NINT,ZMM,ZM,ZMP,ZNM,ZN,ZNP,A)
COMPLEX K1,K2,S1,S2,HALF1,HALF2,INGRL1,INGRL2,J
COMMON/CNSTNS/J,B2,A2,B
H1=(ZN-ZMM)/NINT
H2=(ZMP-ZM)/NINT
H102=0.5*H1
H202=0.5*H2
S1=(0.,0.)
S2=S1
CALL KERNEI(K1,K2,ZMM,ZM,ZMP,ZNM,ZN,ZNP,ZMM+H102,ZM+H202,A)
HALF1=K1
HALF2=K2

```

```

NINTM1=NINT-1
DO 100 I=1,NINTM1
Z1=ZMM+I*H1
Z2=ZM+I*H2
CALL KERNEI (K1,K2,ZMM,ZM,ZMP,ZNM,ZN,ZNP,Z1,Z2,A)
S1=S1+K1
S2=S2+K2
CALL KERNEI(K1,K2,ZMM,ZM,ZMP,ZNM,ZN,ZNP,Z1+H102,Z2+H202,A)
HALF1=HALF1+K1
100 HALF2=HALF2+K2
INGRL1=4.*HALF1+2.*S1
INGRL2=4.*HALF2+2.*S2
CALL KERNEI(K1,K2,ZMM,ZM,ZMP,ZNM,ZN,ZNP,ZMM,ZM,A)
INGRL1=INGRL1+K1
INGRL2=INGRL2+K2
CALL KERNEI(K1,K2,ZMM,ZM,ZMP,ZNM,ZN,ZNP,ZM,ZMP,A)
INGRL1=H1*(INGRL1+K1)/6.
INGRL2=H2*(INGRL2+K2)/6.
INGRL1=INGRL1+INGRL2
RETURN
END
C* THIS SUBROUTINE USES SIMPSON'S RULE TO NUMERICALLY INTEGRATE
C* FOR IMPEDANCE ELEMENTS USING EQUATION (2.4.6)
COMPLEX INGRLM(NINT,ZMM,ZM,ZMP,ZNM,ZN,ZNP,A)
COMPLEX K1,K2,S1,S2,HALF1,HALF2,INGRL1,INGRL2,J
COMMON/CNSTNS/J,B2,A2,B
H1=(ZM-ZMM)/NINT
H2=(ZMP-ZM)/NINT
H102=0.5*H1
H202=0.5*H2
S1=(0.,0.)
S2=S1
CALL KERNEM(K1,K2,ZMM,ZM,ZMP,ZNM,ZN,ZNP,ZMM+H102,ZM+H202,A)
HALF1=K1
HALF2=K2
NINTM1=NINT-1
DO 100 I=1,NINTM1
Z1=ZMM+I*H1
Z2=ZM+I*H2
CALL KERNEM (K1,K2,ZMM,ZM,ZMP,ZNM,ZN,ZNP,Z1,Z2,A)
S1=S1+K1
S2=S2+K2
CALL KERNEM(K1,K2,ZMM,ZM,ZMP,ZNM,ZN,ZNP,Z1+H102,Z2+H202,A)
HALF1=HALF1+K1
100 HALF2=HALF2+K2
INGRL1=4.*HALF1+2.*S1
INGRL2=4.*HALF2+2.*S2
CALL KERNEM(K1,K2,ZMM,ZM,ZMP,ZNM,ZN,ZNP,ZMM,ZM,A)
INGRL1=INGRL1+K1
INGRL2=INGRL2+K2
CALL KERNEM(K1,K2,ZMM,ZM,ZMP,ZNM,ZN,ZNP,ZM,ZMP,A)
INGRL1=H1*(INGRL1+K1)/6.
INGRL2=H2*(INGRL2+K2)/6.
INGRLM=INGRL1+INGRL2
RETURN

```

```

END
C* INVERSION OF A COMPLEX MATRIX ZZ, OF ORDER N, INVERSE IS RETURNED
C* IN PLACE OF ZZ
SUBROUTINE LINEQ(ZZ,N)
COMPLEX ZZ(1),STOR,STO,ST,S
DIMENSION LR(77)
COMPLEX X
CABR(X)=REAL(X)*REAL(X)+AIMAG(X)*AIMAG(X)
DO 20 I=1,N
LR(I)=I
20 CONTINUE
M1=0
DO 18 M=1,N
K=M
DO 2 I=M,N
K1=M1+I
K2=M1+K
IF(CABR(ZZ(K1))-CABR(ZZ(K2))> 2,2,6
6 K=I
2 CONTINUE
LS=LR(M)
LR(M)=LR(K)
LR(K)=LS
K2=M1+K
STOR=ZZ(K2)
J1=0
DO 7 J=1,N
K1=J1+K
K2=J1+M
STO=ZZ(K1)
ZZ(K1)=ZZ(K2)
ZZ(K2)=STO,STOR
J1=J1+N
7 CONTINUE
K1=M1+M
ZZ(K1)=1./STOR
DO 11 I=1,N
IF (I-M)12,11,12
12 K1=M1+I
ST=ZZ(K1)
ZZ(K1)=(0.,0.)
J1=0
DO 10 J=1,N
K1=J1+I
K2=J1+M
ZZ(K1)=ZZ(K1)-ZZ(K2)*ST
J1=J1+N
10 CONTINUE
11 CONTINUE
M1=M1+N
18 CONTINUE
J1=0
DO 9 J=1,N
IF (J-LR(J)) 14,8,14
14 LRJ=LR(J)

```

```
J2=(LRJ-1)*N
21 DO 13 I=1,N
      K2=J2+I
      K1=J1+I
      S=ZZ(K2)
      ZZ(K2)=ZZ(K1)
      ZZ(K1)=S
13 CONTINUE
      LR(J)=LR(LRJ)
      LR(LRJ)=LRJ
      IF (J-LR(J)) 14,8,14
8   J1=J1+N
9   CONTINUE
      RETURN
      END
```

```

C THIS SUBROUTIN COMPUTES VALUES OF INTEGRAND IN EQUATION (2.4.5)
SUBROUTINE KERNEI(K1,K2,ZMM,ZM,ZMP,ZNM,ZN,ZNP,Z1,Z2,A)
COMPLEX K1,K2,J,K11,K12,K21,K22
COMMON/CNSTNS/J,B2,A2,B
Z12=Z1+Z1
Z22=Z2+Z2
DZM=ZMP-ZM
DZN=ZNP-ZN
RNM1=SQRT(A2+(Z1-ZNM)*(Z1-ZNM))
RN1=SQRT(A2+(Z1-ZN)*(Z1-ZN))
RNP1=SQRT(A2+(Z1-ZNP)*(Z1-ZNP))
RNM2=SQRT(A2+(Z2-ZNM)*(Z2-ZNM))
RN2=SQRT(A2+(Z2-ZN)*(Z2-ZN))
RNP2=SQRT(A2+(Z2-ZNP)*(Z2-ZNP))
RNM1R=SQRT(A2+(Z1+ZNM)*(Z1+ZNM))
RN1R=SQRT(A2+(Z1+ZN)*(Z1+ZN))
RNP1R=SQRT(A2+(Z1+ZNP)*(Z1+ZNP))
RNM2R=SQRT(A2+(Z2+ZNM)*(Z2+ZNM))
RN2R=SQRT(A2+(Z2+ZN)*(Z2+ZN))
RNP2R=SQRT(A2+(Z2+ZNP)*(Z2+ZNP))
K11=CEXP(-J*B*RNM1)/RNM1-2.*COS(B*DZN)
**CEXP(-J*B*RN1)/RN1+CEXP(-J*B*RNP1)/RNP1
K12=CEXP(-J*B*RNM1R)/RNM1R-2.*COS(B*DZN)
**CEXP(-J*B*RN1R)/RN1R+CEXP(-J*B*RNP1R)/RNP1R
K1=30.*J*(K11+K12)/SIN(B*DZN)
K21=CEXP(-J*B*RNM2)/RNM2-2.*COS(B*DZN)
**CEXP(-J*B*RN2)/RN2+CEXP(-J*B*RNP2)/RNP2
K22=CEXP(-J*B*RNM2R)/RNM2R-2.*COS(B*DZN)
**CEXP(-J*B*RN2R)/RN2R+CEXP(-J*B*RNP2R)/RNP2R
K2=30.*J*(K21+K22)/SIN(B*DZN)
K1=K1*SIN(B*(Z1-ZNM))/SIN(B*DZN)
K2=K2*SIN(B*(ZNP-Z2))/SIN(B*DZN)
RETURN
END

```

```
C* THIS SUBROUTIN COMPUTES VALUES OF INTEGRAND IN EQUATION (2.4.6)
SUBROUTINE KERNE(M,K1,K2,ZMM,ZM,ZNP,ZNM,ZN,A)
COMPLEX K1,K2,J
COMMON/CNSTNS/J,B2,A2,B
Z12=Z1#Z1
Z22=Z2#Z2
DZM=ZMP-ZM
DZN=ZNP-ZN
RNMI=SQRT(A2+(Z1-DZN)*(Z1-DZN))
RN1=SQRT(A2+Z1#Z1)
RNP1=SQRT(A2+(Z1+DZN)*(Z1+DZN))
RNP2P=SQRT(A2+(Z2+DZN)*(Z2+DZN))
RN2=SQRT(A2+Z2#Z2)
RNP2=SQRT(A2+(Z2-DZN)*(Z2-DZN))
K1=30.*J*(CEXP(-J*B*RNMI)/RNMI-2.*COS(B*DZN)*CEXP(-J*B*RN1)/RN1+
*CEXP(-J*B*RNP1)/RNP1)/SIN(B*DZN)
K2=30.*J*(CEXP(-J*B*RNP2)/RNP2-2.*COS(B*DZN)*CEXP(-J*B*RN2)/RN2+
*CEXP(-J*B*RNP2P)/RNP2P)/SIN(B*DZN)
K1=K1*SIN(B*(Z1-ZMM))/SIN(B*DZN)
K2=K2*SIN(B*(ZMP-Z2))/SIN(B*DZN)
RETURN
END
```

1

INPUT PARAMETERS

N= 3 SEGMENTS.

L= .25 WAVELENGTHS

A= .001000 WAVELENGTHS

NINT= 17

IMPEDANCE MATRIX Z(IJ,JJ)

N REAL IMAGINARY

1	2.85+j-346.2	5.54+j 372.5	5.10+j 47.8
2	5.54+j 372.5	10.79+j-644.6	9.96+j 381.1
3	5.10+j 47.8	9.96+j 381.1	9.27+j-689.4

INVERSION OF COMPLEX MATRIX

	NN=1	NN=2	NN=3
1	.0192+j-.0097	.0168+j-.0103	.0103+j-.0069
2	.0168+j-.0103	.0148+j-.0083	.0091+j-.0058
3	.0103+j-.0069	.0091+j-.0058	.0056+j-.0025

VOLTAGE VECTOR V(N)

N	REAL	IMAGINARY
1	1.000 + j	.000
2	.000 + j	.000
3	.000 + j	.000

CURRENT VECTOR I(N)

N	REAL	IMAGINARY	IMAGNITUDE (mA)	IPHASE
1	.0192 + j -.0097		21.51202	-26.80564
2	.0168 + j -.0103		19.72957	-31.40119
3	.0103 + j -.0069		12.40741	-33.66765

* INPUT IMPEDANCE = 41.49 +j 20.96 *

[ZINMAG = 46.49 , ZINPHASE = 26.81]

```

C *****
C * MM-Extended UTD PROGRAM FOR A BOTTOM-FED MONPOLE WITH *
C * DELTA-GAP VOLTAGE GENERATOR MOUNTED ON A HALF-PLANE. *
C * THIS COMPUTER PROGRAM, USES PIECEWISE SINUSOIDAL BASIS FUNCT-
C * IONS AND GALERKIN'S METHOD TO ANALYSE A BOTTOM-FED LINEAR *
C * MONPOLE. *
C * THE VARIABLES IN THE MAIN PROGRAM ARE:
C *          A = RADIUS OF ANTENNA IN WAVELENGTHS
C *          N = NUMBER OF SEGMENTS
C *          L = LENGTH OF THE MONPOLE IN WAVELENGTHS
C *          NINT = NUMBER OF SIMPSONS'S RULE DIVISION
C *
C *
C *
C *
C *
C *****
C
C DIMENSION ZMAG(23),ZPHASE(23)
REAL L,LL,LLP,IMAX,ZINMAG,ZINPHA
REAL IMAG(23),IPHASE(23),DATA(23,2)
COMPLEX I(23),V(23),J,ZZ(3,3),ZIN,IIN
COMPLEX INGRLI,KERNEI,INGRLM,KERNEM,INGRLK,INGRLD,KERNEL,KERNEF
COMPLEX IZ(23),ZLOAD
COMMON/ARRAY/ZZ,V
COMMON /CNSTS/J,B2,A2,B
OPEN(UNIT=5,FILE='DA2.DAT',STATUS='OLD')
OPEN(UNIT=6,FILE='OUT23.DAT',STATUS='NEW')
DATA DEGRAD,RADdeg/.0174532,57.29577/
DB 1001 IP=1,10
READ(5,1000) A,N,L,NINT,DD
1000 FORMAT(F7.5,12,F4.2,12,F5.2)
C* WRITE OUT INPUT PARAMETERS AND IMPEDANCE MATRIX
WRITE(6,10) N,L,A,NINT,DD
10 FORMAT(1H1,30X,'INPUT PARAMETERS'//1H ,27X,'N=',I3,' SEGMENTS',
//1H ,27X,'L=',F5.2,' WAVELENGTHS'//1H ,27X,'A=',F9.6,' WAVELENGTH
$'//28X,'NINT=',I3//1H ,27X,'DD=',F5.2,'WAVELENGTHS'//1H ,30X,
$' IMPEDANCE MATRIX Z(IJ,JJ)'//1H ,3X,
$'N',2X,'REAL',5X,'IMAGINARY')
PHI0R=45.*DEGRAD
PHI0S=360.*DEGRAD
NP02P1=1
DZ=L/N
PI=3.14159265
J=(0.,1.)
B=2.*PI
B2=B*B
A2=A*A
M=N
ZMM=0.
DO 600 II=2,M
ZM=ZMM+DZ
ZMP=ZMM+2.*DZ

```

```

ZNM=0.
DO 100 JJ=2,N
ZN=ZNM+DZ
ZNP=ZNM+2.*DZ
C* CALL INGRLK(NINT,ZMM,ZM,ZMP,ZNM,ZN,ZNP)
ZZ(1,1)=INGRLI(NINT,ZMM,ZM,ZMP,ZNM,ZN,ZNP,A)-INGRLK(NINT
*,ZMM,ZM,ZNP,ZNM,ZN,ZNP,DD,A)
100 ZNM=ZN
ZMM=ZN
600 CONTINUE
ZMM=0.
ZNM=0.
ZN=0.
ZM=0.
ZMP=DZ
ZNP=DZ
ZZ(1, 1)=INGRLM(NINT,ZMM,ZM,ZMP,ZNM,ZN,ZNP,A)-INGRLD(NINT
*,ZMM,ZM,ZMP,ZNM,ZN,ZNP,DD,A)
ZMM=0.
DO 350 NN=2,M
ZN=0.
ZNM=0.
ZNP=DZ
ZM=ZMM+DZ
ZMP=ZMM+2.*DZ
ZZ(1,NN)=INGRLM(NINT,ZMM,ZM,ZMP,ZNM,ZN,ZNP,A)-INGRLD(NINT
*,ZMM,ZM,ZMP,ZNM,ZN,ZNP,DD,A)
350 ZMM=ZN
ZN=0.
DO 351 NN=2,N
ZMM=0.
ZN=0.
ZMP=DZ
ZN=ZN+DZ
ZNP=ZN+2.*DZ
ZZ(NN, 1)=INGRLI(NINT,ZMM,ZM,ZMP,ZNM,ZN,ZNP,A)-INGRLK(NINT
*,ZMM,ZM,ZNP,ZNM,ZN,ZNP,DD,A)
351 ZNM=ZN
C* DO 250 II=1,M
C* WRITE(6,20) II,(ZZ(II,JJ),JJ=1,N)
C* 20 FORMAT(I2,5(F6.2,'+'F6.1,1X)/4(2X,4(F7.2,'+'F6.1   )/1)
C* 250 CONTINUE
C   CALL COMPLEX MATRIX SOLVING SUBROUTINE
    CALL LINEQ(ZZ,N)
C* WRITE (6,35)
C* 35 FORMAT(//15X,'INVERSION OF COMPLEX MATRIX',//15X,'NN=1',10X,
C* '#NN=2'10X,'NN=3')
C* DO 1250 II=1,M
C*   WRITE(6,120) II,(ZZ(II,JJ),JJ=1,N)
C* 120 FORMAT(1X,I2,2X,3(F6.4,'+'F6.4,1X)/4(5X,4(F6.4,'+'F6.4,1X)/
C* #5X,3(F6.4,'+'F6.4,1X)/5X,2(F6.4,'+'F6.4,1X))
C* 1250 CONTINUE
C   COMPUTE INPUT IMPEDANCE
    DO 203 II=1,M
      V(II)=(0.,0.)

```

```

      IF (II.EQ.NP02P1) V(II)=(1.,0.)
103 CONTINUE
C     WRITE OUT VOLTAGE VECTOR
c$     WRITE(6,130)
c$ 130  FORMAT(1H //1H //,29X,'VOLTAGE VECTOR V(M)'//1H ,19X,'N',12X,
c$     *'REAL',14X,'IMAGINARY')
c$     DO 310 KK=1,N
c$ 310  WRITE(6,140) KK,V(KK)
c$ 140  FORMAT(1H ,17X,I3,11X,F6.3,' + j ',7X,F6.3)
      DO 666 II=1,M
      I(II)=(0.,0.)
      DO 667 JJ=1,N
      I(II)=I(II)+ZZ(II,JJ)*V(JJ)
      IMAG(II)=1000.*CABS(I(II))
      SS2=REAL(I(II))
      SS1=AIMAG(I(II))
      SS=SS1/SS2
      IPHASE(II)=RADDEG*ATAN(SS)
667 CONTINUE
666 CONTINUE
NP=NP02P1
ZIN=V(NP)/I(NP)
C     WRITE OUT CURRENT VECTOR
WRITE(6,30)
30  FORMAT(1H //1H //,20X,'CURRENT VECTOR I(N)'//1H ,8X,'N',2X,'REAL
      *',4X,'IMAGINARY',4X,'IMAGNITUDE (mA)',2X,'IPHASE')
C     DELTAS= LEN/8.
C     S=-LEN/2.
      DO 300 KK=1,N
      WRITE(6,40) KK,I(KK),IMAG(KK),IPHASE(KK)
40  FORMAT(1H ,6X,I3,2X,F6.4,' + j ',F6.4,5X,F9.5,7X,F9.5)
300 CONTINUE
ZINMAG=CABS(ZIN)
S2=REAL(ZIN)
S1=AIMAG(ZIN)
S=S1/S2
ZINPHA=RADDEG*ATAN(S)
WRITE(6,444) ZIN,ZINMAG,ZINPHA
444 FORMAT(//5X,'* INPUT IMPEDANCE =',F11.2,' +j ',F11.2,1X,'*//8X,'['
      $1X,'ZINMAG =',F11.2,2X,', ZINPHASE =',F11.2,1X,']')
1001 CONTINUE
STOP
END
C$ THIS SUBROUTINE USES SIMPSON'S RULE TO NUMERICALLY INTEGRATE
C$ FOR IMPEDANCE ELEMENTS USING EQUATION (4.4.10)
COMPLEX FUNCTION INGRLI(NINT,ZMM,ZM,ZMP,ZNM,ZN,ZNP,A)
COMPLEX K1,K2,S1,S2,HALF1,HALF2,INGRL1,INGRL2,J
COMMON/CNSTNS/J,B2,A2,B
H1=(ZM-ZMN)/NINT
H2=(ZMP-ZM)/NINT
H102=0.5*H1
H202=0.5*H2
S1=(0.,0.)
S2=S1
CALL KERNEI(K1,K2,ZMM,ZM,ZMP,ZNM,ZN,ZNP,ZNM+H102,ZM+H202,A)

```

```

HALF1=K1
HALF2=K2
NINTM1=NINT-1
DO 100 I=1,NINTM1
Z1=ZMM+I*H1
Z2=ZM+I*H2
CALL KERNEI (K1,K2,ZMM,ZM,ZMP,ZNM,ZN,ZNP,Z1,Z2,A)
S1=S1+K1
S2=S2+K2
CALL KERNEI(K1,K2,ZMM,ZM,ZMP,ZNM,ZN,ZNP,Z1+H102,Z2+H202,A)
HALF1=HALF1+K1
100 HALF2=HALF2+K2
INGRL1=4.*HALF1+2.*S1
INGRL2=4.*HALF2+2.*S2
CALL KERNEI(K1,K2,ZMM,ZM,ZMP,ZNM,ZN,ZNP,ZMM,ZM,A)
INGRL1=INGRL1+K1
INGRL2=INGRL2+K2
CALL KERNEI(K1,K2,ZMM,ZM,ZNP,ZNM,ZN,ZNP,ZM,ZMP,A)
INGRL1=H1*(INGRL1+K1)/6.
INGRL2=H2*(INGRL2+K2)/6.
INGRL1=INGRL1+INGRL2
RETURN
END
C* THIS SUBROUTINE USES SIMPSONS'S RULE TO NUMERICALLY INTEGRATE
C* FOR IMPEDANCE ELEMENTS USING EQUATION (4.4.10)
COMPLEX FUNCTION INGRLM(NINT,ZMM,ZM,ZMP,ZNM,ZN,ZNP,A)
COMPLEX K1,K2,S1,S2,HALF1,HALF2,INGRL1,INGRL2,J
COMMON/CNSTNS/J,B2,A2,B
H1=(ZN-ZMM)/NINT
H2=(ZMP-ZM)/NINT
H102=0.5*H1
H202=0.5*H2
S1=0.,0.
S2=S1
CALL KERNEM(K1,K2,ZMM,ZM,ZNP,ZNM,ZN,ZNP,ZMM+H102,ZM+H202,A)
HALF1=K1
HALF2=K2
NINTM1=NINT-1
DO 100 I=1,NINTM1
Z1=ZMM+I*H1
Z2=ZM+I*H2
CALL KERNEM (K1,K2,ZMM,ZM,ZMP,ZNM,ZN,ZNP,Z1,Z2,A)
S1=S1+K1
S2=S2+K2
CALL KERNEM(K1,K2,ZMM,ZM,ZMP,ZNM,ZN,ZNP,Z1+H102,Z2+H202,A)
HALF1=HALF1+K1
100 HALF2=HALF2+K2
INGRL1=4.*HALF1+2.*S1
INGRL2=4.*HALF2+2.*S2
CALL KERNEM(K1,K2,ZMM,ZM,ZMP,ZNM,ZN,ZNP,ZMM,ZM,A)
INGRL1=INGRL1+K1
INGRL2=INGRL2+K2
CALL KERNEM(K1,K2,ZMM,ZM,ZNP,ZNM,ZN,ZNP,ZM,ZMP,A)
INGRL1=H1*(INGRL1+K1)/6.
INGRL2=H2*(INGRL2+K2)/6.

```

```

INGRLM=INGRL1+INGRL2
RETURN
END
C* THIS SUBROUTINE USES SIMPSONS'S RULE TO NUMERICALLY INTEGRATE
C* FOR IMPEDANCE ELEMENTS USING EQUATION (4.4.10)
COMPLEX INGRLK(NINT,ZMM,ZM,ZMP,ZNM,ZN,ZNP,DD,A)
COMPLEX K1,K2,S1,S2,HALF1,HALF2,INGRL1,INGRL2,J
COMMON/CNSTNS/J,B2,A2,B
H1=(ZN-ZMM)/NINT
H2=(ZMP-ZM)/NINT
H102=0.5*H1
H202=0.5*H2
S1={0.,0.}
S2=S1
CALL KERNEL(K1,K2,ZMM,ZM,ZMP,ZNM,ZN,ZNP,ZMM+H102,ZM+H202,DD,A)
HALF1=K1
HALF2=K2
NINTM1=NINT-1
DO 100 I=1,NINTM1
Z1=ZMM+I*H1
Z2=ZM+I*H2
CALL KERNEL(K1,K2,ZMM,ZM,ZMP,ZNM,ZN,ZNP,Z1,Z2,DD,A)
S1=S1+K1
S2=S2+K2
CALL KERNEL(K1,K2,ZMM,ZM,ZMP,ZNM,ZN,ZNP,Z1+H102,Z2+H202,DD,A)
HALF1=HALF1+K1
100 HALF2=HALF2+K2
INGRL1=4.*HALF1+2.*S1
INGRL2=4.*HALF2+2.*S2
CALL KERNEL(K1,K2,ZMM,ZM,ZMP,ZNM,ZN,ZNP,ZMM,ZM,DD,A)
INGRL1=INGRL1+K1
INGRL2=INGRL2+K2
CALL KERNEL(K1,K2,ZMM,ZM,ZMP,ZNM,ZN,ZNP,ZM,ZNP,DD,A)
INGRL1=H1*(INGRL1+K1)/6.
INGRL2=H2*(INGRL2+K2)/6.
INGRLK=INGRL1+INGRL2
RETURN
END
C* THIS SUBROUTINE USES SIMPSONS'S RULE TO NUMERICALLY INTEGRATE
C* FOR IMPEDANCE ELEMENTS USING EQUATION (4.4.10)
COMPLEX INGRLD(NINT,ZMM,ZM,ZMP,ZNM,ZN,ZNP,DD,A)
COMPLEX K1,K2,S1,S2,HALF1,HALF2,INGRL1,INGRL2,J
COMMON/CNSTNS/J,B2,A2,B
H1=(ZM-ZMM)/NINT
H2=(ZMP-ZM)/NINT
H102=0.5*H1
H202=0.5*H2
S1={0.,0.}
S2=S1
CALL KERNEL(K1,K2,ZMM,ZM,ZMP,ZNM,ZN,ZNP,ZMM+H102,ZM+H202,DD,A)
HALF1=K1
HALF2=K2
NINTM1=NINT-1
DO 100 I=1,NINTM1
Z1=ZMM+I*H1

```

```

Z2=ZM+I*H2
CALL KERNED(K1,K2,ZMM,ZM,ZMP,ZNM,ZN,ZNP,Z1,Z2,DD,A)
S1=S1+K1
S2=S2+K2
CALL KERNED(K1,K2,ZMM,ZM,ZMP,ZNM,ZN,ZNP,Z1+H102,Z2+H202,DD,A)
HALF1=HALF1+K1
100 HALF2=HALF2+K2
INGRL1=4.*HALF1+2.*S1
INGRL2=4.*HALF2+2.*S2
CALL KERNED(K1,K2,ZMM,ZM,ZMP,ZNM,ZN,ZNP,ZMM,ZM,DD,A)
INGRL1=INGRL1+K1
INGRL2=INGRL2+K2
CALL KERNED(K1,K2,ZMM,ZM,ZMP,ZNM,ZN,ZNP,ZM,ZMP,DD,A)
INGRL1=H1*(INGRL1+K1)/6.
INGRL2=H2*(INGRL2+K2)/6.
INGRLD=INGRL1+INGRL2
RETURN
END
C* INVERSION OF A COMPLEX MATRIX ZZ, OF ORDER N, INVERSE IS RETURNED
C* IN PLACE OF ZZ
SUBROUTINE LINE0(ZZ,N)
COMPLEX ZZ(1),STOR,ST0,ST,S
DIMENSION LR(77)
COMPLEX X
CABQ(X)=REAL(X)*REAL(X)+AIMAG(X)*AIMAG(X)
DO 20 I=1,N
LR(I)=I
20 CONTINUE
M1=0
DO 18 M=1,N
K=N
DO 2 I=M,N
K1=M1+I
K2=M1+K
IF(CABQ(ZZ(K1))-CABQ(ZZ(K2))) 2,2,6
6   K=I
2   CONTINUE
LS=LR(M)
LR(M)=LR(K)
LR(K)=LS
K2=M1+K
ST0R=ZZ(K2)
J1=0
DO 7 J=1,M
K1=J1+K
K2=J1+M
ST0=ZZ(K1)
ZZ(K1)=ZZ(K2)
ZZ(K2)=ST0/ST0R
J1=J1+M
7   CONTINUE
K1=M1+M
ZZ(K1)=1./ST0R
DO 11 I=1,N
11 IF (I-M)12,11,12

```

```
12 K1=M1+I
    ST=ZZ(K1)
    ZZ(K1)=(0.,0.)
    J1=0
    DO 10 J=1,N
    K1=J1+I
    K2=J1+M
    ZZ(K1)=ZZ(K1)-ZZ(K2)*ST
    J1=J1+N
10  CONTINUE
11  CONTINUE
    M1=M1+N
18  CONTINUE
    J1=0
    DO 9 J=1,N
    IF (J-LR(J)) 14,8,14
14  LRJ=LR(J)
    J2=(LRJ-1)*N
21  DO 13 I=1,N
    K2=J2+I
    K1=J1+I
    S=ZZ(K2)
    ZZ(K2)=ZZ(K1)
    ZZ(K1)=S
13  CONTINUE
    LR(J)=LR(LRJ)
    LR(LRJ)=LRJ
    IF (J-LR(J)) 14,8,14
8   J1=J1+N
9   CONTINUE
    RETURN
    END
```

```

C* THIS SUBROUTIN COMPUTES VALUES OF INTEGRAND IN EQUATION (2.4.5)
SUBROUTINE KERNEI(K1,K2,ZMM,ZM,ZMP,ZNM,ZN,ZNP,Z1,Z2,A)
COMPLEX K1,K2,J,K11,K12,K21,K22
COMMON/CNSTNS/J,R2,A2,B
Z12=Z1#Z1
Z22=Z2#Z2
DZM=ZMP-ZM
DZN=ZNP-ZN
RNM1=SQRT(A2+(Z1-ZNM)*(Z1-ZNM))
RN1=SQRT(A2+(Z1-ZN)*(Z1-ZN))
RNP1=SQRT(A2+(Z1-ZNP)*(Z1-ZNP))
RNM2=SQRT(A2+(Z2-ZNM)*(Z2-ZNM))
RN2=SQRT(A2+(Z2-ZN)*(Z2-ZN))
RNP2=SQRT(A2+(Z2-ZNP)*(Z2-ZNP))
RNM1R=SQRT(A2+(Z1+ZNM)*(Z1+ZNM))
RN1R=SQRT(A2+(Z1+ZN)*(Z1+ZN))
RNP1R=SQRT(A2+(Z1+ZNP)*(Z1+ZNP))
RNM2R=SQRT(A2+(Z2+ZNM)*(Z2+ZNM))
RN2R=SQRT(A2+(Z2+ZN)*(Z2+ZN))
RNP2R=SQRT(A2+(Z2+ZNP)*(Z2+ZNP))
K11=CEXP(-J*B*RNM1)/RNM1-2.*COS(B*DZN)
**CEXP(-J*B*RN1)/RN1+CEXP(-J*B*RNP1)/RNP1
K12=CEXP(-J*B*RNM1R)/RNM1R-2.*COS(B*DZN)
**CEXP(-J*B*RN1R)/RN1R+CEXP(-J*B*RNP1R)/RNP1R
K1=30.*J*(K11+K12)/SIN(B*DZN)
K21=CEXP(-J*B*RNM2)/RNM2-2.*COS(B*DZN)
**CEXP(-J*B*RN2)/RN2+CEXP(-J*B*RNP2)/RNP2
K22=CEXP(-J*B*RNM2R)/RNM2R-2.*COS(B*DZN)
**CEXP(-J*B*RN2R)/RN2R+CEXP(-J*B*RNP2R)/RNP2R
K2=30.*J*(K21+K22)/SIN(B*DZN)
K1=K1*SIN(B*(Z1-ZMM))/SIN(B*DZN)
K2=K2*SIN(B*(ZMP-Z2))/SIN(B*DZN)
RETURN
END

```

```
C THIS SUBROUTIN COMPUTES VALUES OF INTEGRAND IN EQUATION (2.4.6)
SUBROUTINE KERNEM(K1,K2,ZMM,ZM,ZMP,ZNM,ZNP,Z1,Z2,A)
COMPLEX K1,K2,J
COMMON/CNSTNS/J,B2,A2,B
Z12=Z1*Z1
Z22=Z2*Z2
DZM=ZMP-ZM
DZN=ZNP-ZN
RNM1=SQRT(A2+(Z1-DZN)*(Z1-DZN))
RN1=SQRT(A2+Z1*Z1)
RNP1=SQRT(A2+(Z1+DZN)*(Z1+DZN))
RNP2P=SQRT(A2+(Z2+DZN)*(Z2+DZN))
RN2=SQRT(A2+Z2*Z2)
RNP2=SQRT(A2+(Z2-DZN)*(Z2-DZN))
K1=30.4J*(CEXP(-J*B*RNM1)/RNM1-2.*COS(B*DZN)*CEXP(-J*B*RN1)/RN1+
*CEXP(-J*B*RNP1)/RNP1)/SIN(B*DZN)
K2=30.4J*(CEXP(-J*B*RNP2)/RNP2-2.*COS(B*DZN)*CEXP(-J*B*RN2)/RN2+
*CEXP(-J*B*RNP2P)/RNP2P)/SIN(B*DZN)
K1=K1*SIN(B*(Z1-ZMM))/SIN(B*DZN)
K2=K2*SIN(B*(ZMP-Z2))/SIN(B*DZN)
RETURN
END
```

```

C* THIS SUBROUTIN COMPUTES VALUES OF INTEGRAND IN EQUATION (4.4.10)
SUBROUTINE KERNEL(K1,K2,ZMM,ZM,ZNP,ZNM,ZN,ZNP,Z1,Z2,DD,A)
COMPLEX K1,K2,J,D(4),DH11,DH12,DH13,DH21,DH22,DH23,KP11,KP12
COMPLEX DH11P,DH12P,DH13P,DH21P,DH22P,DH23P
COMPLEX D411,D412,D413,D421,D422,D423
COMPLEX DH611,DH612,DH613,DH621,DH622,DH623
COMPLEX D611,D612,D613,D621,D622,D623
COMPLEX KD11,KD12,KD13,KD21,KD22,KD23
COMPLEX K11,K12,K13,K21,K22,K23,KP13,KP21,KP22,KP23
COMMON/CNSTNS/3,B2,A2,B
Z12=Z1#Z1
Z22=Z2#Z2
DZN=ZNP-ZN
DZN=ZNP-ZN
S1=SQRT(DD#DD+Z1#Z1)
S2=SQRT(DD#DD+Z2#Z2)
PHR1=ACOS(DD/S1)
PHR2=ACOS(DD/S2)
DD=DD-A
DD2=DD#DD
SPNM1=SQRT(DD2+ZNM#ZNM)
SPN1=SQRT(DD2+ZN#ZN)
SPNP1=SQRT(DD2+ZNP#ZNP)
SPNM2=SQRT(DD2+ZNM#ZNM)
SPN2=SQRT(DD2+ZN#ZN)
SPNP2=SQRT(DD2+ZNP#ZNP)
SBO=1.
FN=2.
PHPRM1=ACOS(DD/SPNM1)
PHPRN1=ACOS(DD/SPN1)
PHPRP1=ACOS(DD/SPNP1)
PHPRM2=ACOS(DD/SPNM2)
PHPRN2=ACOS(DD/SPN2)
PHPRP2=ACOS(DD/SPNP2)
RPNM1=(S1*SPNM1)/(S1+SPNM1)
RPN1=(S1*SPN1)/(S1+SPN1)
RPNP1=(S1*SPNP1)/(S1+SPNP1)
RPNM2=(S2*SPNM2)/(S2+SPNM2)
RPN2=(S2*SPN2)/(S2+SPN2)
RPNP2=(S2*SPNP2)/(S2+SPNP2)
KP11=CEXP(-J*B*S1)*SQRT(SPNM1/(S1*(S1+SPNM1)))
KP12=CEXP(-J*B*S1)*SQRT(SPN1/(S1*(S1+SPN1)))
KP13=CEXP(-J*B*S1)*SQRT(SPNP1/(S1*(S1+SPNP1)))
KP21=CEXP(-J*B*S2)*SQRT(SPNM2/(S2*(S2+SPNM2)))
KP22=CEXP(-J*B*S2)*SQRT(SPN2/(S2*(S2+SPN2)))
KP23=CEXP(-J*B*S2)*SQRT(SPNP2/(S2*(S2+SPNP2)))
CALL WD(D,RPNM1,PHR1,PHPRM1,SBO,FN)
DH11=D(1)+D(2)+D(3)+D(4)
CALL EWD(D,RPNM1,PHR1,PHPRM1,SBO,FN)
DH11P=D(1)+D(2)+D(3)+D(4)
D411=1./CMPLX(0.,B*RPNM1)*(DH11P-0.5*DH11)
K11=CEXP(-J*B*SPNM1)/SPNM1/COS(PHPRM1)*(DH11-D411)*KP11
CALL WDF(D,RPNM1,PHR1,PHPRM1,SBO,FN)
DH611=D(1)+D(2)+D(3)+D(4)

```

```

D611=-1./CMPLX(0.,B$S1)*DH611
KD11=CEXP(-J*B$SPNM1)/SPNM1/COS(PHPRM1)*D611*KP11
CALL WD(D,RPN1,PHR1,PHPRN1,SBO,FN)
DH12=D(1)+D(2)+D(3)+D(4)
CALL EWD(D,RPN1,PHR1,PHPRN1,SBO,FN)
DH12P=D(1)+D(2)+D(3)+D(4)
D412=1./CMPLX(0.,B$RPN1)*(DH12P-0.5*DH12)
K12=-2.*COS(B$DZN)*CEXP(-J*B$SPN1)/SPN1/COS(PHPRN1)*(DH12-D412)*KP12
CALL WDF(D,RPN1,PHR1,PHPRN1,SBO,FN)
DH612=D(1)+D(2)+D(3)+D(4)
D612=-1./CMPLX(0.,B$S1)*DH612
KD12=-2.*COS(B$DZN)*CEXP(-J*B$SPN1)/SPN1/COS(PHPRN1)*D612*KP12
CALL WD(D,RPNP1,PHR1,PHPRP1,SBO,FN)
DH13=D(1)+D(2)+D(3)+D(4)
CALL EWD(D,RPNP1,PHR1,PHPRP1,SBO,FN)
DH13P=D(1)+D(2)+D(3)+D(4)
D413=1./CMPLX(0.,B$RPNP1)*(DH13P-0.5*DH13)
K13=CEXP(-J*B$SPNP1)/SPNP1/COS(PHPRP1)*(DH13-D413)*KP13
CALL WDF(D,RPNP1,PHR1,PHPRP1,SBO,FN)
DH613=D(1)+D(2)+D(3)+D(4)
D613=-1./CMPLX(0.,B$S1)*DH613
KD13=CEXP(-J*B$SPNP1)/SPNP1/COS(PHPRP1)*D613*KP13
K1=30.*J*((K11+K12+K13)*COS(PHR1)-(KD11+KD12+KD13)
*ISIN(PHR1))/ISIN(B$DZN)
CALL WD(D,RPNM2,PHR2,PHPRM2,SBO,FN)
DH21=D(1)+D(2)+D(3)+D(4)
CALL EWD(D,RPNM2,PHR2,PHPRM2,SBO,FN)
DH21P=D(1)+D(2)+D(3)+D(4)
D421=1./CMPLX(0.,B$RPNM2)*(DH21P-0.5*DH21)
K21=CEXP(-J*B$SPNM2)/SPNM2/COS(PHPRM2)*(DH21-D421)*KP21
CALL WDF(D,RPNM2,PHR2,PHPRM2,SBO,FN)
DH621=D(1)+D(2)+D(3)+D(4)
D621=-1./CMPLX(0.,B$S2)*DH621
KD21=CEXP(-J*B$SPNM2)/SPNM2/COS(PHPRM2)*D621*KP21
CALL WD(D,RPN2,PHR2,PHPRN2,SBO,FN)
DH22=D(1)+D(2)+D(3)+D(4)
CALL EWD(D,RPN2,PHR2,PHPRN2,SBO,FN)
DH22P=D(1)+D(2)+D(3)+D(4)
D422=1./CMPLX(0.,B$RPN1)*(DH22P-0.5*DH22)
K22=-2.*COS(B$DZN)*CEXP(-J*B$SPN2)/SPN2/COS(PHPRN2)*(DH22-D422)*KP22
CALL WDF(D,RPN2,PHR2,PHPRN2,SBO,FN)
DH622=D(1)+D(2)+D(3)+D(4)
D622=-1./CMPLX(0.,B$S2)*DH622
KD22=-2.*COS(B$DZN)*CEXP(-J*B$SPN2)/SPN2/COS(PHPRN2)*D622*KP22
CALL WD(D,RPNP2,PHR2,PHPRP2,SBO,FN)
DH23=D(1)+D(2)+D(3)+D(4)
CALL EWD(D,RPNP2,PHR2,PHPRP2,SBO,FN)
DH23P=D(1)+D(2)+D(3)+D(4)
D423=1./CMPLX(0.,B$RPNP1)*(DH23P-0.5*DH23)
K23=CEXP(-J*B$SPNP2)/SPNP2/COS(PHPRP2)*(DH23-D423)*KP23
CALL WDF(D,RPNP2,PHR2,PHPRP2,SBO,FN)
DH623=D(1)+D(2)+D(3)+D(4)
D623=-1./CMPLX(0.,B$S2)*DH623
KD23=CEXP(-J*B$SPNP2)/SPNP2/COS(PHPRP2)*D623*KP23
K2=30.*J*((K21+K22+K23)*COS(PHR2)-(KD21+KD22+KD23)

```

```
*$SIN(PHR2))/SIN(B*DZN)
K1=K1*$SIN(B*(Z1-ZMM))/SIN(B*DZM)
K2=K2*$SIN(B*(ZNP-Z2))/SIN(B*DZM)
RETURN
END
```

```

C THIS SUBROUTIN COMPUTES VALUES OF INTEGRAND IN EQUATION (4.4.10)
SUBROUTINE KERNED(K1,K2,ZMM,ZM,ZMP,ZNM,ZN,ZNP,Z1,Z2,DD,A)
COMPLEX K1,K2,J,D(4),DH12,DH13,DH22,DH23
COMPLEX K12,K13,K22,K23,KP12,KP13,KP22,KP23
COMPLEX DH12P,DH13P,DH22P,DH23P,D412,D413,D422,D423
COMPLEX DH612,DH613,DH622,DH623,D612,D613,D622,D623
COMPLEX KD12,KD13,KD22,KD23
COMMON/CNSTNS/3,B2,A2,B
Z12=Z1#Z1
Z22=Z2#Z2
DZM=ZNP-ZM
DZN=ZNP-ZN
S1=SQRT(DD#DD+Z1#Z1)
S2=SQRT(DD#DD+Z2#Z2)
PHR1=ACOS(DD/S1)
PHR2=ACOS(DD/S2)
DD=DD-A
DD2=DD#DD
SPN1=SQRT(DD2)
SPNP1=SQRT(DD2+DZN#DZN)
SPN2=SQRT(DD2)
SPNP2=SQRT(DD2+DZN#DZN)
SBO=1.
FN=2.
PHPRN1=ACOS(DD/SPN1)
PHPRP1=ACOS(DD/SPNP1)
PHPRN2=ACOS(DD/SPN2)
PHPRP2=ACOS(DD/SPNP2)
RPN1=(S1#SPN1)/(S1+SPN1)
RPNP1=(S1#SPNP1)/(S1+SPNP1)
RPN2=(S2#SPN2)/(S2+SPN2)
RPNP2=(S2#SPNP2)/(S2+SPNP2)
KP12=CEXP(-J*B*S1)*SQRT(SPN1/(S1*(S1+SPN1)))
KP13=CEXP(-J*B*S1)*SQRT(SPNP1/(S1*(S1+SPNP1)))
KP22=CEXP(-J*B*S2)*SQRT(SPN2/(S2*(S2+SPN2)))
KP23=CEXP(-J*B*S2)*SQRT(SPNP2/(S2*(S2+SPNP2)))
CALL WD(D,RPN1,PHR1,PHPRN1,SBO,FN)
DH12=D(1)+D(2)+D(3)+D(4)
CALL END(D,RPN1,PHR1,PHPRN1,SBO,FN)
DH12P=D(1)+D(2)+D(3)+D(4)
D412=1./CMPLX(0.,B*RPN1)*(DH12P-0.5*DH12)
K12=-COS(B*DZN)*CEXP(-J*B*SPN1)/SPN1/COS(PHPRN1)*(DH12-D412)*KP12
CALL WDF(D,RPN1,PHR1,PHPRN1,SBO,FN)
DH612=D(1)+D(2)+D(3)+D(4)
D612=-1./CMPLX(0.,B*S1)*DH612
K12=-COS(B*DZN)*CEXP(-J*B*SPN1)/SPN1/COS(PHPRN1)*D612*KP12
CALL WD(D,RPNP1,PHR1,PHPRP1,SBO,FN)
DH13=D(1)+D(2)+D(3)+D(4)
CALL END(D,RPNP1,PHR1,PHPRP1,SBO,FN)
DH13P=D(1)+D(2)+D(3)+D(4)
D413=1./CMPLX(0.,B*RPNP1)*(DH13P-0.5*DH13)
K13=CEXP(-J*B*SPNP1)/SPNP1/COS(PHPRP1)*(DH13-D413)*KP13
CALL WDF(D,RPNP1,PHR1,PHPRP1,SBO,FN)
DH613=D(1)+D(2)+D(3)+D(4)

```

```

D613=-1./CMPLX(0.,B*S1)*DH613
K13=CEXP(-J*B*SPNP1)/SPNP1/COS(PHPRP1)*D613*KP13
K1=30.*J*((K12+K13)*COS(PHR1)-(KD12+KD13)*SIN(PHR1))/SIN(B*DZN)
CALL WDF(D,RPN2,PHR2,PHPRN2,SBO,FN)
DH22=D(1)+D(2)+D(3)+D(4)
CALL EWD(D,RPN2,PHR2,PHPRN2,SBO,FN)
DH22P=D(1)+D(2)+D(3)+D(4)
D422=1./CMPLX(0.,B*RPN2)*(DH22P-0.5*DH22)
K22=-COS(B*DZN)*CEXP(-J*B*SPN2)/SPN2/COS(PHPRN2)*(DH22-D422)*KP22
CALL WDF(D,RPN2,PHR2,PHPRN2,SBO,FN)
DH622=D(1)+D(2)+D(3)+D(4)
D622=-1./CMPLX(0.,B*S2)*DH622
K622=-COS(B*DZN)*CEXP(-J*B*SPN2)/SPN2/COS(PHPRN2)*D622*KP22
CALL WDF(D,RPNP2,PHR2,PHPRP2,SBO,FN)
DH23=D(1)+D(2)+D(3)+D(4)
CALL EWD(D,RPNP2,PHR2,PHPRP2,SBO,FN)
DH23P=D(1)+D(2)+D(3)+D(4)
D423=1./CMPLX(0.,B*RPNP2)*(DH23P-0.5*DH23)
K23=CEXP(-J*B*SPNP2)/SPNP2/COS(PHPRP2)*(DH23-D423)*KP23
CALL WDF(D,RPNP2,PHR2,PHPRP2,SBO,FN)
DH623=D(1)+D(2)+D(3)+D(4)
D623=-1./CMPLX(0.,B*S2)*DH623
K23=CEXP(-J*B*SPNP2)/SPNP2/COS(PHPRP2)*D623*KP23
K2=30.*J*((K22+K23)*COS(PHR2)-(KD22+KD23)*SIN(PHR2))/SIN(B*DZN)
K1=K1*SIN(B*(Z1-ZHM))/SIN(B*DZN)
K2=K2*SIN(B*(ZMP-Z2))/SIN(B*DZN)
RETURN
END

```

```

SUBROUTINE EWD(D,R,PHR,PHPR,SBO,FN)
C*
C* THIS SUBROUTINE COMPUTES THE FIRST ORDER WEDGE DIFFRACTION
C* COEFFICIENT.
C*
COMPLEX D(4),CT,TERM,FT(4),EFFECT
DATA CT,UTPI/(-0.05626977,0.05626977),0.15915494/
DATA PI,TPI,SML/3.14159265,6.28318531,0.001/
IF (FN-0.5.LT.SML)GO TO 10
DKL=TPI*R
UFN=1./FN
BETAR=PHR-PHPR
TERM=CT/(FN*SBO)
SGN=1.
I=0
2   I=I+1
DN=UFN*(0.5*SGN+UTPI*BETAR)
N=DN+SIGN(0.5,DN)
ANG=TPI*FN*N-BETAR
A=2.*((COS(0.5*ANG))**2)
X=DKL*A
Y=PI+SGN*BETAR
IF (ABS(X).LT.1.E-10)GO TO 3
FT(I)=EFFECT(X)/TAN(0.5*Y*UFN)
GO TO 4
3   FT(I)=(0.,0.)
IF (ABS(COS(0.5*Y*UFN)).LT.1.E-3)GO TO 4
FT(I)=(1.7725,1.7725)*SIGN(SQRT(DKL),Y)
FT(I)=(FT(I)-(0.,2.)*DKL*(PI-SGN*ANG))/FN
4   SGN=-SGN
D(I)=TERM*FT(I)
IF (SGN.LT.0.)GO TO 2
BETAR=PHR+PHPR
IF (I.LE.3)GO TO 2
C   DI=TERM*(FT(1)+FT(2))
C   DR=TERM*(FT(3)+FT(4))
RETURN
10  DO 5 I=1,4
5   D(I)=(0.,0.)
C10 DI=(0.,0.)
C   DR=(0.,0.)
RETURN
END
COMPLEX FUNCTION EFFECT(XF)
C*
C* THIS ROUTINE COMPUTES THE WEDGE TRANSITION FUNCTION.
C*
COMPLEX FXX(8),FX(8),CJ
DIMENSION XX(8)
DATA XX/.3,.5,.7,1.,1.5,2.3,4.,5.5/
DATA CJ/(0.,1.)/
DATA FX/(0.5729,0.2677),(0.6768,0.2682),(0.7439,0.2549),
      (0.8095,0.2322),(0.873,0.1982),(0.9240,0.1577),(0.9658,0.1073),
      (0.9797,0.0828)/

```

```

DATA FXX/(0.,0.), (0.5195,0.0025), (0.3355,-0.0665),
$(0.2187,-0.0757), (0.127,-0.068), (0.0638,-0.0506),
$(0.0246,-0.0296), (0.0093,-0.0163)/
X=ABS(XF)
IF(X.GT.5.5)GO TO 1
IF(X.GT.0.3)GO TO 10
C* SMALL ARGUMENT FORM
EFFCT=(0.5*(1.253,1.253)*SQRT(X)-(0.,2.)*X-1.334*X*X)*CEXP(CJ*X)+  

$(((1.253,1.253)*SQRT(X)-(0.,2.)*X-0.6667*X*X)*CEXP(CJ*X))*X
GO TO 20
C* LINEAR INTERPOLATION REGION
10 DO 11 N=2,7
11 IF(X.LT.XX(N)) GO TO 12
12 EFFCT=FXX(N)*X
GO TO 20
C* LARGE ARGUMENT FORM
13 EFFCT=0.5*CMPLX(3./X,-1.)/X
20 IF(XF.GE.0.) RETURN
EFFCT=CONJG(EFFCT)
RETURN
END

```



```

SUBROUTINE WD(D,R,PHR,PHPR,SBO,FN)
C*
C* THIS SUBROUTINE COMPUTES THE FIRST ORDER WEDGE DIFFRACTION
C* COEFFICIENT.
C*
COMPLEX D(4),CT,TERM,FT(4),FFCT
DATA CT,UTPI/(-0.05626977,0.05626977),0.15915494/
DATA PI,TPI,SML/3.14159265,6.28318531,0.001/
IF (FN-0.5.LT.SML)GO TO 10
DKL=TPI*R
UFN=1./FN
BETAR=PHR-PHPR
TERM=CT/(FN*SBO)
SGN=1.
I=0
2 I=I+1
DN=UFN*(0.5*SGN+UTPI*BETAR)
N=DN+SIGN(0.5,DN)
ANG=TPI*FN*N-BETAR
A=2.*((COS(0.5*ANG))**2)
X=DKL*A
Y=PI+SGN*BETAR
IF (ABS(X).LT.1.E-10)GO TO 3
FT(I)=FFCT(X)/TAN(0.5*Y*UFN)
GO TO 4
3 FT(I)=(0.,0.)
IF (ABS(COS(0.5*Y*UFN)).LT.1.E-3)GO TO 4
FT(I)=(1.7725,1.7725)*SIGN(SQRT(DKL),Y)
FT(I)=(FT(I)-(0.,2.)*DKL*(PI-SGN*ANG))/FN
4 SGN=-SGN
D(I)=TERM*FT(I)
IF (SGN.LT.0.)GO TO 2
BETAR=PHR+PHPR
IF (I.LE.3)GO TO 2
C DI=TERM*(FT(1)+FT(2))
C DR=TERM*(FT(3)+FT(4))
RETURN
10 DO 5 I=1,4
5 D(I)=(0.,0.)
C10 DI=(0.,0.)
C DR=(0.,0.)
RETURN
END
COMPLEX FUNCTION FFCT(XF)
C*
C* THIS ROUTINE COMPUTES THE WEDGE TRANSITION FUNCTION.
C*
COMPLEX FXX(8),FX(8),CJ
DIMENSION XX(8)
DATA XX/.3,.5,.7,1.,1.5,2.3,4.,5.5/
DATA CJ/(0.,1.)/
DATA FX/(0.5729,0.2677),(0.6768,0.2682),(0.7439,0.2549),
*(0.8095,0.2322),(0.873,0.1982),(0.9240,0.1577),(0.9658,0.1073),
*(0.9797,0.0828)/

```

```
DATA FXX/(0.,0.),(0.5195,0.0025),(0.3355,-0.0665),  
  (0.2187,-0.0757),(0.127,-0.068),(0.0638,-0.0506),  
  (0.0246,-0.0296),(0.0093,-0.0163)/  
  XF=ABS(XF)  
  IF(X.GT.5.5)GO TO 1  
  IF(X.GT.0.3)GO TO 10  
C*  SMALL ARGUMENT FORM  
  FFCT=((1.253,1.253)*SQR(X)-(0.,2.)*X-0.6667*X*X)*CEXP(CJ*X)  
  GO TO 20  
C*  LINEAR INTERPOLATION REGION  
  10  DO 11 N=2,7  
  11  IF(X.LT.XX(N)) GO TO 12  
  12  FFCT=FXX(N)*(X-XX(N))+FX(N)  
  GO TO 20  
C*  LARGE ARGUMENT FORM  
  1  FFCT=1.+CMPLX(-0.75/X,0.5)/X  
  20  IF(XF.GE.0.) RETURN  
      FFCT=CONJG(FFCT)  
      RETURN  
  END
```

```

SUBROUTINE WDF(D,R,PHR,PHPR,SBD,FN)
C*
C* THIS SUBROUTINE COMPUTES THE FIRST ORDER WEDGE DIFFRACTION
C* COEFFICIENT.
C*
COMPLEX D(4),CT,TERM,FT(4),FFCT1,EFFCT1
DATA CT,UTPI/(-0.05626977,0.05626977),0.15915494/
DATA PI,TPI,SML/3.14159265,6.28318531,0.001/
IF (FN-0.5.LT.SML)GO TO 10
DKL=TPI*R
UFN=1./FN
BETAR=PHR-PHPR
TERM=CT/(FN*SBD)
SGN=1.
I=0
2 I=I+1
DN=UFN*(0.5*SGN+UTPI*BETAR)
N=DN+SIGN(0.5,DN)
ANG=TPI*FN*N-BETAR
A=2.*((COS(0.5*ANG))**2
X=DKL*A
Y=PI+SGN*BETAR
IF(ABS(X).LT.1.E-10)GO TO 3
FT(I)=FFCT1(X)/(2.*FN*((COS(0.5*Y*UFN))**2)
$+EFFCT1(X)/TAN(0.5*Y*UFN)*TAN(0.5*ANG))
GO TO 4
3 FT(I)=(0.,0.)
IF(ABS(COS(0.5*Y*UFN)).LT.1.E-3)GO TO 4
FT(I)=(1.7725,1.7725)*SIGN(SQRT(DKL),Y)
FT(I)=(FT(I)-(0.,2.)*DKL*(PI-SGN*ANG))/FN
4 SGN=-SGN
DI=TERM*FT(I)
IF(SGN.LT.0.)GO TO 2
BETAR=PHR+PHPR
IF(I.LE.3)GO TO 2
C DI=TERM*(FT(1)+FT(2))
C DR=TERM*(FT(3)+FT(4))
RETURN
10 DO 5 I=1,4
5 D(I)=(0.,0.)
C10 DI=(0.,0.)
C DR=(0.,0.)
RETURN
END
COMPLEX FUNCTION FFCT1(XF)
C*
C* THIS ROUTINE COMPUTES THE WEDGE TRANSITION FUNCTION.
C*
COMPLEX FXX(8),FX(8),CJ
DIMENSION XX(8)
DATA XX/.3,.5,.7,1.,1.5,2.3,4.,5.5/
DATA CJ/(0.,1.)/
DATA FX/(0.5729,0.2677),(0.6768,0.2682),(0.7439,0.2549),
$(0.8095,0.2322),(0.873,0.1982),(0.9240,0.1577),(0.9658,0.1073),

```

```

*(0.9797,0.0828)/
DATA FXX/(0.,0.),{0.5195,0.0025},{0.3355,-0.0665},
*(0.2187,-0.0757),{0.127,-0.068},{0.0638,-0.0506},
*(0.0246,-0.0296),{0.0093,-0.0163}/
X=ABS(XF)
IF(X.GT.5.5)GO TO 1
IF(X.GT.0.3)GO TO 10
C# SMALL ARGUMENT FORM
FFCT1=((1.253,1.253)*SQR(X)-(0.,2.)*X-0.6667*X*X)*CEXP(CJ*X)
GO TO 20
C# LINEAR INTERPOLATION REGION
10 DO 11 N=2,7
11 IF(X.LT.XX(N)) GO TO 12
12 FFCT1=FXX(N)*(X-XX(N))+FX(N)
GO TO 20
C# LARGE ARGUMENT FORM
1 FFCT1=1.+CMPLX(-0.75/X,0.5)/X
20 IF(XF.GE.0.) RETURN
FFCT1=CONJG(FFCT1)
RETURN
END
COMPLEX FUNCTION EFFCT1(XF)

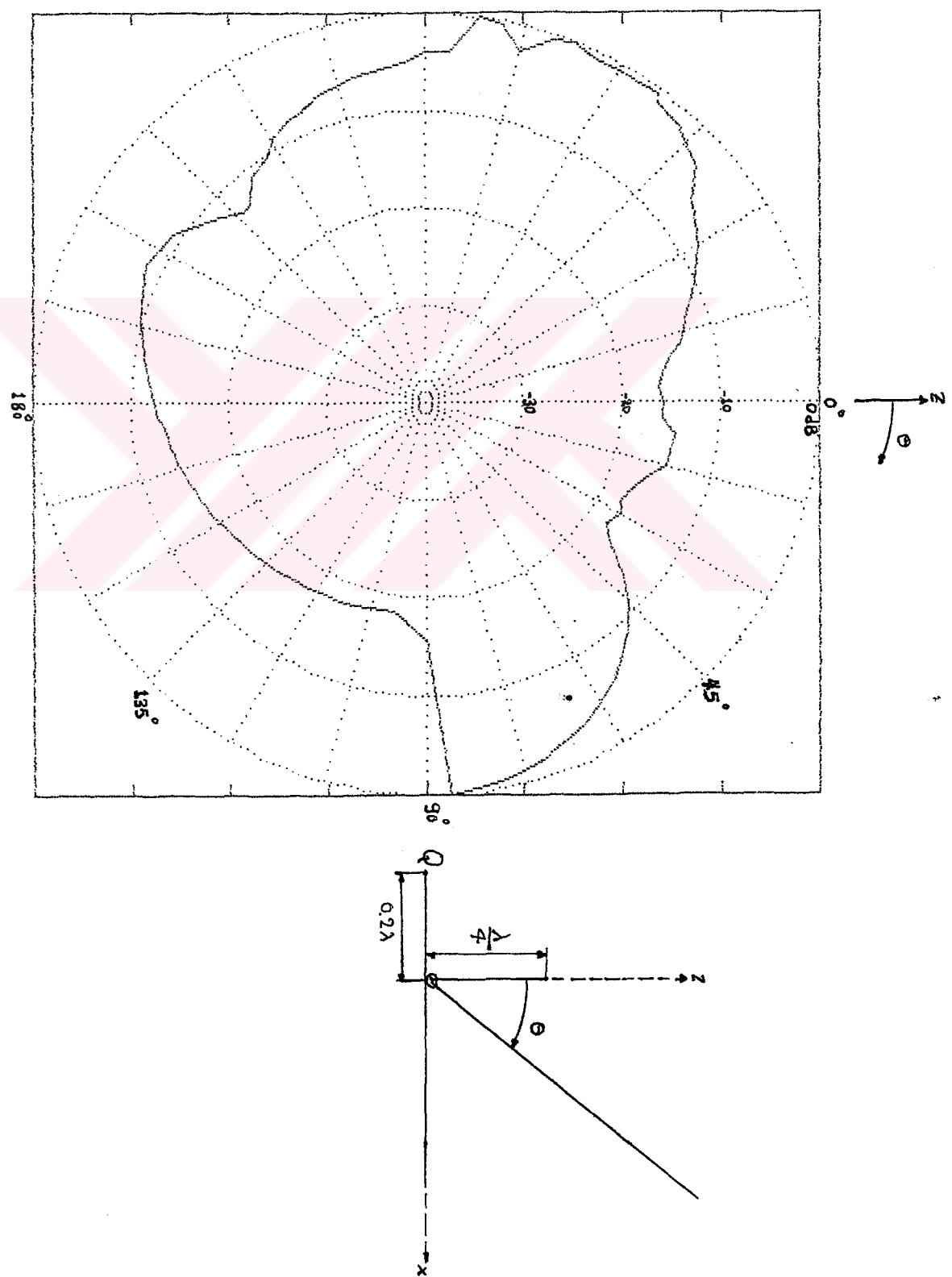
C#
C# THIS ROUTINE COMPUTES THE WEDGE TRANSITION FUNCTION.
C#
COMPLEX FXX(B),FX(B),CJ
DIMENSION XX(B)
DATA XX/.3,.5,.7,1.,1.5,2.3,4.,5.5/
DATA CJ/(0.,1.)/
DATA FX/{0.5729,0.2677},{0.6768,0.2682},{0.7439,0.2549},
*(0.8095,0.2322),{0.873,0.1982},{0.9240,0.1577},{0.9658,0.1073},
*(0.9797,0.0828)/
DATA FXX/(0.,0.),{0.5195,0.0025},{0.3355,-0.0665},
*(0.2187,-0.0757),{0.127,-0.068},{0.0638,-0.0506},
*(0.0246,-0.0296),{0.0093,-0.0163}/
X=ABS(XF)
IF(X.GT.5.5)GO TO 1
IF(X.GT.0.3)GO TO 10
C# SMALL ARGUMENT FORM
EFFCT1=(0.5*(1.253,1.253)*SQR(X)-(0.,2.)*X-1.334*X*X)*CEXP(CJ*X)+
*((1.253,1.253)*SQR(X)-(0.,2.)*X-0.6667*X*X)*CEXP(CJ*X))*X
GO TO 20
C# LINEAR INTERPOLATION REGION
10 DO 11 N=2,7
11 IF(X.LT.XX(N)) GO TO 12
12 EFFCT1=FXX(N)*X
GO TO 20
C# LARGE ARGUMENT FORM
1 EFFCT1=0.5*CMPLX(3./X,-1.)/X
20 IF(XF.GE.0.) RETURN
EFFCT1=CONJG(EFFCT1)
RETURN
END

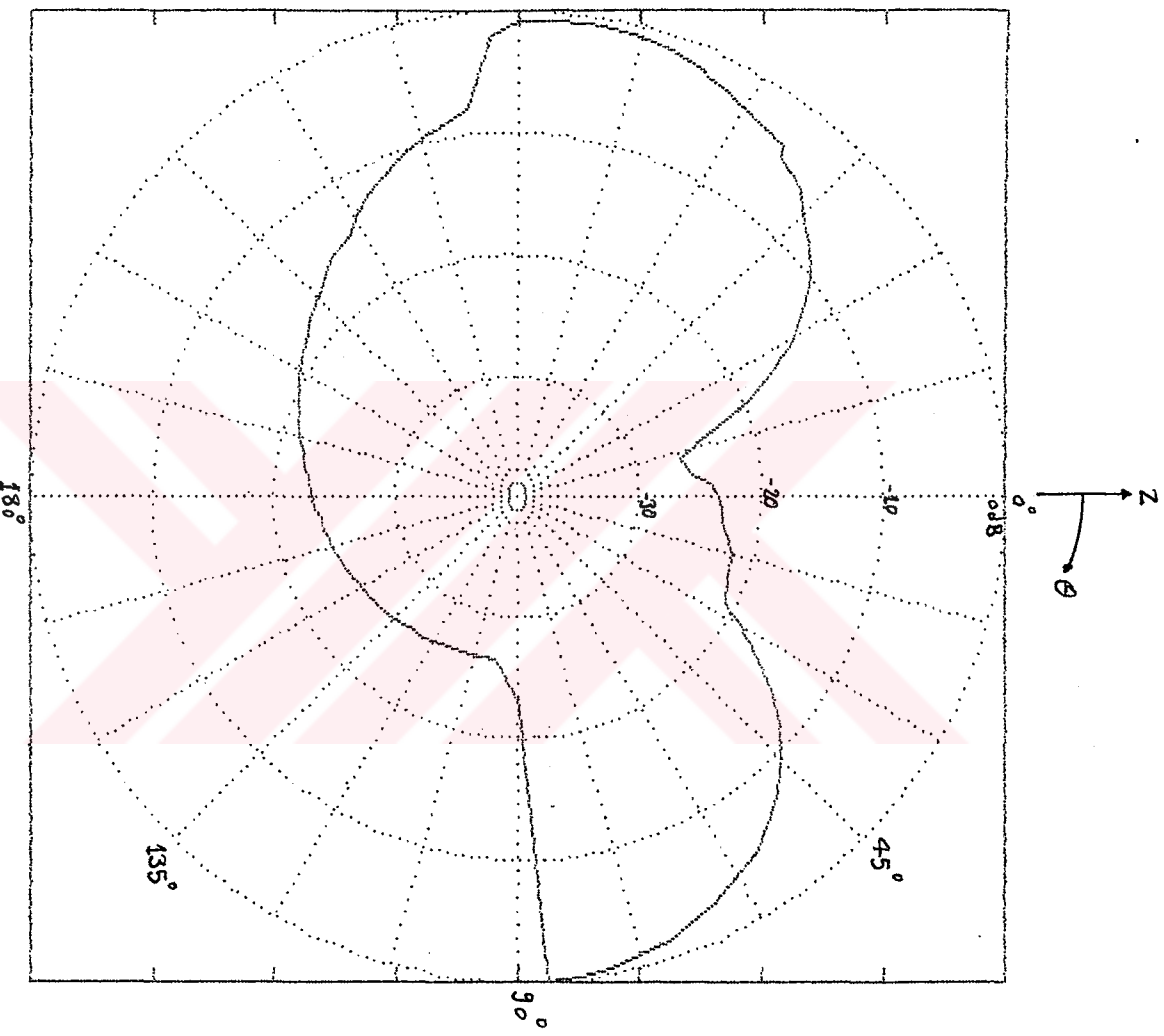
```

APPENDIX D

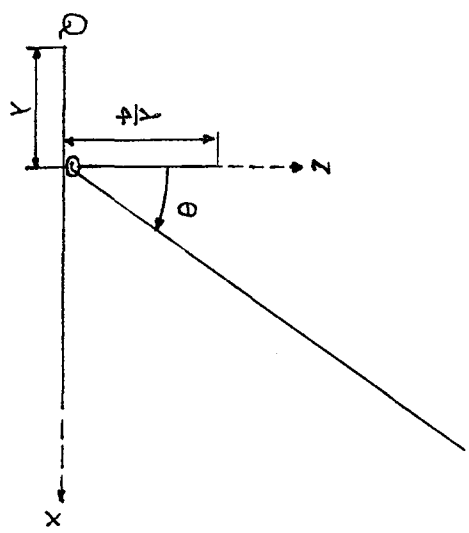
In this appendix, the radiation pattern of a quarter wavelength monopole mounted near the edge of a conducting half-plane is investigated. The wire radius is 0.001λ . The current distribution is obtained using the MM-UTD method. The pattern due to the known current distribution is calculated using the UTD. The vertical plane and horizontal plane patterns are given for different values of d , the edge-monopole separation of 0.2λ , λ , 2λ , 3λ , 4λ and 5λ , respectively.

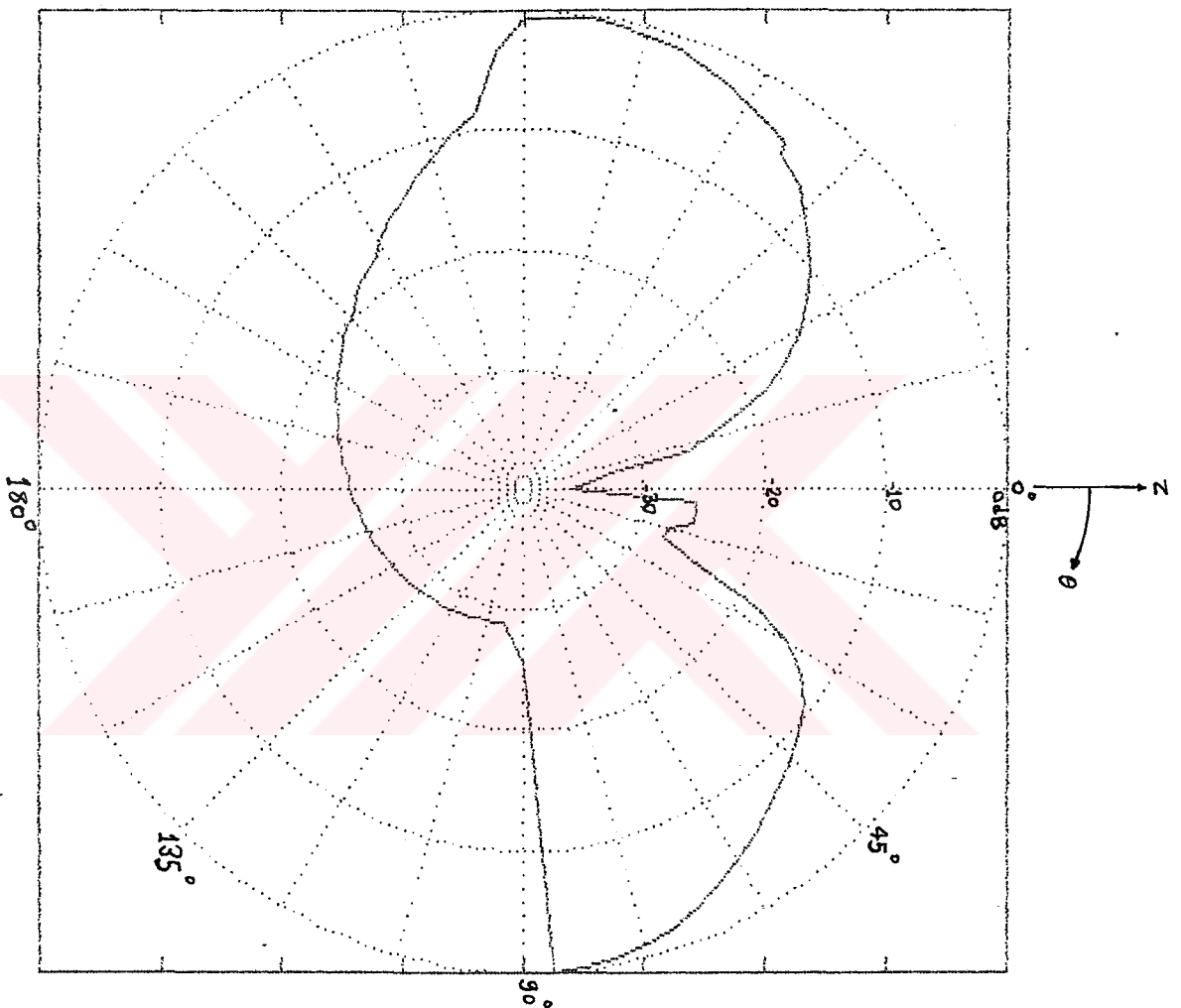
It is observed that beyond of the edge does not significantly alter the radiation pattern.



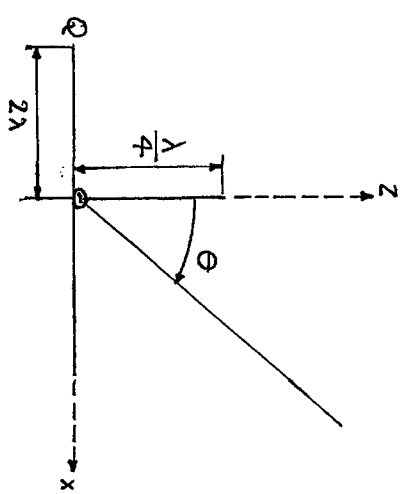


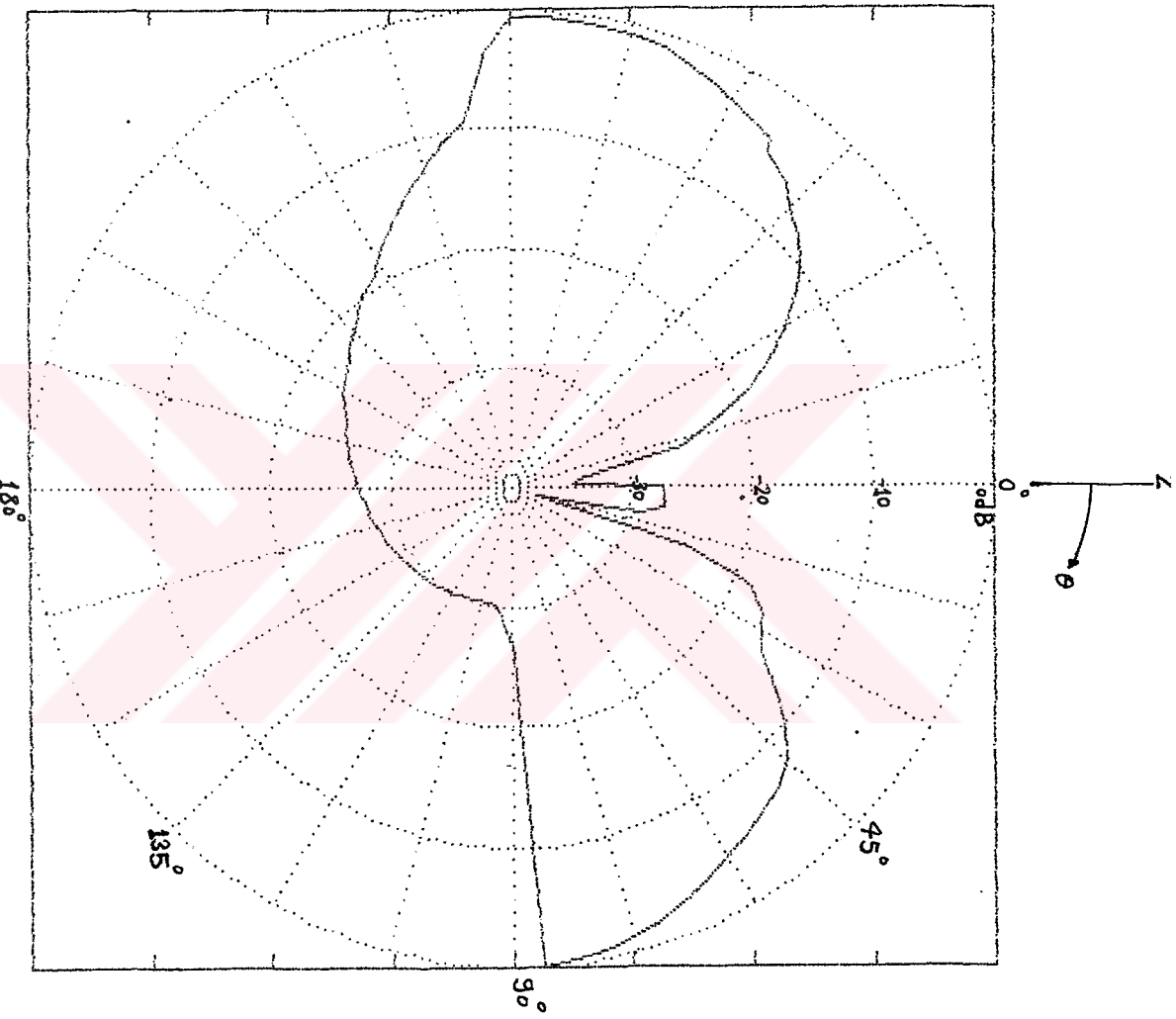
COMPUTED VERTICAL PLANE PATTERN OF A $\lambda/4$ MONOPOLE
MOUNTED NEAR THE EDGE OF A HALF-PLANE (dB).





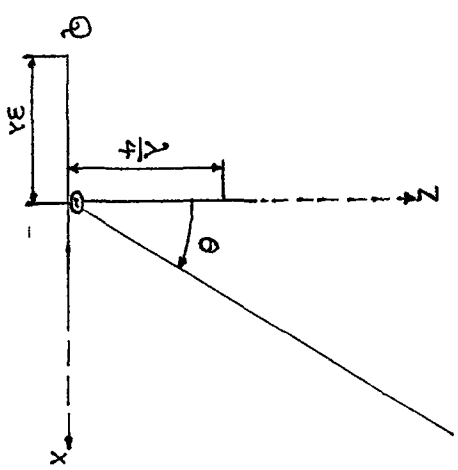
COMPUTED VERTICAL PLANE PATTERN OF A $\lambda/4$ MONOPOLE
MOUNTED NEAR THE EDGE OF A HALF-PLANE (dB).

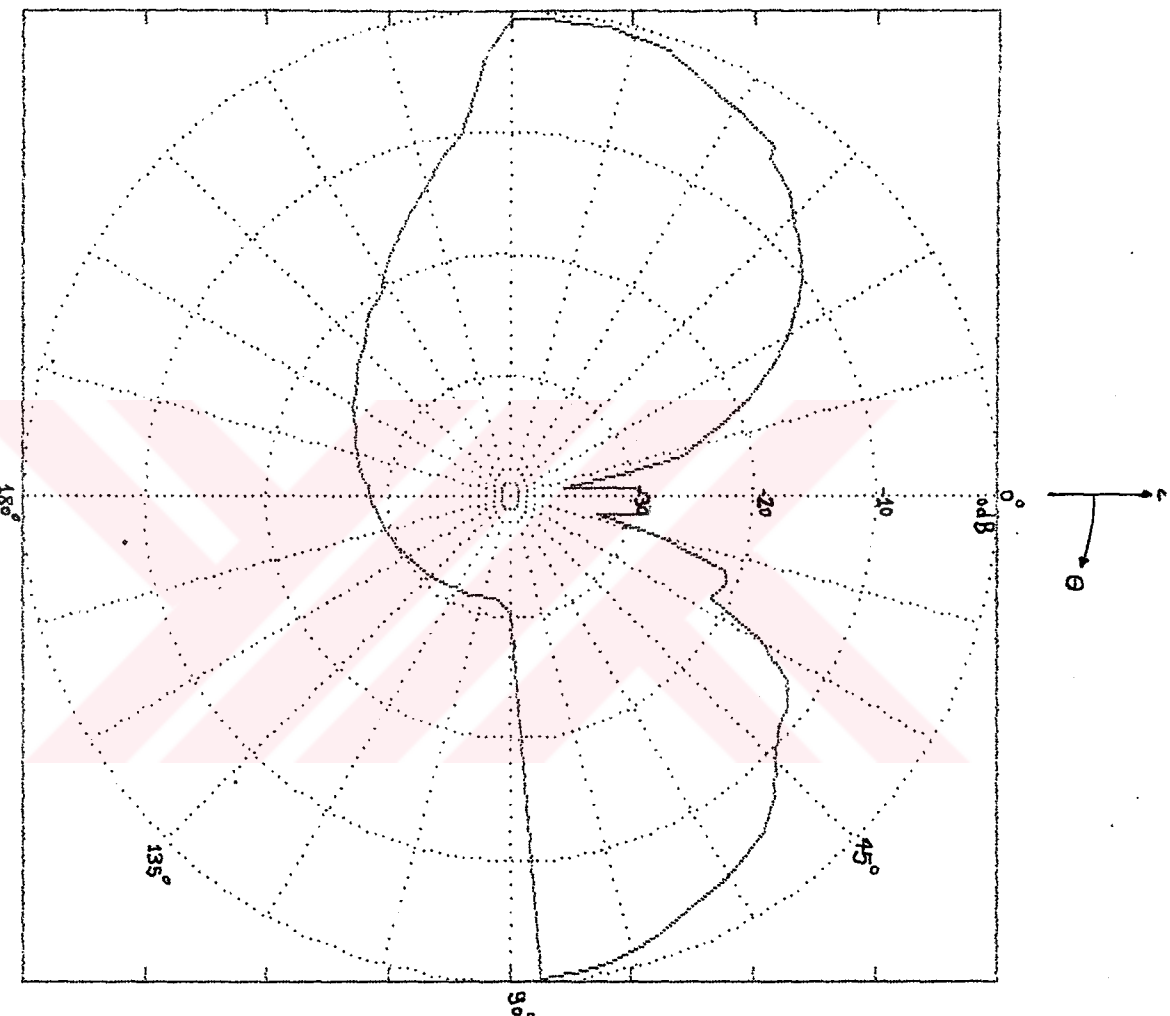




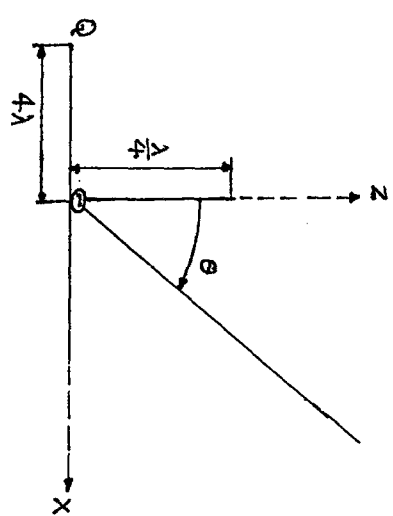
COMPUTED VERTICAL PLANE PATTERN OF A $\lambda/4$ MONOPOLE

OUNTED NEAR THE EDGE OF A HALF-PLANE (dB).

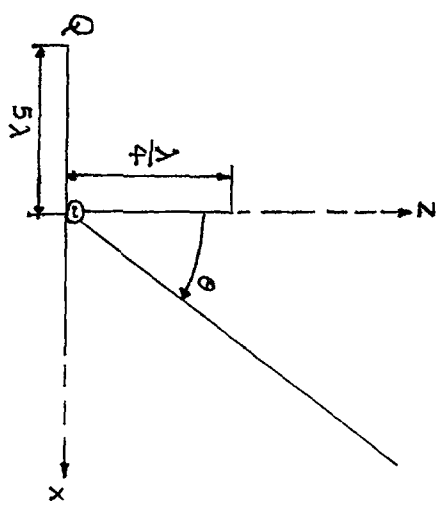
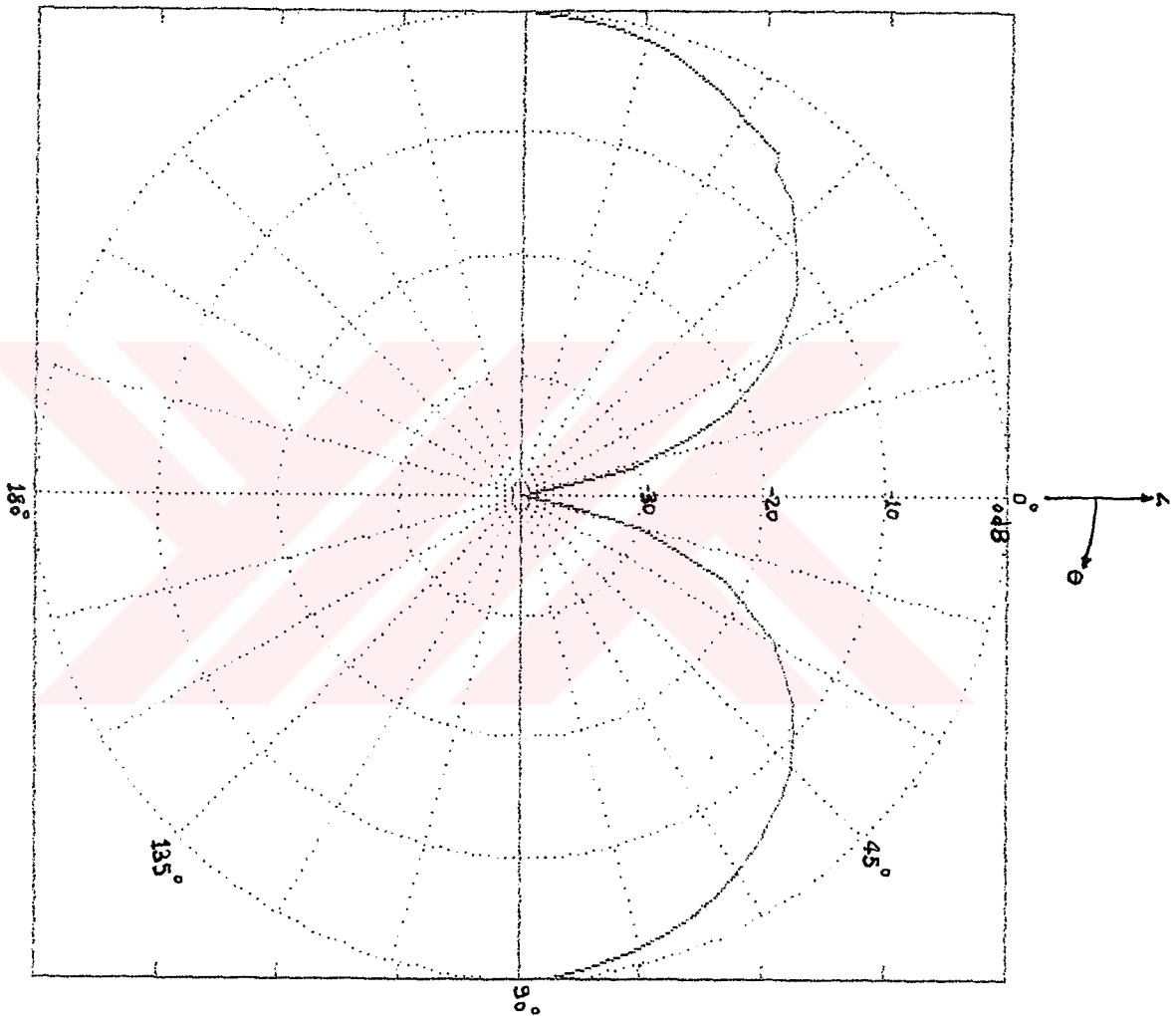


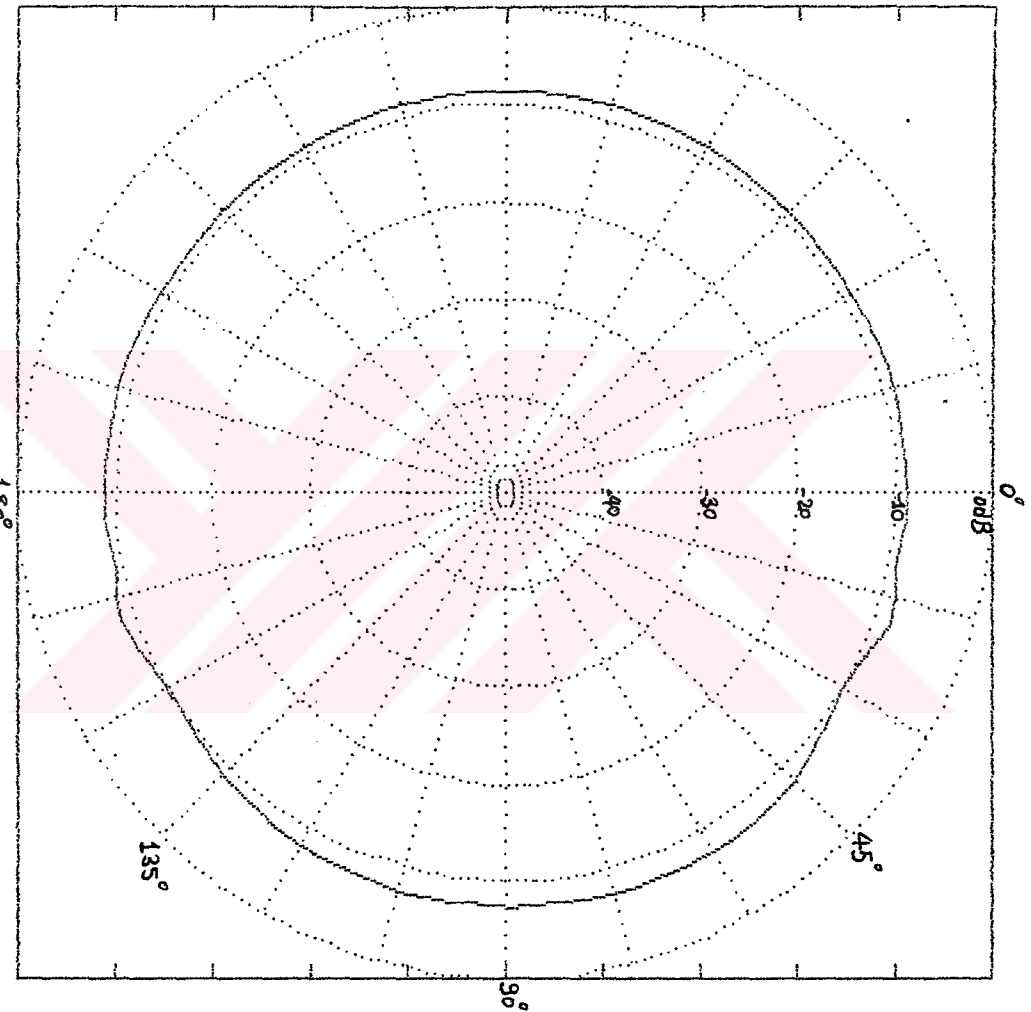


COMPUTED VERTICAL PLANE PATTERN OF A $\lambda/4$ MONOPOLE
MOUNTED NEAR THE EDGE OF A HALF-PLANE (dB).

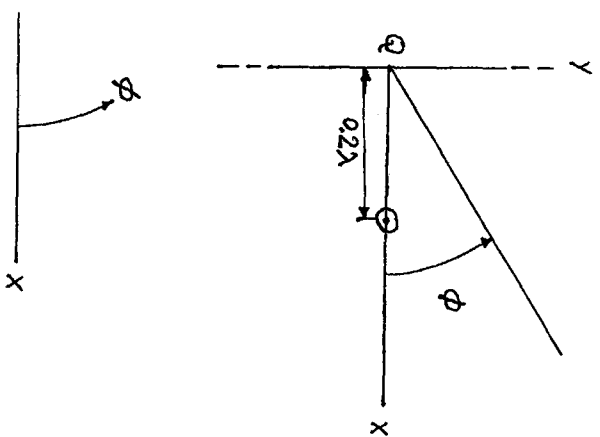


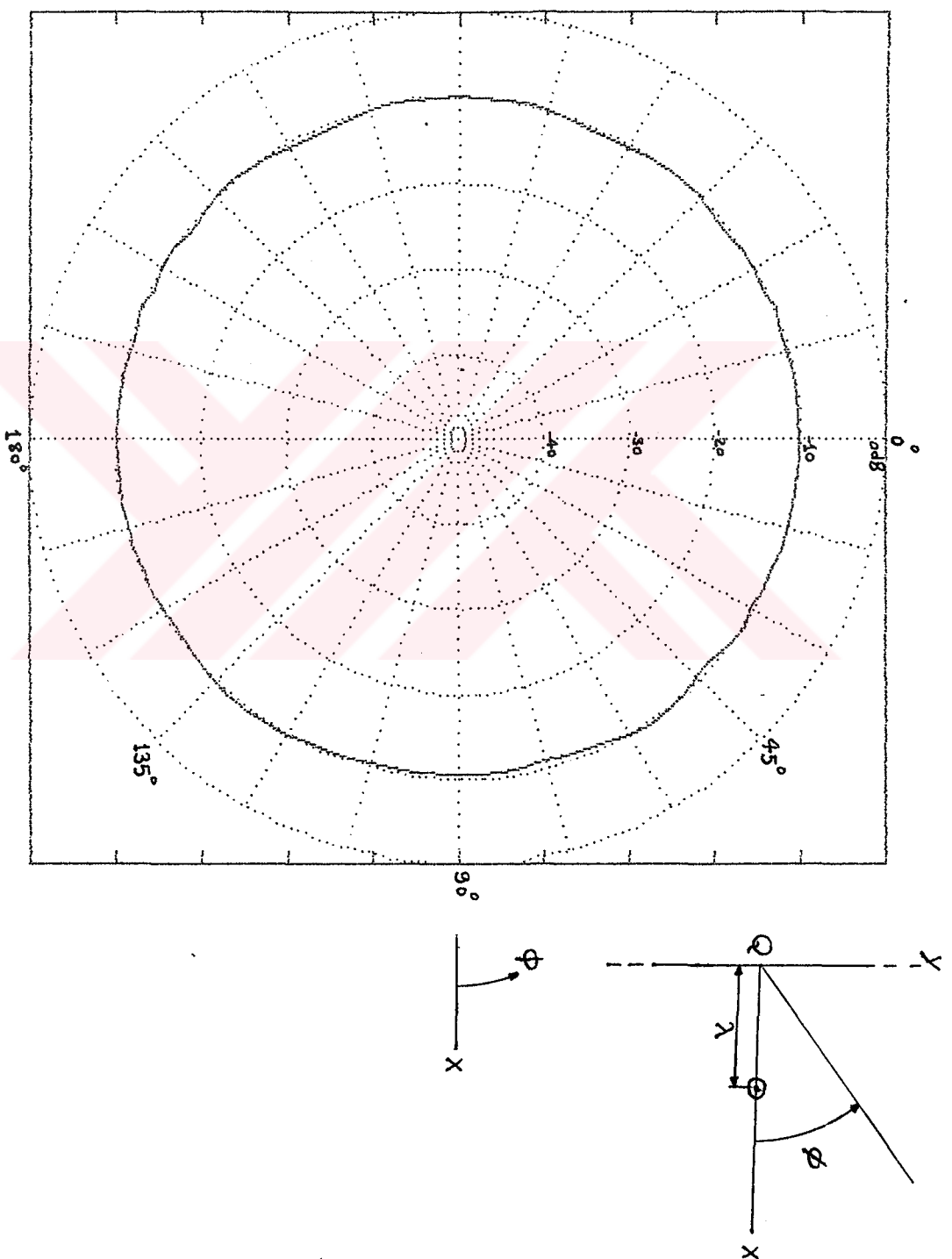
COMPUTED VERTICAL PLANE PATTERN OF A $\lambda/4$ MONOPOLE
MOUNTED NEAR THE EDGE OF A HALF-PLANE (dB).



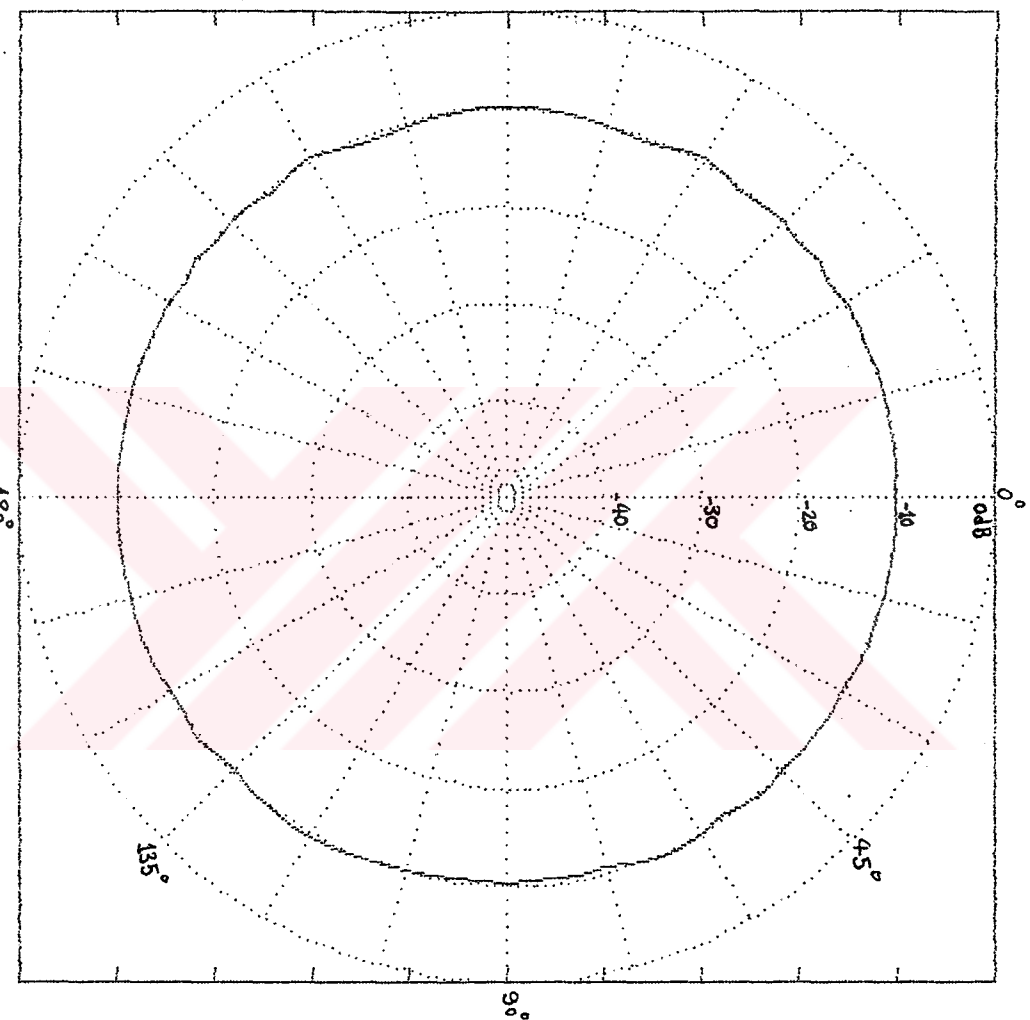


COMPUTED HORIZONTAL PLANE PATTERN OF A $\lambda/4$ MONOPOLE
MOUNTED NEAR THE EDGE OF A HALF-PLANE (dB).

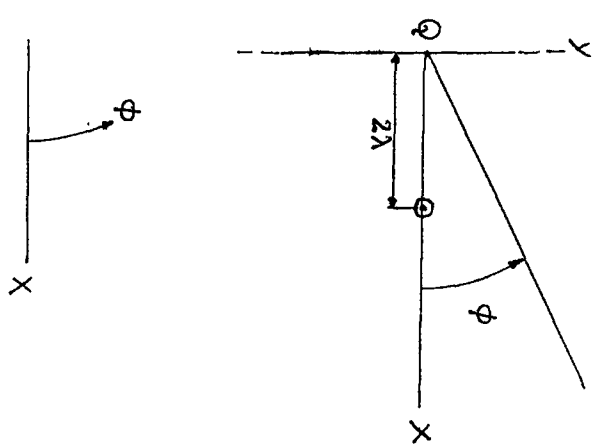




COMPUTED HORIZONTAL PLANE PATTERN OF A $\lambda/4$ MONPOLE
MOUNTED NEAR THE EDGE OF A HALF-PLANE (dB).

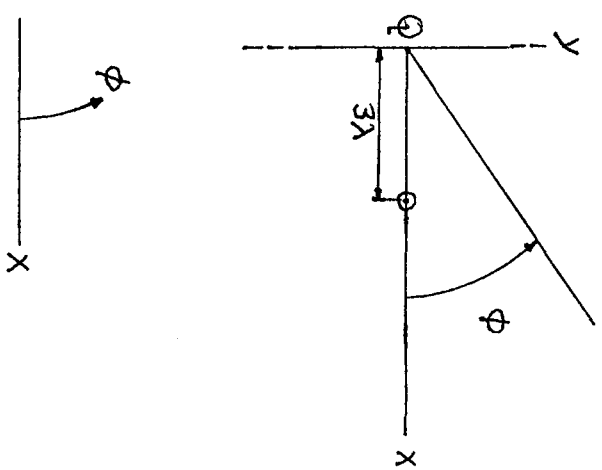
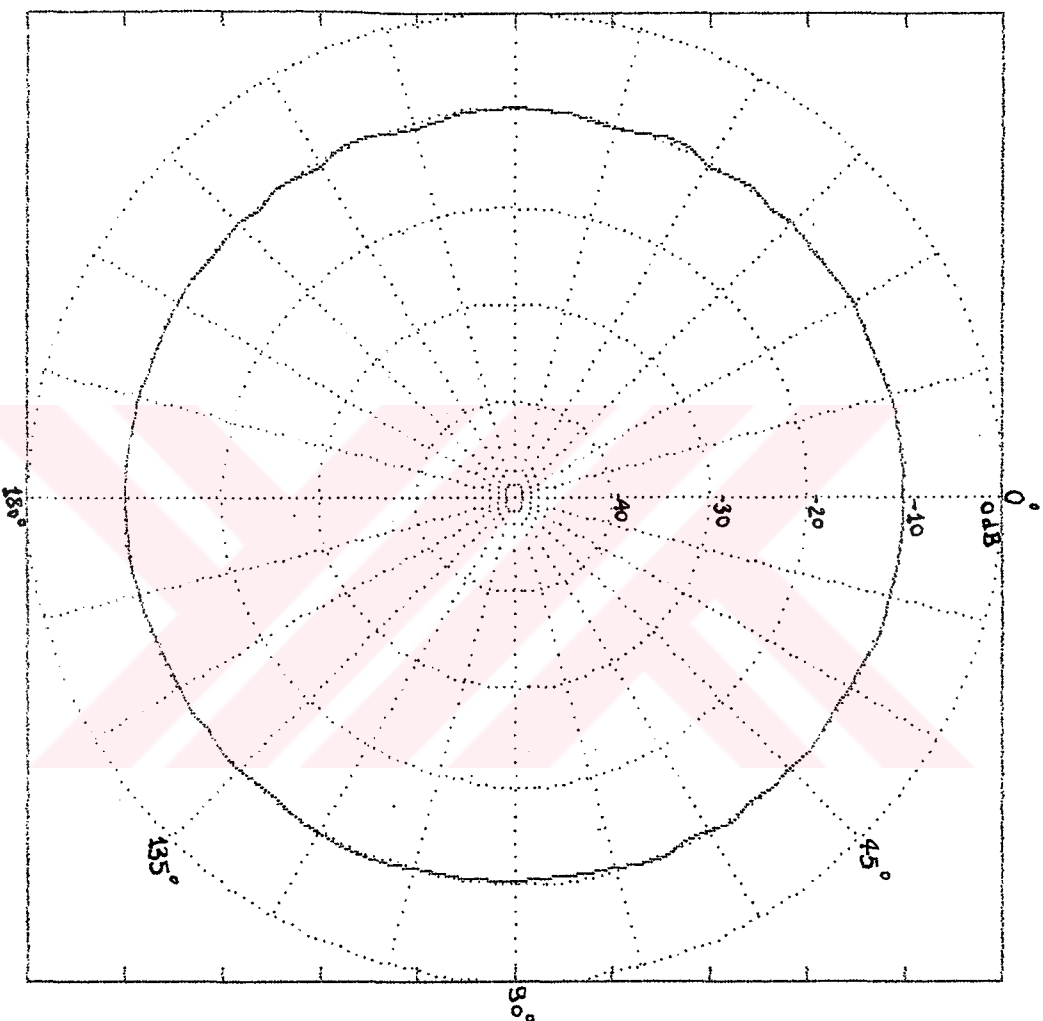


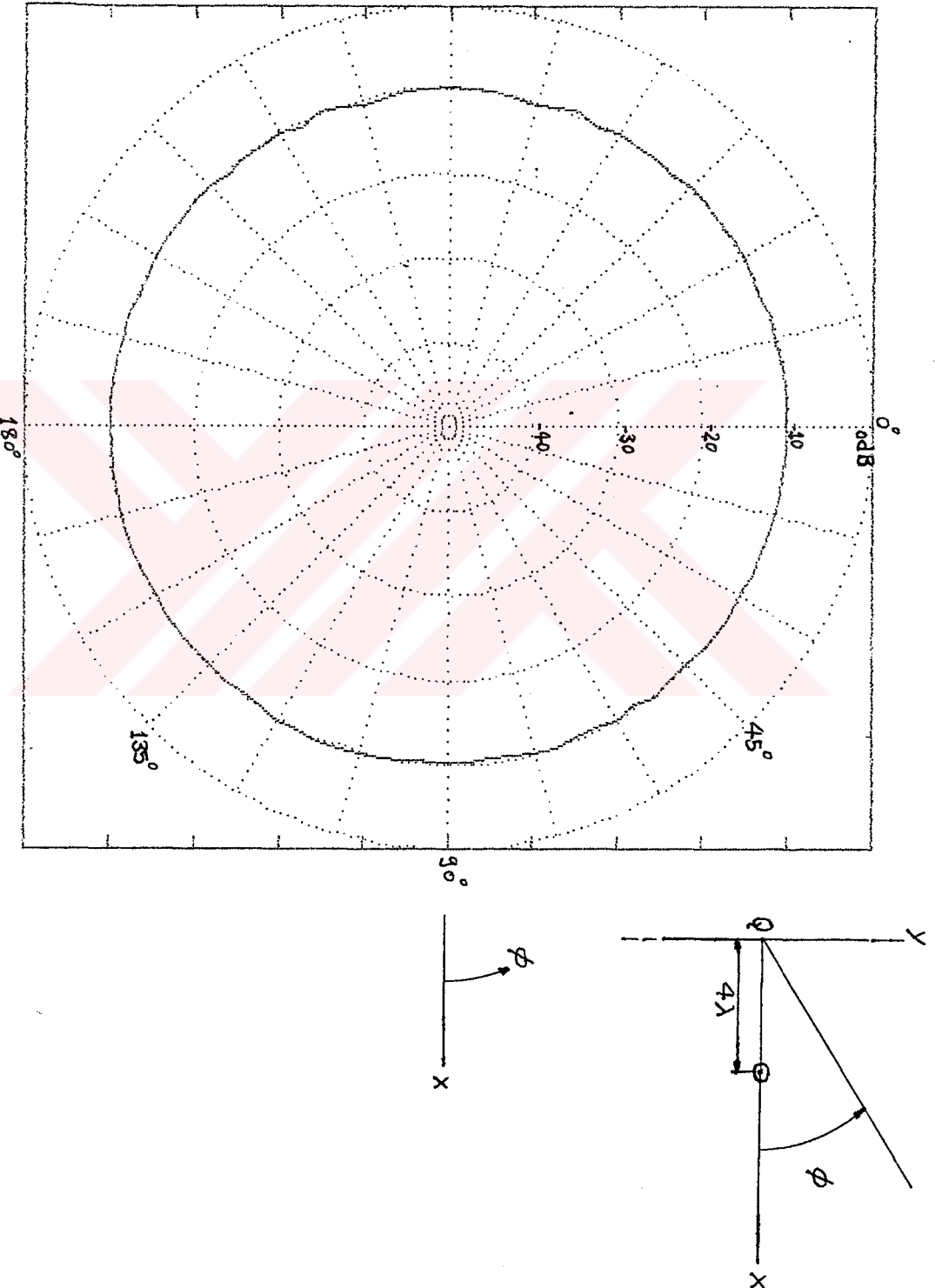
COMPUTED HORIZONTAL PLANE PATTERN OF A $\lambda/4$ MONOPOLE
MOUNTED NEAR THE EDGE OF A HALF-PLANE (dB).



COMPUTED HORIZONTAL PLANE PATTERN OF A $\lambda/4$ MONPOLE

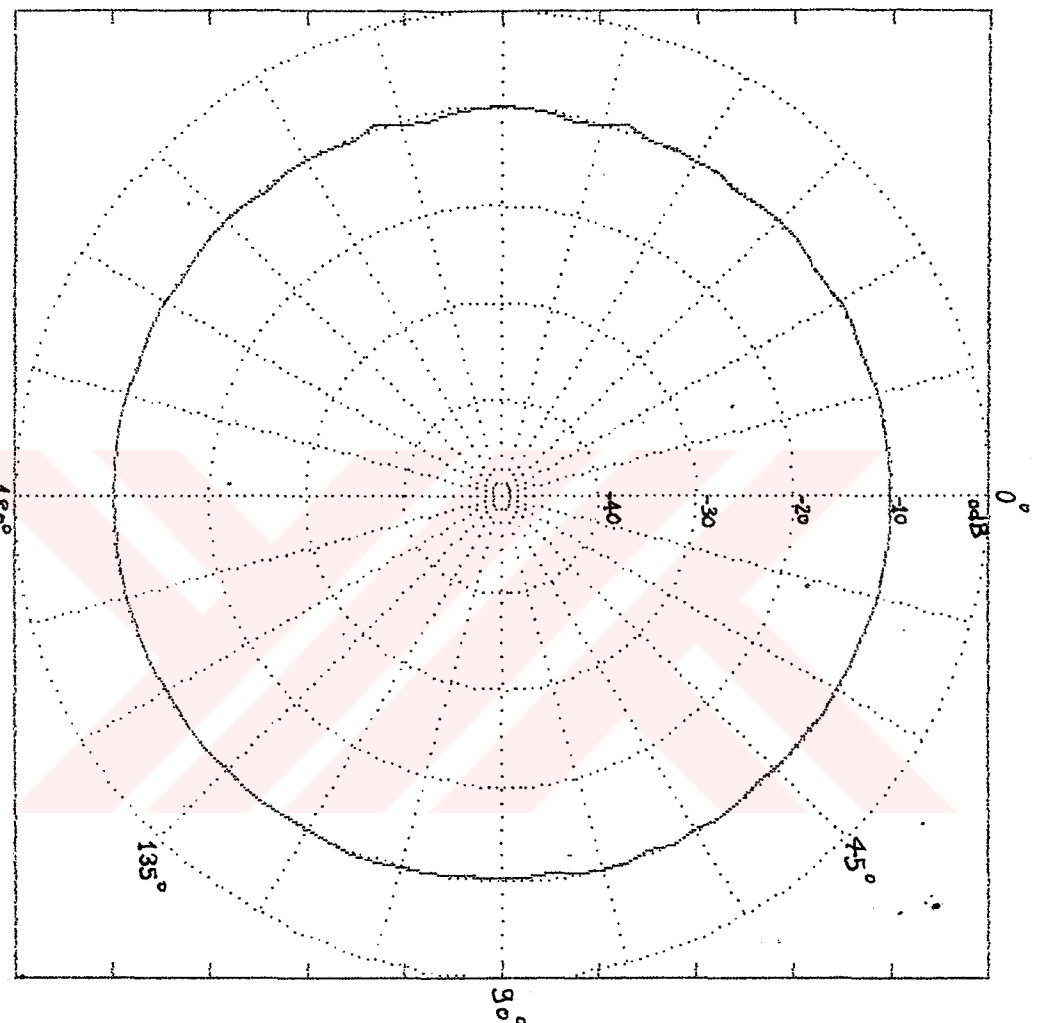
OUNTED NEAR THE EDGE OF A HALF-PLANE (dB).



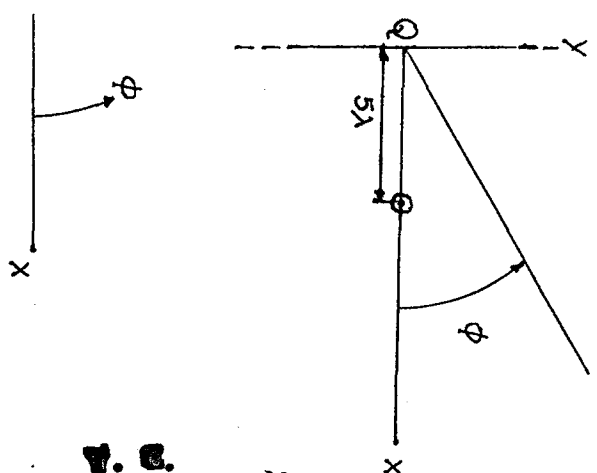


COMPUTED HORIZONTAL PLANE PATTERN OF A $\lambda/4$ MONOPOLE

OUNTED NEAR THE EDGE OF A HALF-PLANE (dB).



COMPUTED HORIZONTAL PLANE PATTERN OF A $\lambda/4$ MONOPOLE
MOUNTED NEAR THE EDGE OF A HALF-PLANE (dB).



W. E.
Yükseköğretim Kurulu
Dokumentasyon Merkezi